BEER FOAM PHYSICS

A.D. Ronteltap

BEER FOAM PHYSICS

Proefschrift

ter verkrijging van de graad van

doctor in de landbouwwetenschappen,

op gezag van de rector magnificus,

dr. H.C. van der Plas,

in het openbaar te verdedigen

op vrijdag 1 december 1989

des namiddags te vier uur in de aula

van de Landbouwuniversiteit te Wageningen

1. Stikstofgas kan in bierschuim de kwaliteit zowel verbeteren
    als verslechteren.
    Dit proefschrift.

2. De door Hartong uitgevoerde proef met één wel en één niet
    afgedekt bierglas is een goede proef om te laten zien
    waardoor bierschuim inzakt. Zijn verklaring, dat in een
    afgedekt bierglas verdamping en daarmee coalescentie wordt
    voorkomen, zou een goede verklaring kunnen zijn, maar het is
    niet de juiste.
    Vancraenenbroeck, R., Cerevisia 4:191 (1982).

3. Het is onjuist aan te nemen dat de bellengrootteverdeling in
    de bovenste bellenlaag van bierschuim representatief is voor
    de bellengrootteverdeling in het gehele schuim.
    Glenister, P.R., Segel, E., Koeppl, D.G., ASBC Proc. pp. 150 (1966).

4. Een hoge oppervlakte dilatatie of shear viscositeit werkt
    niet per definitie stabiliserend op schuim.
    Barbeau, W.E., Kinsella, J.E., Colloids and Surfaces. 17:169 (1986).

5. "Bubble ghosts" zijn dissipatieve structuren.
    Prigogine, I., Stengers, I., "Orde uit Chaos." Ed: Uitgeverij Bert Bakker, Amsterdam. (1988).

6. Men verwacht dat de produktiviteit per manuur als gevolg van
    automatisering toeneemt, terwijl men vergeet dat een manuur
    tijdens het automatiseren vaak weinig produktief is.

7. De in de praktijk vaak gehanteerde methode om de gevoeligheid
    voor oproming van emulsies te voorspellen door middel van
    centrifugeren kan makkelijk tot verkeerde conclusies leiden.
    Pearce, K.N., Kinsella, J.E., J. Agric. Food Chem. 26(3):716 (1978).

8. De stelling, dat natuurkundigen zich niet zouden mogen
    bezighouden met de "Fundamentele Vragen", is reductionistisch
    van aard.
    Lagendijk, A., "De arrogantie van de fysicus." Intermediair 38:17 (1989).

Stellingen bij het proefschrift "Beer Foam Physics" door A.D. Ronteltap, 1 december 1989 te Wageningen.

9. Het terugdringen van de CO_2-uitstoot in Nederland met jaarlijks 2% zal een invloed op het broeikaseffect hebben die in omvang ongeveer gelijk is aan de invloed op de inzaksnelheid van bierschuim.

10. Het is onjuist te veronderstellen dat aan alcoholgebruik slechts negatieve aspecten zijn verbonden voor de volksgezondheid.
Stampfer, M.J., Colditz, G.A., Willett, W.C., Speizer, F.E., Hennekens, C.H., N. Engl. J. Med. 319:267 (1988).

11. Het feit dat vandalisme als noodzakelijk kwaad wordt geaccepteerd brengt de oplossing van dit probleem niet naderbij.

12. "Vergrijzen" is een ongelukkige term om het ouder worden van mensen aan te geven.

13. Bij mooi weer is het schuimgedrag van bier van minder belang.

Voor Mariëlle

ABSTRACT

Abstract:

   The physical aspects of beer foam behavior were studied in terms of the four physical processes, mainly involved in the formation and breakdown of foam. These processes are, bubble formation, drainage, disproportionation and coalescence. In detail, the processes disproportionation and coalescence were studied. The mechanism of coalescence was determined using, amongst others, a falling film apparatus. The spreading of surface active material on the film surface proved to initiate coalescence. Disproportionation in a foam is mainly influenced by partial gas pressure differences. Surface rheological aspects dominate the rate of disproportionation when the gas composition throughout a foam is uniform. The effect of the four physical processes on various foam phenomena can be explained. The disappearance of beer foam is a result of the combined action of drainage and gas diffusion from the foam to the surrounding atmosphere. When spreading substances are added to beer foam from an external source, coalescence is initiated and foam collapse occurs. The four physical processes have a different effect on foam behavior. Therefore, a distinction between these processes was made using an optical glass-fibre probe technique. With this technique the bubble-size distribution, the gas fraction in the foam, the height of the foam and the level of the foam-liquid interface can be measured as a function of time.

PREFACE

This thesis is not the work of a single person. It could never have been written if I would not have been helped by so many people. It is not possible to mention all of them here, and to thank each of them in person. However, I would like to express my gratitude to several contributors.

The research work on beer foam, described in this thesis, would not even have started if Gert Jan Muts of Heineken Technisch Beheer B.V. had not initiated it with such enthusiasm. The collaboration between him and professor A. Prins has been a great inspiration. After Gert Jan Muts was transferred to another job within the company, Marja Hollemans replaced him, guiding the research on beer foam into the right direction. Time after time, she succeeded to bridge the distance between the fundamental view, prevailing at the university of Wageningen, and the general, practical approach at the brewery in Zoeterwoude. Her contribution has been of immense value.

The fatherly coaching of professor A. Prins during the entire period of this research work has been a tremendous learning experience. The patient way he teaches his PhD students makes it a day to day joy to work with him. His original research approach, his vivid flexibility and reassuring attitude has never failed to be a continuing encouragement.

In this thesis results are presented acquired by Jacco Wijkmans, Ellen de Jong, Adriaan Garritsen and Bart Schulte who, as students, helped me to carry out some of the experiments. I thank each of them for their contribution and hope that they have learned as much from me as I learned from them. In addition, Chris Bisperink contributed to the experimental work presented here. His support in the laboratory has been a great help and I hope that he will succeed to unravel more of the physical mysteries of beer foam within the near future.

I would also like to express my thanks to Bart Damsté and Maarten de Gee of the Mathematics department of the Agricultural University, Wageningen, who with dedication spent many hours to help me to develop a numerical model that describes the transport of gas.

The development of a new method to determine bubble-size distributions in foam would not have been possible without the spontaneous help of Jacob Jan Frijlink and Peter van Halderen who made available their time and their knowledge of the optical glass-fibre technique. I would like to thank Jan Daniël Houthuijsen and Ton Erenst for their contribution to the complex automation of the apparatus.

The scientific discussions I had with my colleagues Hans Westerbeek, Karin Boode and Coen Akkerman have been an inspiring challenge to me each time. They made a significant contribution to the completion of this thesis.

I thank B.W. Drost of Heineken for his confidence in this beer foam study and for his willingness to support the Heineken financial contribution wholeheartedly.

The support of the LEB fonds, has made it possible to distribute this thesis in an appropriate edition.

CONTENTS

1. OUTLINE OF THIS STUDY

The appearance is one of the most important quality characteristics of beer to the consumer. It is believed to be even more important than taste, although this may be disputed. The appearance of the beer depends mainly on the behavior of the foam. It has become evident that the quality of the foam influences the overall perception of the consumer to a great extent. Therefore, the control of foam behavior is essential. For that reason, an extensive research on the behavior of beer foam has been carried out in the last decades, all over the world.

The approach has mostly been to analyze the chemical components of beer, like proteins, metal ions and hop constituents, and to try to find a correlation with a foam number. These efforts have given an enormous amount of experimental results, that are partly useful, but are sometimes also very inconclusive and confusing. There is a lot of contradiction in beer foam literature. The research work so far has not satisfactory led to a better control of beer foam behavior.

One of the main reasons for the lack of insight is that research has predominantly been concentrated on the chemical aspects of foam. The behavior of beer foam can not be explained with the knowledge of the chemical composition alone. For example, the contribution of surface active components to the behavior of the foam may be either negative or positive or both, depending on, amongst others, their concentration, their interaction with other components and their location in the foam. Two chemical components, each having a positive effect on foam behavior, may have a negative effect when they are mixed and vice versa. In addition, two foams, that have exactly the same chemical composition, may behave very different. Several examples of the latter will be given in chapter 6.8.

At the beginning of this research work, the need was expressed for an additional approach in order to be able

to fully understand beer foam behavior. The ultimate objective was to acquire more fundamental, physical and phenomenological knowledge of beer foam behavior. It was anticipated that, if fundamental knowledge about beer foam could be obtained, the effect of the composition on the behavior of the foam could be explained. In other words, the opinion dominated that the gap between the chemical composition and the behavior of the foam was too large to explain various phenomena. It was expected that more fundamental and physical research could relate foam behavior to the chemical composition of beer in a better way.

The scope of this study has been to explain beer foam behavior in terms of four physical processes that mainly determine foam formation and breakdown. They are (i) bubble formation and growth, (ii) creaming and drainage, (iii) coalescence and (iv) disproportionation. An effort has been made to distinguish between these processes, to discover the main physical process, and to find the predominant parameters, that are involved in beer foam behavior. Unfortunately, the behavior of foam does not mainly depend on one single physical process. All four processes, mentioned above, are involved. In addition, the processes are interrelated and their progress depends very much on the progress of the other processes.

The four physical processes are discussed in chapter 2 trough 5 and the important parameters for the progress of these processes are reviewed. Chapter 2 and 3, where respectively bubble formation and drainage are discussed, are reviews of available literature. Research work was not carried out on these subjects. In chapter 4 and 5, the results of research work are also included. In chapter 4, coalescence is discussed in detail. In particular, coalescence, initiated by the spreading of surface active material is considered. In chapter 5, the effect of the gas composition in the foam and of the surface dilational viscosity on the rate of disproportionation is elucidated. Experimental results of bubble dissolution are compared to model calculations. In chapter 6, the appearance of the

2

foam and the occurrence of several phenomena, like the creaminess of the foam, foam collapse and cling, are explained in terms of the four physical processes. In chapter 7, a definition of the stability of foam properties is given. The measurement of beer foam behavior is discussed in chapter 8, where a review is given of several methods to measure foam characteristics. A newly developed apparatus to determine foam characteristics by means of the measurement of the bubble-size distribution is also presented in that chapter. In chapter 9, final conclusions on foam behavior are given. The influence of the four physical processes on beer foam behavior is explained.

2. BUBBLE FORMATION

2.1. Introduction

Although the bubble formation process does not seem to influence foam behavior at first sight, this influence is quite pronounced. Very important factors for beer foam behavior, like the gas composition, bubble size, bubble surface composition and the structure of the foam, are determined during the bubble formation process.

In general, bubbles can be produced in a liquid by (i) agitating or whipping, (ii) by sparging or diffusing gas through a porous material, and (iii) by decreasing the pressure of a with gas saturated liquid. In the latter case, the liquid becomes supersaturated as a result of the pressure release. Consequently, bubbles can nucleate and grow.

In beer, bubbles may be formed by air entrapment during dispense. However, the most important mechanism for bubble formation in beer is nucleation, because beer is supersaturated with carbon dioxide after pressure release.

A review on bubble nucleation was given by Blander (1979). He explained that two kinds of bubble nucleation can be distinguished, *viz.* homogeneous nucleation and heterogeneous nucleation. As a result of the creation of a new surface during bubble formation an energy barrier has to be overcome. For homogeneous nucleation, *i.e.* the spontaneous formation of a bubble nucleus, the energy barrier is high and therefore homogeneous nucleation will only occur at very high supersaturation values. The value of the supersaturation pressure can be estimated, assuming that the Laplace pressure of a very small bubble must be overcome in the course of bubble formation. Walstra (1989) simply calculates that homogeneous nucleation does not take place unless the supersaturation is in the order of 10^8 Nm^{-2} (supposing that the minimum radius for a bubble is 1 nm and the surface tension is 50 mNm^{-1}). For beer, a pressure of that value is quite unrealistic. This means

4

that bubbles do not originate spontaneously in beer, but that heterogeneous nucleation occurs. Bubbles grow from a catalytic site in order to overcome the energy barrier for bubble formation. This site may be for example a crack in the wall of a container, or a gas pocket in dispersed material.
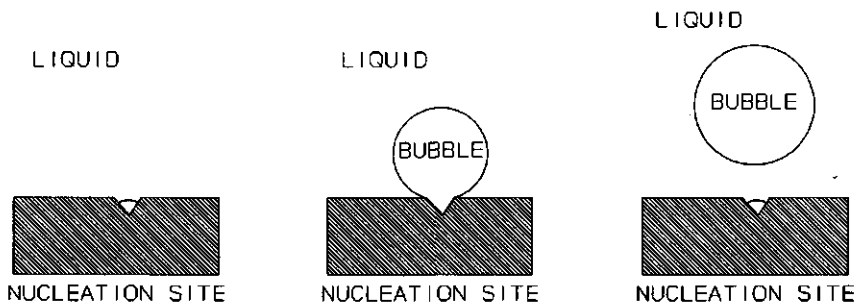
Ward et al (1970) developed a theory for heterogeneous bubble formation using a generalized Kelvin equation to describe the relation between the pressure at which nucleation occurs and the gas concentration in the liquid. They put forward the concept of the critical radius. The concept is based on the fact that the radius of a nucleus must have at least a minimal, critical size to allow bubble growth. If the radius of the nucleus is smaller than that critical radius the nucleus is unstable and will rapidly dissolve. The critical radius therefore is an unstable equilibrium, threshold value. The concept was extended by Ward et al (1982) and conditions for a second stable critical radius were formulated. The other critical radius is larger than the first, and is a result of the fact that the concept was developed for a confined volume of liquid. Ward et al (1983) described the growth of a bubble from a conical pit. In addition, the emergence of a bubble is discussed in relation to the wetting proper-ties of the liquid and the conical pit. Ward and Levart (1984) stated that a number of bubble nuclei may be in stable equilibrium with the liquid if the value of the supersaturation is low and the contact angle is small. Ward et al (1985) described the evolution of a bubble to a final stable equilibrium size.

More quantitative work on bubble nucleation was put forward by Wilt (1986), who reported a model for the homogeneous and heterogeneous nucleation rates of bubbles in carbonated beverages. Confirmation is given that a supersaturation ratio of carbonated beverages should at least be a thousand fold in order to allow homogeneous nucleation. He estimated that the supersaturation ratio of an opened carbonated beverage is about 5 and therefore homogeneous nucleation is quite impossible. Heterogeneous

nucleation however is likely to occur in depressurized carbonated beverages, depending on the contact angle between the liquid and the nucleation site and on the shape of this site. He reported that especially cavities are good nucleation spots. The effect of the surface tension on the nucleation growth rate is discussed. Ciholas and Wilt (1988) extended this model for the spherical cavity case.

The experimental measurement of the bubble nucleation rate and of the amount of bubbles formed per unit of time has been difficult. Therefore, experimental confirmation of nucleation theories has not been put forward until recently. Lubetkin and Blackwell (1988) described an acoustic method, that allows the measurement of the bubble nucleation rate.

The initial bubble-size distribution in a foam depends on the conditions during bubble formation. Heterogeneous bubble formation is schematized in figure 1.1.

LIQUID   LIQUID   LIQUID

                                                    BUBBLE

                                    BUBBLE

NUCLEATION SITE   NUCLEATION SITE   NUCLEATION SITE

Figure 1.1: Heterogeneous bubble nucleation, growth and detachment. The nucleation site is wetted by the liquid.

The moment of bubble detachment from the nucleation site is if buoyancy ($\Delta\rho gV$) becomes bigger than the adhesive force (the vertical component of $\sigma*O$), where $\Delta\rho$ is the density difference between the gas and the liquid, g is gravity, V is the volume of the bubble, O is the perimeter of the bubble where it is attached to the nucleation site and σ is the surface tension. Therefore, the bubble size is mainly determined by the surface tension at the moment of bubble detachment. The nucleation and growth of a

6

bubble goes very swift. The bubble surface is expanded rapidly during the growth of the bubble. Therefore, the increased surface tension under expansion conditions is significant. The history of the bubble surface and the surface dilational viscosity at given expansion rate determine the surface tension. The expansion rate is, amongst others, determined by the supersaturation value. If small bubbles are desired in a foam the dynamic surface tension under expansion conditions should be low.

Another important factor that may influence the initial bubble size is tangential convection during the dispense of the beer. As a result of convection, the moment of bubble detachment will be advanced. Consequently, the bubbles will remain smaller.

References

- Blander, M., Adv. in Colloid and Interface Sci. 10:1 (1979).
- Ciholas, P.A., Wilt, P.M., J. Colloid and Interface Sci. 123(1):296 (1988).
- Lubetkin, S., Blackwell, M., J. Colloid and Interface Sci. 26(2):610 (1988).
- Walstra, P., "Principles of Foam Formation and Stability." In: Focus on Foams. Ed: A.J. Wilson, Wiley and sons. (1989). To be published.
- Ward, C.A., Balakrishnan, A., Hooper, F.C., J. Basic Eng. 92:695 (1970).
- Ward, C.A., Tikuisis, P., Venter, R.D., J. Appl. Phys. 53(9):6076 (1982).
- Ward, C.A., Johnson, W.R., Venter, R.D., Ho, S., Forest, T.W., Fraser, W.D., J. Appl. Phys. 54(4):1833 (1983).
- Ward, C.A., Levart, E., J. Appl. Phys. 56(2):491 (1984).
- Ward, C.A., Yee, D., Tikuisis, P., J. Appl. Phys. 58(1):273 (1985).
- Wilt, P.M., J. Colloid and Interface Sci. 112(2):530 (1986).

3. CREAMING AND DRAINAGE

3.1. Introduction

The creaming of bubbles is the rise of the bubbles to the top of the system. Drainage is the liquid flow from a foam to the liquid underneath. It is not well defined where creaming stops and drainage begins. In fact, one could argue that it is the same process because both processes have many things in common. *E.g.* the main driving force for both processes is gravity. One could also argue that creaming becomes drainage as soon as the bubbles start to interfere and to influence each other in their motion.

The creaming process may be described with Stokes law. However, this law can only be applied if the bubble surface is immobile and the Reynolds number is low.

The effect of the mobility of the surface was discussed by Van 't Riet et al (1984). As a result of the tangential shear on the surface of the rising bubble, the surface is expanded at the top polar end of the bubble and compressed at the bottom of the bubble. Consequently, the surface tension gradient, that is a result of the surface defor-mation, counteracts the shear. The surface reaches a stationary-state and the surface becomes less mobile or even motionless. In the latter case, bubbles can be regarded as solid particles, as far as the rise of the bubbles is concerned. For beer this condition is most likely met because sufficient surface active components are present.

The other condition for Stokes law, *i.e.* the condition of low Reynolds numbers, is probably not met for beer. The density difference between the liquid and the gas is high, bubbles are comparatively large, the viscosity of beer is low and therefore creaming will advance rapidly. In addition, the bubbles may hydrodynamically interact. For these reasons, the rise of larger bubbles will not obey Stokes law.

Deviations from Stokes law may also be explained by variations in size during the rise of the bubble. The pressure in the liquid decreases as a function of the height in the glass. Therefore, the bubble will expand during the rise of the bubble. However, this effect is very small. A variation in bubble size as a consequence of gas uptake or dissolution can be more important as discussed in chapter 5.1.

Drainage occurs if the bubbles become more densely packed. The foam becomes dryer and the bubbles become deformed. This leads to a series of events, that is described by Ivanov and Jain (1979) and Wasan and Malhotra (1986) and Ivanov and Dimitrov (1989). During drainage, the foam evolves gradually from a foam with spherical bubbles to a foam with polyhedral bubbles. In a polyhedral foam the Plateau border suction contributes as a driving force for drainage (e.g. Scheludko (1957)), in addition to gravity. As a consequence of the curvature of a Plateau border, the pressure inside the Plateau border is lower than inside the bubble and in the plane film. Therefore, liquid will flow from the film to the Plateau border. Through the Plateau borders this liquid will drain from the foam as a result of gravity.

The driving forces for drainage, Plateau border suction and gravity, are counteracted by a complex interplay of surface and bulk rheological properties. Drainage depends very much on the viscosity of the film liquid. Slow drainage is the result of high bulk viscosity as can be seen from Eq. [3.1]. Another balancing parameter for drainage may be a surface tension gradient, that is driven by liquid motion (Djabbarah and Wasan (1985)). As a result of this surface tension gradient, the bubble surface may come to a total stand still (Rao et al (1982)). In that case, drainage can be described as the liquid flow from between two rigid surfaces. Consequently, the drainage rate decelerates because shear forces slow down the liquid flow. For the same reasons, the surfaces of Plateau borders may be immobile too (Kann (1984)). However, the volume-surface ratio of Plateau borders is higher than the

volume-surface ratio of films and therefore no sound conclusion can be drawn about the mobility of Plateau border surfaces. Drainage from films with (partly) mobile surface has been described by Ivanov (1985). Film drainage for uneven film thinning has been described by Liem and Woods (1974).

The rate of drainage from films can be approximated with the classical Reynolds (1886) law for liquid drainage, if the surfaces of the film can be described as two circular, plane parallel plates (*Eq.* [3.1]):

$$- \frac{d\theta}{dt} = \frac{2\theta^3 \Delta P}{3\eta r^2} \qquad [3.1]$$

where θ is the film thickness, ΔP is the driving pressure, t is time, η is the viscosity of the film liquid and r is the radius of a circular plane parallel film. From this equation an order of magnitude calculation can be made to determine the rate of film drainage. The drainage time for a plane parallel film to reach the critical film thickness of rupture can be described with *Eq.* [3.2] (see *e.g.* Malysa et al (1980)):

$$t_c \approx \frac{3\eta A}{4\pi\theta_c^2 \Delta P} \qquad [3.2]$$

where t_c is the critical drainage time, *i.e.* the time to reach the critical film thickness, A is the surface area of the plane parallel film and θ_c is the critical film thickness. The interpretation of ΔP is not always easy. The driving force for drainage from between two liquid plane parallel, horizontal films in a polyhedral foam is Plateau border suction. In that case, ΔP is equal to the capillary pressure (P_c). Assuming that ΔP is equal to $(2\sigma/r)$, the critical drainage time becomes:

$$t_c = \frac{3\eta r^3}{4\theta_c^2\sigma} \qquad [3.3]$$

Eq. [3.3] clearly indicates that the critical time for film rupture very much depends on both the radius and the critical film thickness.

For thinner films the assumption that ΔP is equal to the Laplace pressure is not valid. As the surfaces of the film approach, the Van der Waals attractive force may start to contribute as a driving force for drainage. In addition, a counteracting pressure can be present, that becomes more important if the film thickness decreases. This counter-acting pressure was called disjoining pressure (Π) by Derjaguin (1941). Taking into account this disjoining pressure the driving pressure for drainage can then be written as:

$$\Delta P = P_c - \Pi \qquad [3.4]$$

ΔP is not a constant during drainage because, as the film becomes thinner, the disjoining pressure increases and ΔP decreases. The liquid drainage from films may come to a complete stop if the disjoining pressure between the two surface layers can balance the capillary pressure. In that case a film can be stabilized, that may exist over a very long period of time if evaporation can be excluded. Scheludko (1962) formulated the conditions for the equili-brium film with the following equation:

$$\frac{dP_c}{d\theta} = \frac{d\Pi}{d\theta} \qquad [3.5]$$

The disjoining pressure may be either based on electro-static repulsion or steric effects, mostly of polymer

molecules like proteins. For low molecular weight surface active material, very thin equilibrium films may be formed typically in the range smaller than 1 μm. Films may become so thin that grey or black spots appear in the film. These spots, called Newton Black spots, were, amongst others, described by Scheludko (1967). The local thickness of the film at these spots determines whether the film will rupture or not (Radoev et al (1983). The critical film thickness of films of high molecular weight material is mostly thicker than the equilibrium thickness, which means that these films will rupture before the equilibrium thickness is reached. For these films, a correlation between the drainage time and film rupture can be found as described by Djabbarah and Wasan (1985).

References

- Derjaguin, B.V., Landau, L.D., Acta Physicochimica USSR 14:633 (1941).
- Djabbarah, N.F., Wasan, D.T., AIChE J. 31(6):1041 (1985).
- Ivanov, I.B., Dimitrov, D.S., Somasundaran, P., Jain, R.K., Chem. Eng. Sci. 40(1):137 (1985).
- Ivanov, I.B., Jain, R.K., "Dynamics and Instability of Fluid Interfaces." In: Lecture Notes in Physics. Ed: T.S. Sorensen. Springer-Verlag, New York. pp. 121. (1979).
- Ivanov, I.B., Dimitrov, D.S., "Thin Film Drainage" In: Thin Liquid Films. Ed: I.B. Ivanov. pp. 379 (1989).
- Liem, A.J.S., Woods, D.R., Can. J. Chem. Eng. 52:222 (1974).
- Kann, K.B., Colloid J. 46(3):508 (1984).
- Malysa, K., Cohen, R., Exerowa, D., Romianowski, A., J. Colloid and Interface Sci. 80(1):1 (1980).
- Radoev, P.B., Scheludko, A.D., Manev, E.D., J. Colloid and Interface Sci. 95(1):254 (1983).
- Rao, A.A., Wasan, D.T., Manev, E.D., Chem. Eng. Commun. 15:63 (1982).
- Reynolds, O., Phil. Trans. Roy. Soc. London A177:157 (1886).

- Scheludko, A., Kolloid Z. **155**:39 (1957).
- Scheludko, A., Proc. Kon. Nederl. Akad. Wetensch. Ser. **B65**:87 (1962).
- Scheludko, A., Adv. Colloid and Interface Sci. **1**:391 (1967).
- Van 't Riet, K., Prins, A., Nieuwenhuijse, J.A., "Some Effects of Foam Control by Dispersed Natural Oil on Mass Transfer in a Bubble Column." Eur. Congr. Biotechnol. 3rd, Volume 3, Verlag Chemie: Weinheim, West Germany. pp. 521. (1984).
- Wasan, D.T., Malhotra, A.K., AIChE Symp. Ser. **82**(252, Thin Liquid Film Phenomena):5 (1986).

4. COALESCENCE

4.1. Introduction

Coalescence in foams is the merge of two bubbles caused by the rupture of the film between the bubbles. Two smaller bubbles become one larger bubble. Many mechanisms for coalescence have been proposed. All mechanisms have in common, that coalescence occurs preferentially if the film thickness is low.

In literature, coalescence is often related to drainage. Films can drain to a certain equilibrium thickness. When this equilibrium thickness is reached, the film may persist over a very long period of time. Equilibrium films only rupture when the film liquid evaporates, or when disturbances occur. The rupture of films may also occur at a certain critical film thickness (θ_c), that is higher than the equilibrium film thickness. A possible mechanism for this rupture at the critical film thickness is given by Vrij and Overbeek (1967). They stated that comparatively thick films may rupture as a result of spontaneous fluctuations in film thickness.

The rupture of films, at a higher thickness than the equilibrium thickness, may occur as a consequence of external influences. Two possible mechanisms, that have been described, are the "hydrophobic particle mechanism" and the so called "spreading mechanism".

The hydrophobic particle mechanism was described by Garrett (1979), Dippenaar (1982) and Aronson (1986). A small hydrophobic particle, positioned in a liquid film, can initiate coalescence. The surface of the film next to the particle is curved as a consequence of the poor wetting properties. Therefore, the Laplace pressure in the film is locally higher than in the gas phase and in the part of the film with plane surfaces. Consequently, there will be a pressure gradient in the film, which causes the liquid to flow away from the particle. Rupture of the film occurs as schematically displayed in figure 4.1.

14
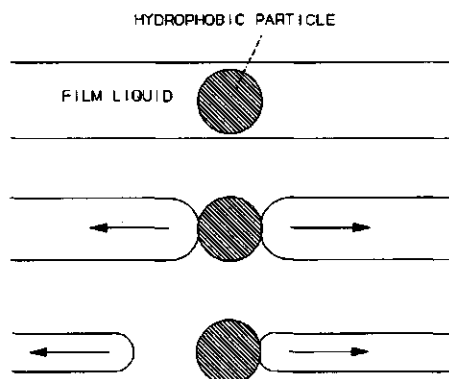
Figure 4.1: Film rupture, initiated by the hydrophobic particle mechanism.

About this mechanism several remarks can be made. (i) The particle has to pierce through both surfaces of the film and therefore, the diameter of the hydrophobic particles must be at least equal to or larger than the film thickness. If the particle has a diameter smaller than the film thickness the mechanism does not work. (ii) The contact angle of the liquid onto the hydrophobic surface must be close to 180°. (iii) The Laplace pressure depends on two radii of curvature. The driving force is not only based on the curvature of the film next to the particle. This curvature can be compensated by a curvature perpendicular to the plane of the display in figure 4.1. In that case, the pressure throughout the film is in equilibrium and coalescence will not occur. For that reason, hole formation in a film is also determined by the shape of the hydrophobic particle. In general, spherical particles will not initiate coalescence because the radius of a spherical particle can be equal to both radii of curvature of the film on the particle surface. However, anisometric hydrophobic particles can very successfully initiate film rupture. (iv) The influence of surface viscosity on this process is ambiguous. On one hand, the liquid motion in the film will cause a surface tension gradient in the film that opposes the liquid motion (Gibbs-Marangoni effect). Therefore, the surface viscosity will slow down the liquid motion, but the rupture of the

15

film can not be stopped by a surface tension gradient. On the other hand however, the surface tension next to the particle increases as a result of surface expansion and therefore the Laplace pressure increases. This may enhance coalescence since the Laplace pressure is the driving force for film rupture.

The second possible mechanism for coalescence, induced by particles or droplets, is the "spreading mechanism". This mechanism was first described by Ross (1950) and Ross et al (1953). Recently, the mechanism was discussed by Kruglyakov (1989). In figure 4.2, the spreading mechanism is displayed schematically.
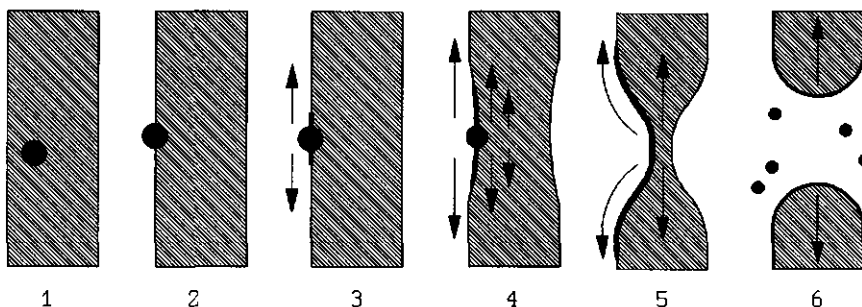
Figure 4.2: Film rupture, initiated by the spreading mechanism. For the sake of clarity the dimensions of the film were exaggerated.

If small droplets come into the surface of a beer film (2), surface active material may spread onto the bubble surface (3). By viscous forces the liquid of the film is dragged along radially in the direction of the spreading material (4). A thin spot in the film results (5). The thin spot may eventually become unstable and coalescence may occur (6).

Film rupture is only caused by the spreading mechanism if the droplets come to the surface of the film, the spreading of surface active material occurs, and enough material spreads. Therefore, there are several important parameters, which influence coalescence by the spreading mechanism: (i) Within the relevant time scale the film layer between the droplet and the atmosphere surrounding the film must drain. The critical drainage time for this

16

process may be estimated with *Eq.* [3.3] as described. (ii) The spreading mechanism only works if material spreads. In figure 4.3 an illustration is given of the spreading conditions. To spread, the surface tension of the film liquid (σ_w) must be higher than the sumvector of the surface tension of the droplet (σ_o) and the interfacial tension of the film liquid and the droplet (σ_{ow}). For this reason, the composition of the particle is important.
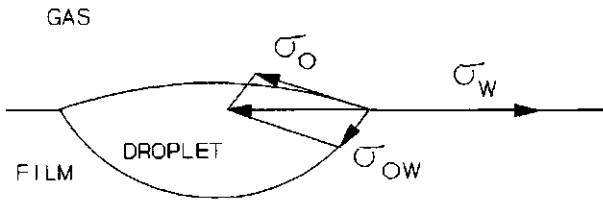

Figure 4.3: The spreading condition; if $\sigma_w > \sigma_{ow} + \sigma_o$ surface active material will spread.

For the same reason, the surface rheological aspects of beer foam are very important. The surface tension of beer in a foam can vary approximately between 9-55 mNm^{-1} under dynamic conditions (see also chapter 5.5). The dynamic surface tension depends strongly on the deformation and the deformation rate of the bubble surface. The spreading of surface active material on a film will predominantly occur if the surface tension is high. This means that film rupture is most likely to occur if a foam film surface is expanded. (iii) The droplet has to have a minimum size in order to contain enough spreading material to cause film rupture. If the droplet is too small, it may happen that spreading occurs but that the spreading does not proceed far enough to form a hole in the film. In that case the film can be restored. This is only valid for a given droplet composition. (iv) The composition of the droplet is also important for yet another reason than mentioned above. If the droplet does not contain enough spreading material, spreading may occur, but the film does not rupture. (v) Thin films will rupture easier than thick films, because less liquid has to be dragged along by the

spreading layer. (vi) The bulk viscosity of the film liquid contributes to the mechanism. At higher viscosity of the film liquid, the penetration depth of the spreading motion in the film increases and coalescence will occur more easily (Eq. [4.1]).

More quantitative work on this subject was reported by Prins (1986,1988). Assuming that the droplet completely spreads on the film surface and that film rupture will take place if the penetration depth (p) of the spreading motion is larger than the film thickness, the penetration depth can be determined with Eq. [4.1]:

$$p = R(\eta^2/\sigma_s d\rho)^{1/3} \qquad [4.1]$$

where R is the initial radius of the droplet, η is the bulk viscosity of the film liquid, σ_s ($=\sigma_w-(\sigma_{ow}+\sigma_o)$) is the spreading tension, d is the thickness of the spread layer and ρ is the density of the film liquid. This equation shows that, with increasing viscosity of the film liquid, the penetration depth increases and therewith the chance that film rupture occurs.

Coalescence in comparatively thick films can be studied by means of a falling film apparatus as described by Lin (1981[a,b]). With the falling film apparatus a thin liquid sheet is produced from a container with a slit. The sheet falls continuously between two guide wires, until it falls into a vessel. From this vessel the liquid is pumped back to the container (figure 4.5). The falling rate of the film is determined by the flow rate of the liquid and gravity. Van Havenbergh and Joos (1983,1984) described the behavior of the falling film quantitatively. The initial velocity of the liquid (v_o) can be calculated if the width of the slit (θ_o), the flow rate (Q) and the slit length (l) are known. Assuming that the flow rate is constant and that the film falls obeying the gravity law, the film thickness (θ) and the liquid velocity (v) at every distance from the slit (x) can be calculated (Brown (1961)):

$$Q = v_o \theta_o l = v \theta l \qquad [4.2]$$

and:

$$v^2 = v_o^2 + 2gx \qquad [4.3]$$

The effect of the bulk viscosity of the film liquid on the velocity of the film was neglected in *Eq.* [4.3]. This is allowed because the viscosity has minor effect on the velocity of the film for low viscosity aqueous solutions as shown by Van Havenbergh and Joos (1983).

If the free falling film is disturbed by some sort of obstruction, a V-shaped edge can appear in the film. The V-shaped edge appears if the falling velocity is higher than the bursting velocity (u) of the disturbance. The angle of the edge is determined by the velocity of the film and the bursting velocity of the disturbance. After a negligible short period of time the bursting velocity reaches a maximum, that can be described by the Culick equation (Culick (1960)):

$$u = (2\sigma/\rho\theta)^{\frac{1}{2}} \qquad [4.4]$$

The V-shaped edge is a Mach wave. The bursting velocity is related to the falling velocity by *Eq.* [4.5]:

$$u = v \sin(\alpha) \qquad [4.5]$$

where α is the Mach angle of the edge. The surface tension of the film at the location of the disturbance can be calculated if *Eq.* [4.4] and *Eq.* [4.5] are combined to give Brown's relation:

$$\sigma = \frac{1}{2}\rho\theta v^2 \sin^2(\alpha) \qquad [4.6]$$

Using *Eq.* [4.6], the dynamic surface tension in the film can be obtained if the Mach angle is measured and the film thickness is known.

In the free falling film coalescence can be initiated by adding emulsion droplets of the right composition and size. The formation of holes can be studied. With stroboscopic light, a pattern as displayed in figure 4.4 can be obtained. With every flash of the stroboscopic light the same hole is observed. However each time the hole is seen larger, because it expands, and lower because it moves along with the free falling film. Because the eye can not distinguish between separate flashes and holds a picture for a certain amount of time, the pattern as displayed in figure 4.4 is perceived.
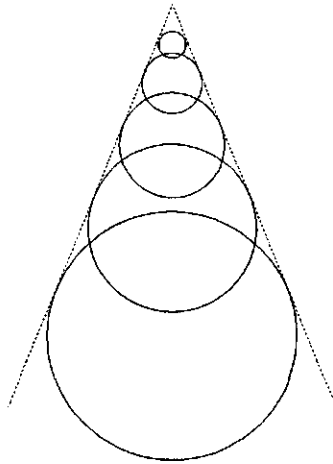

Figure 4.4: The picture obtained with stroboscopic light when film rupture occurs in the free falling film.

The envelope drawn as a dotted line along the holes in figure 4.4 has the same Mach angle as the V-shaped edge that was introduced in the film by a disturbance. The film velocity and the bursting velocity have the same value in both cases. Therefore, the actual surface tension at film rupture conditions can be calculated from Eq. [4.6], if a picture like figure 4.4 is obtained.

4.2. Aim and Approach

It is a well known fact that the behavior of beer foam is highly susceptible to the influence of lipid components

(Jackson et al (1980)). A small amount of lipid can cause rapid foam collapse. Beer contains a small amount of lipid components, like fatty acids and phospholipids. These components have a negative effect on beer foam behavior. However, the effect, that these dissolved lipid components have on the behavior of beer foam, is much smaller than the effect of lipid components coming from other sources than the beer itself. For example, dirty beer glasses or lipid material from the consumer lips may increase foam collapse enormously. Therefore, it can be argued that not only the presence of lipid material, but also the actual condition of the lipid material is important. If lipid material is molecularly dissolved relatively little harm is done to foam behavior, but if it is present as small lipid particles or droplets it can ruin a nice head in no time.

In the foam literature two possible explanations for this exceptional behavior are given. In both cases lipid particles or droplets initiate coalescence. Coalescence can either be caused by the interaction between a hydrophobic particle and the film liquid or by the motion of spreading material on the film surface. A distinction between the hydrophobic particle mechanism and the spreading mechanism can be made because the effect of several parameters on both mechanisms is different.

The particle size can be used to distinguish between these mechanisms. For the hydrophobic particle mechanism the diameter of the particle must be at least equal to the thickness of the film. For the spreading mechanism the diameter of the droplet may be smaller than the film thickness. In addition, as a consequence of the spreading of material, the droplet-size distribution will shift to smaller droplets if the spreading mechanism prevails. It is expected that the particle size will remain the same if the hydrophobic particle mechanism occurs. The surface tension that prevails under dynamic conditions will have a paramount effect on film rupture. If it is the spreading mechanism that initiates film rupture, the dynamic surface tension of the falling film must be so high that the

spreading tension is greater than zero. Therefore, the surface tension in expansion must be low in order to prevent coalescence. In the case of the hydrophobic particle mechanism, the effect of the surface rheological aspects are not well known. In addition, at higher bulk viscosity, the process will be accelerated in the case of the spreading mechanism and decelerated in the case of the hydrophobic particle mechanism. In order to determine which of the mechanisms of film rupture occurs and to study the effect of the above mentioned parameters on film rupture, various techniques were used.

The stability of a liquid film as affected by the presence of small droplets of different composition and size was measured with a falling film apparatus. The effect of the dynamic surface tension on the stability of the falling film was investigated by performing surface rheological and spreading experiments. The spreading experiments were carried out to determine whether surface active material spreads from emulsion droplets onto a beer surface. The lowest surface tension at which the spreading of surface active material occurs was determined for emulsion droplets of different composition.

In order to be able to compare the outcome of the spreading experiments with the results obtained with the falling film apparatus the dynamic surface tension in expansion of several beers was measured with various surface rheological methods. The falling film apparatus was used as described in chapter 4.1. Additional surface rheological experiments were carried out with a Langmuir trough and with an overflowing cylinder technique.

The Langmuir trough could be used in two different configurations. In one configuration, the apparatus is equipped with a single barrier. The trough with a single barrier was used to simulate the transient phenomena that occur in the foam, like bubble formation and film rearrangements. In the other configuration, the Langmuir trough is equipped with a caterpillar belt. The apparatus equipped with the caterpillar belt was used to measure the surface tension at steady-state conditions. The relative

deformation rate of the surface (dlnA/dt) is constant during this experiment (Prins (1976)).

The maximum surface expansion rate in the Langmuir trough is lower than the expansion rate in the falling film apparatus. In addition, in practical situations, surfaces can be expanded more rapidly than can be achieved with the Langmuir trough. Therefore, an overflowing cylinder technique as described by Piccardi and Ferroni (1951, 1953), Padday (1957) and Joos and De Keyser (1980) was used to measure the surface tension at higher steady-state expansion rates. The experiments were carried out with beers of different bulk viscosity to study the effect of bulk viscosity on film stability.

4.3. Experimental

The falling film apparatus consists of a temperature controlled vessel containing 2 liter of beer, from which liquid can be pumped up to a container with a thin slit (θ_o=750 μm, l=13 cm). From the slit the liquid falls as a film, between two side wires, back into the vessel. The apparatus is displayed in figure 4.5. The length of the film is approximately 40 cm. The liquid flow rates, that could be used, were from 1×10^{-5} $m^3 s^{-1}$ to 2.9×10^{-5} $m^3 s^{-1}$.

Emulsions of known droplet-size distribution and droplet composition were added to the beer in the falling film apparatus to study hole formation. The emulsions were made of beer and 2% commercial soya oil (Reddy) with varying amounts of emulsifier (either glycerol-mono-oleate (GMO) or Tween 80). A Rannie homogenizer was used at various pressures (0.5 to 8 Bar) in order to produce emulsions with different droplet-size distributions. The droplet-size distributions were measured either with a light scattering technique as described by Walstra (1968), with a microscope technique or with a Coulter Counter, depending on the droplet-size distribution of the emulsion.

The number of holes that could be produced in the falling film apparatus were measured. This was, unless

indicated otherwise, done with a 2% soya-oil, containing 1% GMO, emulsion homogenized at 0.5 Bar. The amount of emulsion added to the beer was 0.1 %(v/v). The temperature during these measurements was 20°C. The number of holes is expressed as number per unit of volume to make a fair comparison at different flow rates possible.
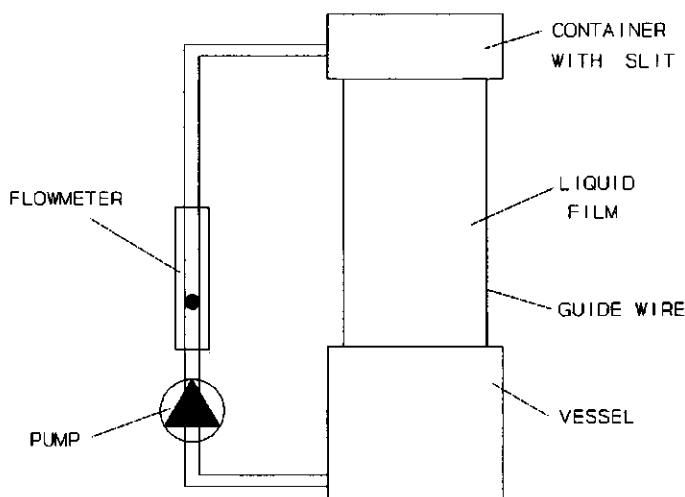

Figure 4.5: The falling film apparatus.

In order to determine whether a certain material spreads onto a surface, simple spreading experiments were carried out. Into a small container the surface tension of beer was measured using a Wilhelmy plate technique. When the equilibrium surface tension was reached, small oil droplets, containing different amounts of emulsifier, were added to the surface of the beer. A sudden decrease of the measured surface tension was taken as evidence of the spreading of surface active material. In order to simulate the increased surface tension in the falling film, the beer was diluted with water. The equilibrium surface tension of the beer was thus increased.

Additional surface rheological experiments were carried out with a Langmuir trough equipped with a single barrier. At the beginning of each experiment the surface had a total area of 90 cm^2. The surface was then expanded to a

total area of 450 cm^2, an increase of 400%. The rate of expansion could be chosen between 2.3x10^{-5} and 2.3x10^{-2} ms^{-1}. The Langmuir trough is displayed in figure 4.6.
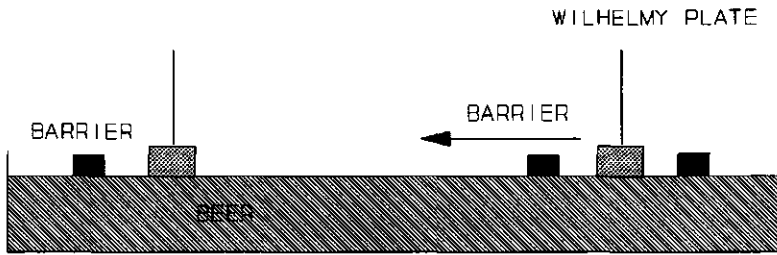

Figure 4.6: The langmuir trough equipped with a single barrier.

The Langmuir trough, equipped with a caterpillar belt with several barriers, was used to measure the surface rheological behaviour at steady-state conditions. The measurements were carried out with expansion rates varying from 2x10^{-4} to 2x10^{-1} s^{-1}. The experimental setup is displayed in figure 4.7.
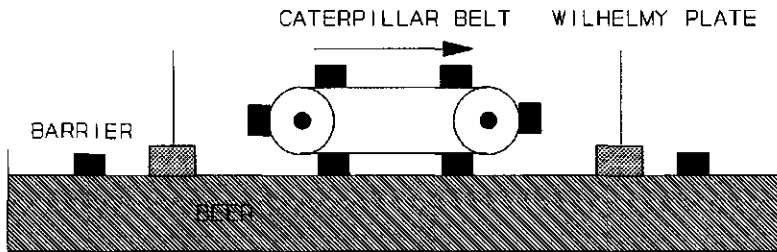

Figure 4.7: The Langmuir trough equipped with the caterpillar belt.

An overflowing cylinder technique was used to measure the dynamic surface tension of beer under expansion conditions. The overflowing cylinder technique is displayed in figure 4.8. The liquid under investigation is pumped from below into a vertical cylinder, and is allowed to overflow radially at the top of the cylinder. The diameter of the inner cylinder at the top is 8 cm. The liquid overflows into an outer cylinder, from which it is pumped again into the inner cylinder. At the top of the inner cylinder the liquid is radially expanded. After a

25

certain short period of time a steady-state equilibrium is achieved, in which surface expansion and diffusion of surface active material to the surface are in equilibrium. The surface tension under expansion conditions can be easily measured with a Wilhelmy plate technique. For the Wilhelmy plate a roughened glass plate was used.
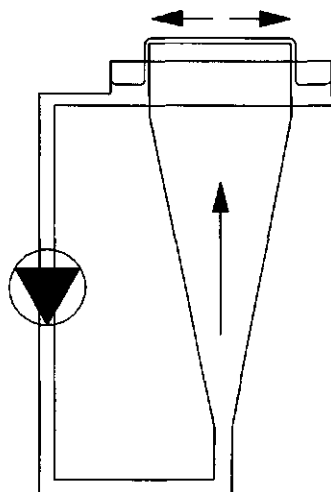

Figure 4.8: The overflowing cylinder.

The measurement of the relative surface expansion rate is more elaborate. (Bergink-Martens et al (1989)). The relative expansion rate that can be reached with the apparatus has a maximum of about 5 s^{-1}, depending on the kind of liquid under investigation, the flow rate and the distance from the center of the cylinder. The relative surface expansion rate (dlnA/dt), that is essential to determine the surface dilational viscosity defined in equation [5.9], can only be acquired by measuring the surface velocity. This can be carried out by adding small floating particles to the surface and measure their velocity.

The bulk viscosity of the beer was measured using a Ubbelohde capillary viscometer (capillary constant *ca.* 5x10^{-9} m^{2}s^{-2}). The experiments were carried out using 7 different aliquots of beer (beer A to G).

26

4.4. Results

In order to establish whether coalescence is initiated according to the hydrophobic particle mechanism or according to the spreading mechanism, the effect of the size of the particles was determined in relation to the film thickness. The thickness of the film as a function of the distance from the slit is displayed in figure 4.9 for different liquid flows. The film thickness was calculated with *Eq.* [4.2] and *Eq.* [4.3].
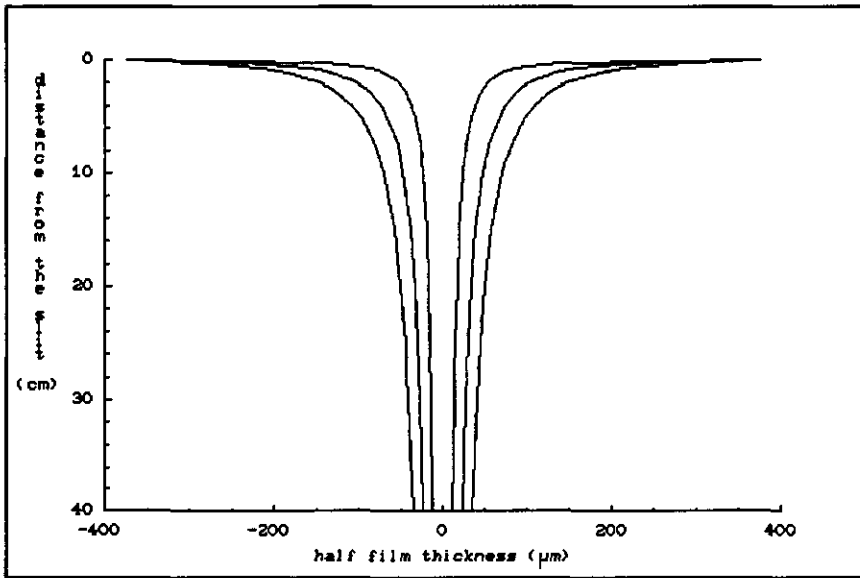
Figure 4.9: The calculated half film thickness of the free falling film as a function of the distance from the slit. The flow rates were resp. 3, 2 and 1×10^{-5} $m^3 s^{-1}$.

As can be seen from figure 4.9 the film thickness is initially the same as the thickness of the slit (750 μm). Thereafter, the film thickness rapidly decreases to about 100 μm. The thickness of the film at a certain distance from the slit is proportional to the flow rate. It can be concluded that the thickness of the film can only be manipulated by a factor of three. Higher flow rates than 2.9×10^{-5} $m^3 s^{-1}$ could not be established with the available pump. At a flow rate lower than 1×10^{-5} $m^3 s^{-1}$ the film becomes unstable.

As described above holes can be formed in the film by adding emulsions. The emulsions used were prepared at different homogenization pressures and with various emulsifier concentrations.
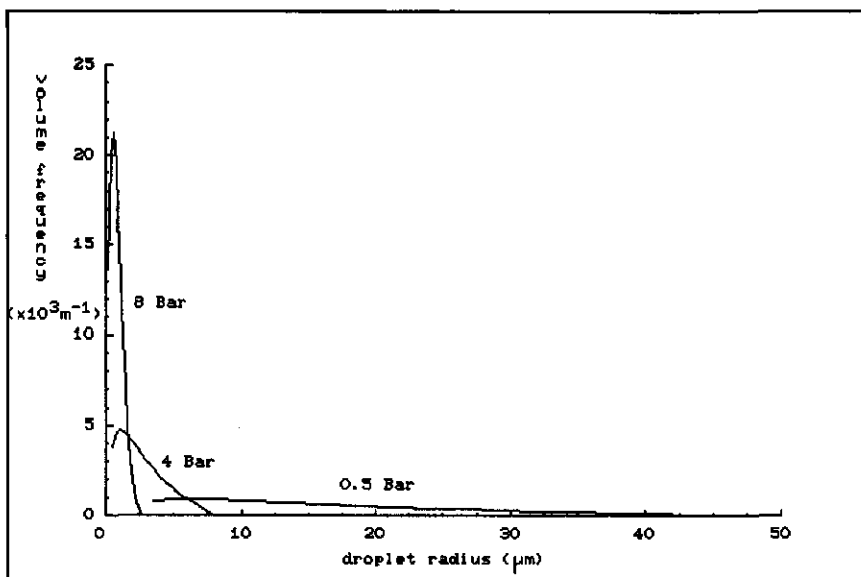
Figure 4.10: The droplet size distribution of different emulsions. The 8 and 4 Bar emulsions contain 2% soya–oil. The 0.5 Bar emulsion contains 2% soya–oil with 1% GMO.

In figure 4.10 the droplet-size distributions of the emulsions prepared with beer E and 2% soya-oil at homogenization pressures of 8 and 4 Bar are given. Also, the droplet-size distribution of an emulsion prepared with beer and 2% soya-oil, containing 1% GMO, is presented. The latter emulsion was prepared at a homogenization pressure of 0.5 Bar. In general, the droplet-size distributions of emulsions prepared with beer and 2% soya-oil containing GMO, omnibus paribus, were somewhat more narrow than emulsions prepared without GMO, but the mean droplet size was approximately the same.

When 2 ml of the emulsions, prepared with 1% GMO at 8 and 4 Bar homogenization pressure, were added to the falling beer film (2 liter of Beer E), the film remained stable at all normal flow rates. No hole formation did occur. However, in the light of a stroboscope a flickering

or twinkling of small light spots in the film was visible. The twinkling can be described as "stars in sky". This twinkling may be explained by the spreading of material on the film surface. In that case, the spreading layer reflects light in a different way than the film without a spreading layer. Hole formation does not take place because the amount of spreading material may be too low to accomplish the required penetration depth.

When 2 ml of emulsion, prepared at 0.5 Bar with beer E and 2% soya-oil, containing 1% GMO, was added to 2 liter of beer E, hole formation occurred in the film. The number of holes, measured at standard conditions, is given in table 4.1.

Table 4.1: The number of holes formed in a free falling beer film. The beer under investigation was beer E.

flow rate $(m^3 s^{-1})$	number of holes (m^{-3})	number of holes (s^{-1})
2.94×10^{-5}	2×10^3	5.9×10^{-2}
2.54×10^{-5}	4×10^3	10.2×10^{-2}
2.21×10^{-5}	9×10^3	19.9×10^{-2}
1.72×10^{-5}	13×10^3	22.4×10^{-2}

One of the reasons that the number of holes formed in the film is very low compared to the concentration of droplets (ca. 10^8 in the film) must undoubtedly be that not all the droplets present in the film come to the surface of the film. Another reason may be that on the basis of the number of droplets in the system and the flow rate the conclusion can be made that only the larger droplets in the system initiate hole formation. This is supported by the fact that the film remained undisturbed when the emulsions with smaller emulsion droplets were added. For the same reason the number of holes depends very much on the film thickness.

Even larger droplets (radius of ca. 1 mm) were added to the film by injecting soya-oil containing 1% GMO into the container with the slit. In contradiction with the expec-

tations these droplets did not cause hole formation. The explanation for this phenomenon can be that droplets larger than a certain size do not come in contact with the surface of the film. The thin liquid beer film between the droplet and the atmosphere surrounding the film does not drain completely within the short time span in the falling film. The film falls in approximately 0.3 s. With *Eq.* [3.3] the critical drainage time (t_c) for the film between the oil droplet and the surrounding atmosphere can be estimated. If the critical thickness (θ_c) of beer films is assumed to be 300 nm (Ivanov and Dimitrov (1989)), the critical drainage time as given in table 4.2 can be calculated for different droplet radii. Also given in table 4.2 is an overview of the observations made in the falling film when droplets of different composition and size are added to the film. The most likely explanation for the behavior of the film is added.

Table 4.2: The observations made in the falling film when droplets of various size and composition are added.

droplet radius (μm)	t_c (s)	observation (s^{-1})	explanation
without emulsifier:			
1	10^{-7}	no holes no twinkling	droplets come to the surface but do not spread
10	10^{-4}	no holes no twinkling	droplets come to the surface but do not spread
100	10^{-1}	no holes no twinkling	droplets come to the surface but do not spread
1000	100	no holes no twinkling	droplets do not come to the surface
with emulsifier:			
1	10^{-7}	no holes twinkling	droplets come to the surface and spread but the droplets are to small to initiate holes
10	10^{-4}	no holes twinkling	droplets come to the surface and spread but the droplets are to small to initiate holes
100	10^{-1}	holes no twinkling	droplets come to the surface, spread and initiate holes
1000	100	no holes no twinkling	droplets do not come to the surface

Summarizing the above, the droplets with a diameter of approximately the same size as the film thickness caused film rupture. Material from droplets of smaller size appeared to spread, but did not cause the film to rupture. Droplets with a diameter much larger than the film thickness do not initiate hole formation, probably because they do not come through the beer film between the droplet and the surrounding atmosphere.

From these experiments no definite conclusions can be drawn about the mechanism for hole formation. Either the hydrophobic particle mechanism or the spreading mechanism can occur.
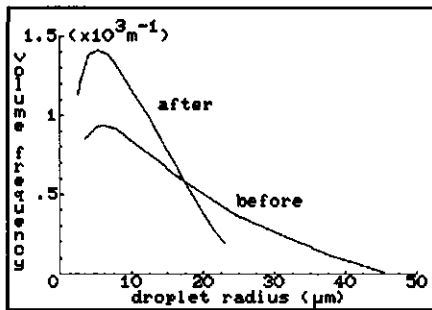

Figure 4.11[a]: The droplet–size distribution of the 0.5 Bar 2% soya oil/1% GMO emulsion before and after the experiment determined with a microscope.
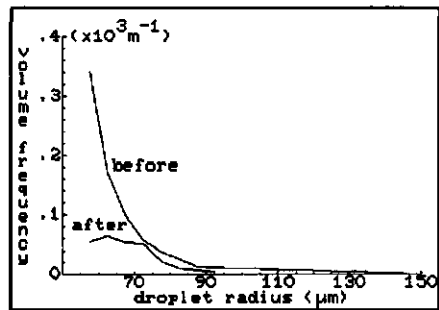
Figure 4.11[b]: The droplet–size distribution of the 0.5 Bar 2% soya oil/1% GMO emulsion before and after the experiment determined with a Coulter Counter for droplets >50 μm.

In figure 4.11[a,b] the droplet-size distribution is given of the 0.5 Bar emulsion containing 1% GMO before and after the experiment as determined with a microscope technique and a Coulter Counter. With both methods it can be clearly seen that the droplet-size distribution shifts to smaller droplets during the falling film experiment, meaning that the larger droplets become smaller. This observation was also made by Roberts (1977) who describes the spontaneous emulsification of defoamer during the breakdown of a foam. This may be a result of the spreading of material on the surface of the film. The spread layer breaks up and forms smaller droplets. This observation is in agreement with the observation that after a certain period of time the

formation of holes stops. These results indicate that the formation of holes is caused according to the spreading mechanism. By decreasing the flow rate and thus the film thickness the formation of holes can be initiated again.

Emulsions, homogenized at 8, 4 and 0.5 Bar were also prepared without GMO. When they were added to the film, omnibus paribus, no holes were formed. In addition, the "stars in the sky" were not observed. The addition of a certain amount of GMO to the emulsion appears to be necessary for hole formation. The essential addition of emulsifier can be explained in favor of both coalescence mechanisms. The addition may change the contact angle between the beer film and the emulsion droplet in such a way that the hydrophobic particle mechanism works. This is not very likely, because it can be expected that the addition of an emulsifier would alter the wetting properties to make the droplet more hydrophilic. However, no definite conclusions can be drawn. On the other hand, the addition of GMO to the emulsion droplet may alter the spreading pressure from negative to positive. This means that no surface active material spreads from an emulsion droplet without GMO and that material spreads if it contains a certain minimum amount of GMO.

In order to establish which of the above mentioned mechanisms of film rupture occurs spreading experiments of soya-oil droplets onto a beer surface were carried out as a function of the GMO concentration (table 4.3).

Table 4.3: Spreading experiments of soya-oil onto the surface of beer E carried out as a function the GMO concentration. The initial surface tension was 41 mNm^{-1}.

droplet composition	spreading	final surface tension (mNm^{-1})
soya-oil	no	41
soya-oil as emulsion	no	41
soya-oil 1% GMO	no	41
soya-oil 2% GMO	yes	39
soya-oil 3% GMO	yes	37
soya-oil 4% GMO	yes	37

It becomes clear that in order to spread surface active material onto a beer surface a certain minimum amount of GMO must be added to the soya-oil. The pure soya-oil does not spread on the surface of the beer. If the spreading of surface active material initiates hole formation in the falling film the minimum amount of GMO, added to the oil, must be larger than 1%, because the soya-oil containing 1% GMO does not spread on the beer surface. This assumption is not in agreement with the observation that holes are formed in the falling film when the 2% soya-oil containing 1% of GMO is added to the film. The disagreement may be a consequence of the fact that the surface tension of the falling film is higher than the equilibrium surface tension. This is a result of the creation of a new surface at the slit and the surface expansion that takes place in the film.

Figure 4.12: The dynamic surface tension of a free falling beer film as a function of the distance from the slit for various flow rates. Determined according to Van Havenbergh.

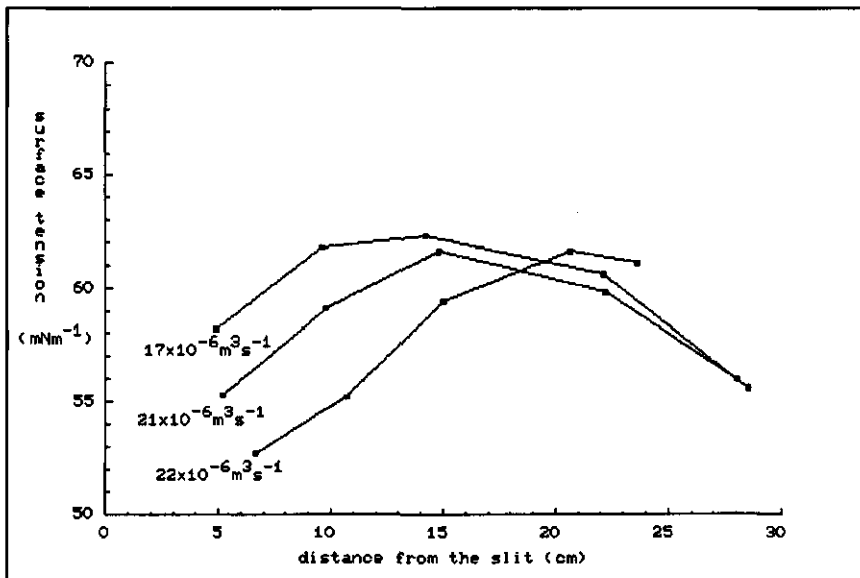In figure 4.12 the dynamic surface tension is given for beer E as a function of the distance from the slit for various flow rates. The observations are not completely in agreement with the results of Van Havenbergh and Joos (1983), made with SDS solutions. These authors found that

33

the surface tension in the film continuously decreases from about 72 mNm^{-1} close to the slit to lower values at the lower part of the falling film depending on the SDS concentration. The deviation between results presented in figure 4.12 and the results of Van Havenbergh and Joos (1983) may be explained by the fact that the dynamic surface tension of beer instead of SDS was measured. The surface tension of the beer film is between 50 mNm^{-1} and 65 mNm^{-1}. This is relevant, because surface active material, that does not spread on a beer surface in equilibrium, may spread on the expanded surface of the falling beer film.

To investigate this supposition in more detail, the beer was diluted with water to simulate the prevailing surface conditions in the free falling film. As a consequence of this manipulation the surface tension can be made equal for both situations, although the surface composition may be different. For this reason, the comparison has limited value. The results of the spreading experiments on diluted beer surfaces are given in table 4.4. The surface tension at which spreading occurs for various concentrations of GMO is lower than the surface tension measured in the free falling beer film. Even from soya-oil droplets containing low concentrations of GMO (0.25%), surface active material spreads on the surface of diluted beer ($\sigma \geq 50$ mNm^{-1}) and initiates hole formation in the free falling beer film. This is a strong argument in favor of the occurrence of the spreading mechanism.

Table 4.4: Spreading experiments of soya–oil onto diluted beer surfaces carried out as a function the GMO concentration.

droplet composition	spreading surface tension (mNm^{-1})
soya–oil 2% GMO	41
soya–oil 1% GMO	44
soya–oil 0.75% GMO	46
soya–oil 0.5% GMO	48
soya–oil 0.25% GMO	50
soya–oil 0% GMO	>72[*]

[*] no spreading on water.

The dynamic surface tension of the beer in expansion appears to be important for coalescence, initiated by soya-oil droplets, because it determines whether a given droplet spreads or not. Therefore, the dynamic surface tension of beer was measured in various ways. Experiments were carried out in a Langmuir trough either equipped with a single barrier or equipped with a caterpillar belt. The results obtained with the experiment using a single barrier are displayed in figure 4.13.
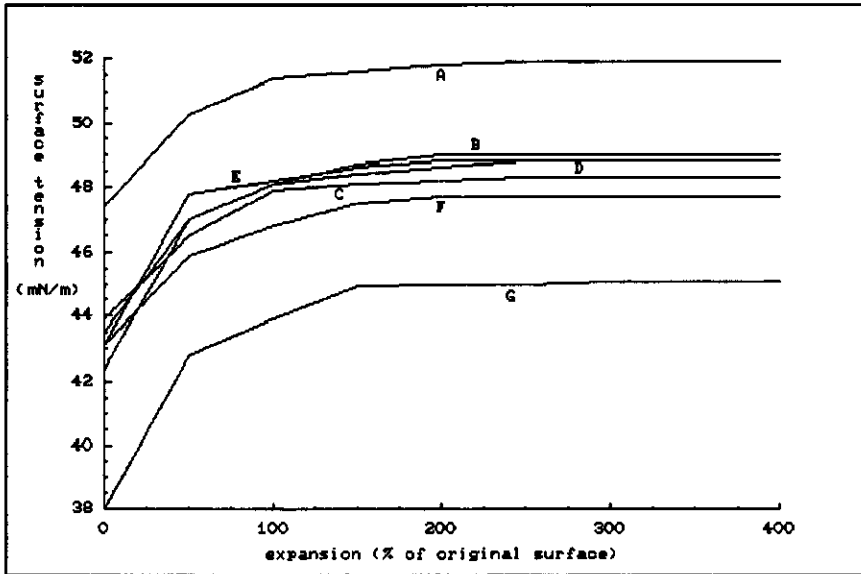
Figure 4.13: The surface tension as a function of the expansion for various beers.

The linear expansion rate of the barriers was 2.3×10^{-2} ms^{-1}. As can be clearly seen the surface rheological behavior of the beers is remarkably different. The equilibrium surface tension varies from 38 mNm^{-1} to 47.4 mNm^{-1}. When the surface is expanded 400% the surface tension of all beers rises. The final surface tension of beers under dynamic conditions lies between 45.1 mNm^{-1} and 51.9 mNm^{-1}. It seems that the curves are shifted over approximately the same distance as the difference in equilibrium surface tension.

The surface rheological behaviour of beer, under the steady-state conditions in the Langmuir trough equipped with the caterpillar belt, is displayed in figure 4.14. As can be seen the surface tension of the beers depends very

35

much on the deformation rate. At high deformation rate the surface tension does not increase as much as at lower deformation rate showing that beer is shear thinning with respect to the surface dilational viscosity. The sequence for the beers is very much the same as in figure 4.13.
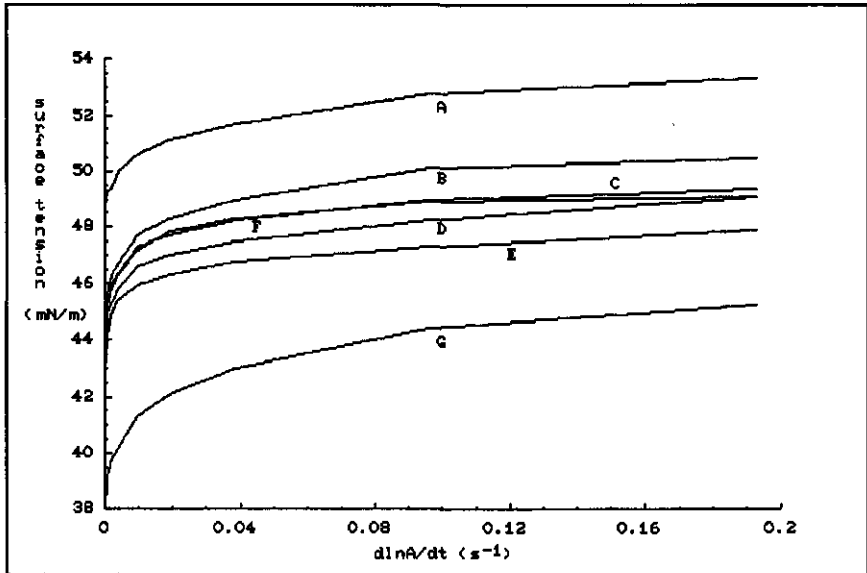
Figure 4.14: The dynamic surface tension as a function of the steady state expansion rate as measured with the Langmuir trough equipped with the caterpillar belt.

The overflowing cylinder was used to measure the dynamic surface tension at higher steady-state expansion rates than with the caterpillar belt method (max. 0.2 s^{-1}). In figure 4.15 the value of the surface expansion rate of beer D is given as a function of the distance from the center of the inner cylinder. As can be seen the relative expansion rate is not uniform over the cylinder. Instead the dlnA/dt increases from about 2 to 8 s^{-1}. The surface tension is measured at the center of the cylinder, where dlnA/dt is approximately constant. The plate has a width of 2.6 cm.

However, since the dlnA/dt at that place can not be determined exactly the surface viscosity can not be calculated. In addition, the surface viscosity is unknown for a second reason. As stated before, the relative expansion rate at the top of the overflowing cylinder

depends on the surface and bulk rheological properties of the liquid under investigation. Depending on the liquid, the flow rate and the geometry of the system, the surface adapts itself. A steady-state of a certain surface tension and surface relative expansion rate is accomplished. This means that it is not certain whether the dlnA/dt for all beers, measured in the overflowing cylinder, is equal. The surface viscosity can not be calculated unless the dlnA/dt for every beer can be measured.
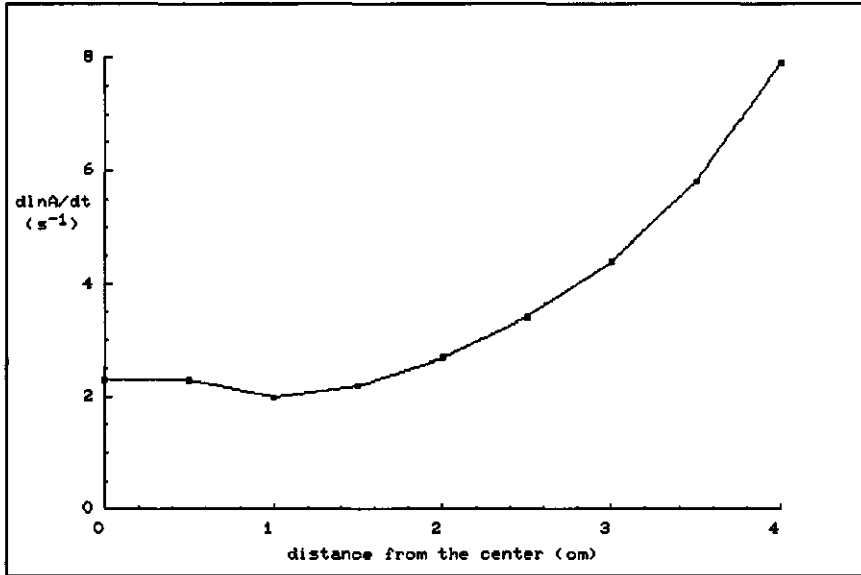
Figure 4.15: The dlnA/dt in the overflowing cylinder as a function of the distance from the center of the inner cylinder. The examined beer was beer D.

This is not a real drawback of the method for these kind of measurements since the surface dilational viscosity is not the relevant parameter for the spreading of surface active material. The relevant parameter is the dynamic surface tension (σ_{dyn}), which can easily be measured.

In table 4.5 the dynamic surface tension of 7 different beers are given as measured with the overflowing cylinder technique. It can be concluded that the surface tension in expansion for the 7 beers is approximately similar. The differences at high expansion rates have become very low. The large differences between the beers found at lower expansion rate with the caterpillar belt method seem to

almost disappear at higher expansion rates. Nevertheless, the sequence of the 7 beers remains very much the same.

Table 4.5: The dynamic surface tension for various beers as measured with the overflowing cylinder technique. The flow rate was 5.6 m^3s^{-1}. The dlnA/dt was approximately 2 s^{-1}.

beer	σ_e (mNm^{-1})	σ_{dyn} (mNm^{-1})
A	47.4	55.0
B	42.2	52.9
C	43.0	53.0
D	42.8	52.6
E	41.6	52.0
F	41.9	52.1
G	38.0	52.8

The last parameter that can be used to distinguish between the hydrophobic particle mechanisms and the spreading mechanism is bulk viscosity. Therefore, the viscosity of the beer was increased with different amounts of dextran and emulsion droplets were added to the film.
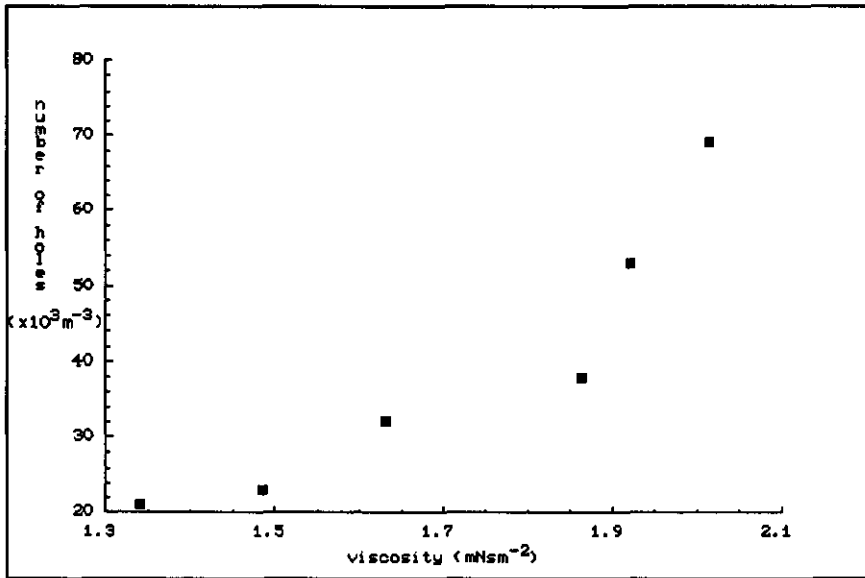
Figure 4.16: The number of holes in a falling film of beer E as a function of the viscosity. The viscosity was increased by adding dextran.

The number of holes in the falling film is given in figure

4.16 as a function of the bulk viscosity. The number of
holes formed in the film depends very much on the bulk
viscosity of the beer. The increase of the number of holes
can not be explained with the increase in penetration
depth alone (*Eq.* [4.1]). Apparently, by increasing the
viscosity, the spreading of smaller droplets becomes
effective as well. Because there are increasingly more
small droplets going from right to left in the right tail
of the droplet-size distribution, the number of holes
formed in the falling film increase at higher viscosity in
a spectacular way.

Table 4.6: The number of holes formed in a free falling beer film for various beers. The bulk viscosity of the beers is given. The flow rate was 1.7×10^{-5} m^3s^{-1}. 30 ml emulsion of beer E, 2% soya–oil, 1% Tween 80 was added to 3 l beer. The d_{vs} of the emulsion was 9.7 μm.

beer	η (mNsm^{-2})	number of holes (m^{-3})
A	1.21	13
B	1.34	17
C	1.34	19
D	1.29	15
E	1.34	21
F	1.34	29
G	1.32	16

The number of holes formed in the falling film apparatus
for different beers, omnibus paribus, is very different as
can be seen in table 4.6. However, the differences seem to
be influenced mainly by the viscosity of the beer as can
be seen in figure 4.17. Under the extreme expansion
conditions in the falling film apparatus the beers had
very similar dynamic surface tension (table 4.5). The
dynamic surface tension apparently does not influence the
results obtained with the falling film apparatus to a
large extent.
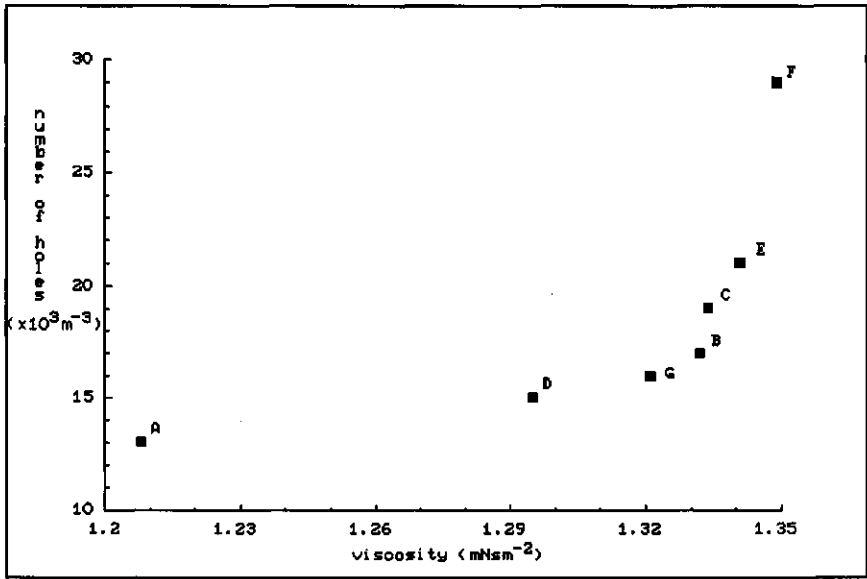
Figure 4.17: The number of holes in a falling beer film as a function of the bulk viscosity. The results are given for various beers.

4.5. Discussion

The results, obtained with the falling film apparatus, can not be directly translated into coalescence in beer foam. The film thickness in foams is at least an order of magnitude smaller than the film thickness in the falling film apparatus, whereas emulsion droplets added to the film in the experiment have about the same diameter as in practice. Therefore, the penetration depth, essential for hole formation in a foam film, will mostly be small. Consequently, droplets with about the same diameter as the film thickness will, depending on their composition, initiate coalescence. In practice, the lipid droplets are added externally to the foam films. In that case, there is no upper limit to the droplet size. All droplets come to the surface. In addition, the film in the falling film apparatus is created at high surface expansion rate. It may be anticipated that the film surfaces in a foam are closer to equilibrium.

Another observation made with the falling film apparatus that can not be directly translated to beer foam, is the result that high bulk viscosity decreases film stability. The effect of bulk viscosity on drainage may be more pronounced than the effect on coalescence by the spreading mechanism. As a consequence of high viscosity, the rate of drainage will be slower and the film thickness in the foam will remain higher over a longer period of time. The effect of the film thickness on the spreading mechanism is more important than the effect of bulk viscosity as can be seen in *Eq.* [4.1].

Although not all observations made with the falling film apparatus can be directly related to beer foam, conclusive results were obtained to distinguish whether film rupture initiated by lipid components is according to the hydrophobic particle mechanism or according to the spreading mechanism. The emulsion droplets, essential to initiate coalescence in the falling film apparatus, must have about the same diameter as the film thickness. This does not give conclusive evidence that hole formation in a liquid film is caused merely by the spreading mechanism and not by the hydrophobic particle mechanism. However, from all other experiments it becomes clear that the spreading of surface active material must be responsible for film rupture. The detrimental effect to beer foam of externally added lipid material is a result of coalescence, initiated by the spreading mechanism.

One of the indications is that the emulsion droplets become smaller during the measurement in the falling film apparatus. Hole formation stops after a period of time. When the flow is decreased the process starts again to show the susceptibility of the process on the film thickness and the droplet size. Another strong argument is that coalescence by the spreading mechanism depends on the composition of the droplet. Soya-oil, although itself a "dirty" system, does not spread on the (expanded) surface of beer. Experiments show that a minimum concentration of emulsifier in the soya-oil is essential for film rupture. The minimum emulsifier concentration that is necessary to

spread on a equilibrium surface of diluted beer is about the same as the concentration that is necessary to cause hole formation in the falling film, whereas the surface tension in both experiments is equal.

Yet another reasoning is that the process in the falling film apparatus very much depends on the bulk viscosity of the beer. An increased viscosity leads to an increase of the number of holes. This is an additional argument in favor of the spreading mechanism.

Because the detrimental effect of externally added lipid components is according to the spreading mechanism, it may be concluded that the surface tension of the beer must be low to avoid the spreading of surface active material. This does not only apply to equilibrium conditions but also to the actual expansion conditions of foam formation and breakdown. For different beers the surface rheological behaviour in expansion is different. In particular, the dynamic surface tension may differ for different beers depending on the expansion rate of the surface. At lower expansion rates the differences are more pronounced. From this observation, it may be expected that beers, that have different surface rheological behaviour in expansion, also differ in their susceptibility to externally added lipid components.

The bulk viscosity of the beer, although its effect was very pronounced in the experiments with the falling film, is less important in beer foam as far as the spreading mechanism is concerned. In practice, it may be expected that the thickness of foam films is smaller than the added spreading droplets. Consequently, the penetration depth of the spreading motion will, in general, be large enough to initiate coalescence.

From these last considerations, it can be concluded that, in practice, the collapse of foam by coalescence, initiated by externally added lipid material, can only be avoided if the fat material does not spread on the surface of the beer. The dynamic surface tension is therefore the most important parameter.

References

- Aronson, M.P., Langmuir **2**:653 (1986).
- Bergink-Martens, D.J.M., Bos, H.J., Prins, A., Schulte, B.C., Submitted to J. Colloid and Interface Sci. (June 1989).
- Brown, D.R., J. Fluid Mech. **10**:297 (1961).
- Culick, F.E.C., J. Appl. Phys. **31**:1128 (1960).
- Dippenaar, A., Int. J. Miner. Process. **9**(1):15 (1982).
- Garrett, P.R., J. Colloid and Interface Sci. **69**:107 (1979).
- Ivanov, I.B., Dimitrov, D.S., "Thin Film Drainage" In: Thin Liquid Films. Ed: I.B. Ivanov. pp. 379 (1989).
- Jackson, G., J. Inst. Brew. **87**:242 (1981).
- Joos, P., De Keyser, P., "The overflowing funnel as a method for measuring surface dilational properties." In: Levich Birthday Conf. Madrid. (1980).
- Kruglyakov, P.M., "Equilibrium Properties of Free Film and Stability of Foams and Emulsions." In: Thin Liquid Foams. Ed: I.B. Ivanov. pp. 767. (1989).
- Lin, S.P., J. Fluid Mech. **104**:111 (1981[a]).
- Lin, S.P., Roberts, G., J. Fluid Mech. **112**:443: (1981[b]).
- Padday, J.F., Proc. Intern. Congr. Surf. Activity, London **1**:1 (1957).
- Piccardi, G., Ferroni, E., Ann. Chim. (Rome) **41**:3 (1951).
- Piccardi, G., Ferroni, E., Ann. Chim. (Rome) **43**:328 (1953).
- Prins, A., "Dynamic Surface Properties and Foaming Behavior of Aqueous Surfactant Solutions." In: Foams. Ed: R. J. Akers, Academic Press. London, New York. pp. 51. (1976).
- Prins, A., "Theory and Practice of Formation and Stability of Food Foams." In: Food emulsions and foams. Ed: E. Dickinson, Royal Society of Chemistry, Leeds. pp. 30. (1986).
- Prins, A., "Principles of Foam Stability." In: Advances in Food Emulsions and Foams. Ed: E. Dickinson, G. Stainsby, Elsevier Applied Science. pp. 91. (1988).

- Roberts, K., Axberg, C., Osterlund, R., J. Colloid and Interface Sci. **62**:264 (1977).
- Ross, S., J. Phys. Colloid Chem. **54**:429 (1950).
- Ross, S., Hughes, A.F., Kennedy, M.L., Mardoian, A.R., J. Phys. Colloid Chem. **57**:684 (1953).
- Van Havenbergh, J., Joos, P., J. Colloid and Interface Sci. **95**(1):173 (1983).
- Van Havenbergh, J., Bussmann, H., Joos, P., J. Colloid and Interface Sci. **101**(2):462 (1984).
- Vrij, A., Overbeek, J.Th.G., J. Am. Chem. Soc. **90**(12):3074 (1968).
- Walstra, P., J. Colloid and Interface Sci. **27**(3) (1968).

5. DISPROPORTIONATION

5.1. Introduction

Disproportionation is a coarsening process, that is the result of inter-bubble gas diffusion, caused by a gas pressure difference between bubbles. If a single gas is present, this pressure difference corresponds to a difference in Laplace pressure. This pressure difference may be a result of a difference in size. According to the law of Laplace the pressure in a smaller bubble is higher than the pressure in a larger bubble, assuming that the surface tensions (σ) of both bubbles are equal:

$$\Delta P_{tot} = P_1 - P_2 = 2\sigma/r_1 - 2\sigma/r_2 \qquad [5.1]$$

ΔP_{tot} being the total pressure difference, and P_1 and P_2 being the Laplace pressures in the bubbles respectively with radii r_1 and r_2. Disproportionation may also be called Ostwald ripening or isothermal destillation.

The pressure difference causes a concentration gradient in the liquid layer separating the bubbles. As a result of this concentration gradient, transport of gas will take place from a smaller to a larger bubble. The larger bubble will grow at the expense of the smaller one. The smaller bubble will eventually disappear. Consequently, coarsening of the foam will take place. The disproportionation rate depends on several parameters, in particular, the gas solubility and the film thickness, which may have very different values in different foams.

Although gas transport in foams may be very important for the behavior of the foam, limited literature about this subject is available. This is probably a consequence of the fact that a quantitative description of gas transport in a multibubble system is very complex. However, although there are some fundamental differences between gas transport in foams and the dissolution of a single

bubble in an infinite amount of liquid, a lot of under-
standing on gas transport in foams can be obtained from
the well developed knowledge on bubble dissolution.

Ever since a first attempt to describe the dissolution
of a bubble by Epstein and Plesset (1950) a vast develop-
ment and improvement of bubble dissolution theory has
occurred. Scriven (1959) gave the exact solution for the
growth rate of a bubble using a similarity transformation
technique. Unfortunately this method can only be used for
bubbles with zero initial radius. Cable and Evans (1967)
extended this method and used it to describe the growth
and dissolution of a sphere with finite initial size.
Later Duda and Vrentas (1969,1971) presented new results
using finite difference solutions and found that previous
methods using perturbation solutions have only limited
validity. In general the finite difference method predicts
faster growth and dissolution rates. Ruckenstein and
Davies (1970) solved the convective diffusion equation for
radial and translational convection for small Reynolds
numbers and potential flow and concluded that, in various
regimes, both convection terms have a significant effect
on the bubble dissolution or growth rate. They also found
that, if surface active material is present, transport by
translational convection is reduced. This reduction may
be a result of the fact that the surface layer at the
bubble boundary is immobile because the liquid driven
surface tension gradient off-sets the translational liquid
flow (Van 't Riet et al (1984)). Tao (1978,1979) described
growth and dissolution of a bubble in a supersaturated or
undersaturated liquid. The influence of the surface
tension as a driving force is included into the model,
that is based on the solution if infinite series of error
integral functions. Vrentas and Vrentas (1982) evaluated
the model presented by Tao and concluded that it gives
good results for systems with a low density difference
between the continuous and the dispersed phase *i.e.* for
gas-liquid systems the model is less suitable than for
liquid-liquid systems.

Both model calculations and experimental evidence of bubble dissolution were presented by Ward and coworkers. Ward and Tucker (1975) were the first to describe the dissolution and growth of bubbles containing more than one diffusing gas, taking into account the vapor pressure in the bubble and the gas expansion effect, that is a result of the surface tension and the curvature of the bubble surface. Ward et al (1982[a,b]) extended their theory using a first order perturbation analysis of the Schrödinger equation and the Boltzmann definition of entropy and concluded that the diffusion of the gas in the liquid is rate determining, and not the transition of gas at the bubble boundary. Ward et al (1982[c]) calculated the value of two possible stable equilibrium bubble sizes for a bubble in a closed volume of liquid. One unstable critical radius is the result of an equilibrium between the amount of supersaturation of the gas in the liquid and the Laplace pressure inside the bubble. If the bubble radius is larger than this critical radius the bubble will grow, and if the bubble radius is smaller than this critical radius the bubble will shrink. The other critical radius is stable and is a result of the closed volume of the system. Ward et al (1986) described a diffusion model taking into account non-equilibrium gas concentrations in the liquid and the vapor pressure in the bubble. He gave experimental evidence for the validity of this model using purified water for the bubble dissolution experiments. The effect of the surface tension close to equilibrium saturation was repeated by Cable and Frade (1988) who stated that low concentrations of impurities in molten glass may have a retarding influence on bubble dissolution by lowering the surface tension. Cable and Frade (1987) also stated that the presence of traces of poorly dissolving or slowly diffusing gases may have a paramount effect on the rate of bubble dissolution or growth. Also involved in bubble dissolution in glassmelts were Weinberg and coworkers. Zak and Weinberg (1980) proposed a model of multibubble dissolution but they assumed that the average distance between bubbles is large compared to the diameter of the

47

bubble and described the bubbles to be concentration point sources of gas. This theory can not be applied to foams because in foams the bubbles interfere with each other. Weinberg (1981) stated that the surface tension of the bubble is more important for the rate of bubble growth or dissolution than convective transport as long as the gas concentration in the liquid is close to the equilibrium value. He also stated that the rate limiting step for bubble dissolution is diffusion in the liquid rather than interfacial mass transfer. Subramanian and Weinberg (1980) studied the role of radial convective transport in more detail and found that it affects bubble dissolution only at sufficiently large values of the driving force. They concluded that convective transport may enhance the bubble dissolution rate. Subramanian and Weinberg (1981) used a short time asymptotic expansion analysis which is less accurate for long time spans. Weinberg et al (1980^{a,b}) and Onorato et al (1981) repeated the importance of incorporating the expansion effect in the bubble dissolution equations and stressed that a multigas system may have a dominant influence on the rate of dissolution or growth of a bubble. Most recently, Yung (1989) gave a review of papers on the dissolution of spheres in an infinite amount of liquid. He described a model using an finite difference method, that makes it easier to account for all sorts of parameters that other authors have neglected. The gas expansion effect, the influence of vapor pressure, the presence of more than one gas with different solubility, radial convection terms, and the surface tension are included in the model. An extensive comparison between the work of various other authors is made.

In some respects the description of the dissolution of a single bubble in an infinite amount of liquid is more complex than the description of gas diffusion in foams. However in other respects the description of gas transport in foams is much more complicated. Non equilibrium gas concentrations in the liquid will practically not occur in foams, because the concentration of the gas at the bubble boundary will be rapidly in equilibrium with the pressure

in the adjacent bubble and the film thickness in general is small. In addition, the radial convection problem does not exist in foams.

On the other hand, the geometry and topology of (polyhedral) bubbles in a foam is too complex to be solved, whereas the geometry of a dissolving sphere is relatively elementary. The size and gas composition of surrounding bubbles determine the gas concentration differences in a very complex way. The diffusion distance varies with time and location. The dimensions of Plateau borders are entirely different from the dimensions of films and the decrease of the film thickness between bubbles with time can only be estimated. Therefore the diffusion distance is not well known.

In spite of these difficulties research work on disproportionation and gas transport in foams has been reported in the last decades. Dewar (1917) was one of the first to describe the rate of air diffusion through soap films. Another attempt to describe the rate of disproportionation was made by Clark and Blackman (1948). They proposed a simple model to describe the growing and shrinking rate of bubbles in a foam having respectively a larger and a smaller radius than the mean bubble radius. They also calculated the decrease of the specific surface area of a foam over a period of time, caused by disproportionation.

Brown et al. (1953) developed another model describing the bubble radius as a function of time. They emphasized that theory and experiment do not always have to coincide, because theory does not include the permeability of the adsorbed surface film, nor high surface viscosity slowing down the evolution of the bubble. The effect of surface viscosity on gas transport in polyurethane foams was repeated by Owen and Kendrick (1968). Princen (1963,1965) improved the theory presented by Brown et al (1953), incorporating the exact shape of a bubble situated at a liquid-gas interface, the film thickness and changing gas composition. Princen (1965) also stresses that the permeability of monolayers on both sides of the film plays an important role in the rate of transport, but later Princen

et al (1967) gave evidence that transport of gases through soluble monolayers is governed by simple Fickean diffusion (Princen (1967)), that can be described as diffusion through pores in an otherwise insoluble layer.

Several other models have been proposed to describe the rate of disproportionation in foams, among which are the LSW theory and the De Vries model. The LSW theory, named after Lifshitz, Slyozov (1961) and Wagner (1951), predicts that the mean bubble radius in a foam will decrease as the third root of time. The De Vries model (1958,1972) is based on Fickean diffusion and predicts that the decrease of the radius of a shrinking bubble is proportional to the square root of time, according to the following equation:

$$r_o^2 - r_t^2 = \frac{4RT\mathbb{D}S\sigma}{P_{atm}\theta} t \qquad [5.2]$$

where t is time, r_o is the bubble radius at t=0, r_t is the bubble radius at t=t, R is the gas constant, T is the absolute temperature, $\mathbb{D}$ is the diffusion coefficient, S is the gas solubility, σ is the surface tension, P_{atm} is the atmospheric pressure and θ is the film thickness between the bubbles. The model was used to estimate the mean film thickness in foams but gave erroneous results as discussed by the author.

Gal-or and Hoelscher (1966) calculated unsteady-state mass transfer in dispersions with a Maxwell-Boltzman like model and included the effect of the bubble-size distribution. They were able to calculate the diffusion rate per unit area of interface.

This work was later reviewed by Lemlich and coworkers. Ranadive and Lemlich (1979) emphasized the important effect of the initial bubble-size distribution on disproportionation and compared the results obtained with the empirical distribution of De Vries and the theoretical distribution of Gal-or. They found that the empirical distribution of De Vries gives the best results. The

important effect of the initial size distributions in foams was repeated by Monsalve and Schechter (1984) and by Cheng and Lemlich (1985). The combined effort of Lemlich and coworkers finely resulted in the development of an apparatus to determine the permeability of thin liquid films by following the evolution of the bubble-size distribution of a initially bimodal foam (Rieser and Lemlich (1988)). From the results they concluded that gas diffusion may be enhanced by convection in the liquid film between the bubbles. Cook and Tock (1974) and Haas and Tock (1975) also determined permeability parameters for several gases. They emphasized the important influence of the gas solubility on the migration rate of gases and used thin liquid surfactant films to purify gases based on their difference in solubility. Ramchandran et al (1981) evaluated gas permeation properties of N_2, O_2 and CO_2 through a monolayer of foam bubbles. They described that a monolayer of gas bubbles can be used to study gas diffusivities, but that problems may be encountered caused by the time-varying surface area of the foam bubbles. The work was reviewed by Markworth (1985) who comments on Ostwald ripening and grain growth in foams and gives a short review on earlier studies. Narsimhan and Ruckenstein (1986) used a foam stability model not only covering gas transport, but also the size distribution of bubbles, film rupture and drainage of liquid films and Plateau borders, in order to be able to describe foam behavior in foam fractionation experiments.

Yet another approach to study gas transport in foams was mentioned recently by Stavans and Glazier (1989). They applied Von Neumans law to describe the rate of disproportionation in a two-dimensional foam. Von Neumans law states that the decrease of the total surface area of a bubble is proportional to the number of sides of the bubble minus 6. This means that bubbles with six sides are stable, bubbles with more sides than 6 grow and bubbles with less than 6 sides shrink and disappear.

5.2. Aim and Approach

Discrepancy between the presented models is clear and none of the models is completely satisfactory owing to assumptions made in the course of derivation. Also, in general, the models can be applied to model systems only. For practical multicomponent systems the models are inexact, mostly overestimating the rate of gas transport.

A number of investigators have suggested explanations for the overestimation of the gas transport rate, among which are: (i) low gas-permeability of insoluble or soluble layers at the film surfaces, (ii) changes in gas composition, caused by a different solubility of the gas components, (iii) non equilibrium gas concentration at the bubble boundary, (iv) simplification of the topology of the bubble, including shape, effective surface area of the bubble and (the evolution of) the film thickness, (v) the neglect of the vapor pressure of the liquid solvent, (vi) the formation of a structure at the bubble surface, (vii) the influence of convection of the film liquid caused by liquid drainage and (viii) high surface viscosity.

The statement that most existing models overestimate the rate of gas transport is also supported by simple observation of bubbles situated at a liquid surface. The observed radius-versus-time curves do not always have the shape of a more or less second or third power dependence as suggested by some authors. Instead, these curves may show an inflection point. This inflection point indicates that transport of gas from a bubble can decelerate.

A high surface viscosity may be responsible for this decrease of the rate of disproportionation because the compression of the bubble surface during the shrinking process in a surfactant solution results, in principle, in a lowering of the surface tension and thus in a decrease of driving force. Another reason for the appearance of an inflection point is the possible presence of more than one gas with different solubilities.

To study the effect on bubble dissolution of the surface dilational viscosity and of the gas composition, a model

52

was developed and experiments were carried out. The radius of bubbles, resting at a beer-gas interface, was measured as a function of time. Gasses of different solubility and beers with different surface dilational viscosities were used. The surface dilational viscosity of beers was measured with a Langmuir trough.

5.3. Theory

Here a new model is presented to give insight in the role of the surface viscosity and the role of changing gas composition in the rate of gas transport in foams. Several assumptions had to be made in the course of the derivation of the model. The local equilibrium supposition was made meaning that the gas concentration at the bubble boundary is supposed to be equal to the equilibrium value during the shrinking process of the bubble. The vapor pressure of the solvent was neglected. Ward et al. (1986) clearly described in which situations and circumstances these assumptions may lead to erroneous results. In the examples given here the vapor pressure is small compared to the total pressure in the bubble and the liquid films are so thin that the local equilibrium supposition can be made. Therefore, these assumptions have minor effect on the outcome of the experiments.

Also postulated is that the presence of an adsorbed monolayer does not form a barrier for gas transport (Princen (1967)) and that the diffusion in the liquid is the rate determining step for gas transport through a liquid film and not the transition rate of the gas from the bubble into the liquid surface. (Ward (1982[b])). If convection does not take place, transport of gases through the liquid layer is a diffusion controlled process that can be described with Ficks law:

$$- \frac{dn_{tot}}{dt} = D\,A\,\frac{\delta c}{\delta z} \qquad [5.3]$$

In *Eq.* [5.3], n_{tot} is the total amount of gas, A is the total area, c is the activity of the gas, and z is the distance over which diffusion takes place. Now, the presence of more than one gas is incorporated into the model. Assuming that gases behave thermodynamically ideal and that gases are distributed homogeneously throughout the bubble, Ficks law may be applied to each gas (i) in the system:

$$-\frac{dn_i}{dt} = D_i A \frac{\delta c_i}{\delta z} \qquad [5.4]$$

For thin films the concentration gradient over the film will be almost linear. In analogy to De Vries (1958) $\delta c/\delta z$ can be written as $\Delta c_i/\vartheta$, where ϑ is a topology factor. The value of ϑ depends on the position of the bubble. In general, five situations can be distinguished: (i) the bubble is surrounded by other bubbles in a foam, (ii) two bubbles are separated by a film and surrounded by an infinite amount of liquid, (iii) the bubble is completely surrounded by an infinite amount of liquid, (iv) one bubble rests at a liquid-gas interface and (v) the bubble is completely surrounded by gas, only separated from the surrounding atmosphere by a thin liquid film. For all these situations a different interpretation for ϑ must be made. ϑ therefore is an adjustable parameter. For the sake of clarity from now on situation (iv) is discussed. The atmosphere above the liquid is regarded as an infinite large bubble, in which the Laplace pressure is zero. The situation can thus be described as a two bubble system. The ϑ in this system accounts for the film thickness of the cap of the bubble, *i.e.* the liquid film between the submerged bubble and the surrounding atmosphere. ϑ is also a correction parameter for the effective diffusion area. *Eq.* [5.4] becomes:

$$- \frac{dn_i}{dt} = D_i \frac{A}{\vartheta} \Delta C_i \qquad [5.5]$$

With the aid of Henry's law, this last equation can be written as:

$$- \frac{dn_i}{dt} = D_i S_i \frac{A}{\vartheta} \Delta P_i \qquad [5.6]$$

In $Eq.$ [5.6] S_i is the solubility of gas i, and ΔP_i is the partial pressure difference of gas i across the film. The value of ΔP_i depends on the Laplace pressure, the atmospheric pressure (P_{atm}), and the gas composition in the bubble and in the atmosphere above the liquid. The gas composition in the atmosphere will practically remain constant during the diffusion proces. Therefore, ΔP_i can be written as:

$$\Delta P_i = (P_{atm} + 2\sigma/r)(n_i/n_{tot}) - k_i P_{atm} \qquad [5.7]$$

where the fraction of gas i in the atmosphere is k_i. Although the Laplace pressure ($2\sigma/r$) is small compared to the atmospheric pressure (P_{atm}), it can not be neglected in $Eq.$ [5.7]. If the gas composition in- and outside the bubble is equal ($i.e.$ $n_i/n_{tot} = k_i$) the Laplace pressure is the only driving force for gas diffusion. Substitution of $Eq.$ [5.7] in $Eq.$ [5.6], and $4\pi r^2$ for the total diffusion area (A) gives:

$$- \frac{dn_i}{dt} = \frac{D_i S_i 4\pi r^2}{\vartheta} [(P_{atm} + 2\sigma/r)(n_i/n_{tot}) - k_i P_{atm}] \qquad [5.8]$$

This equation describes the gas diffusion rate from a bubble situated at a liquid-gas interface to the atmosphere if the surface tension of the bubble is constant.

55

In an attempt to account for the rheological behavior of the bubble surface the model can be extended. To this end a mathematical expression is needed to describe the rheological behavior of the bubble surface. The shrinking of a spherical bubble surface is an all-sided compression where no shear occurs. To describe this surface behavior the surface dilational viscosity (η_s) can be used since this parameter is valid for compression as well as expansion *Eq.* [5.9]:

$$\eta_s = \frac{\sigma - \sigma_e}{d\ln A/dt} \qquad [5.9]$$

where σ_e is the equilibrium surface tension. The value of the relative surface deformation rate ($d\ln A/dt$) is then defined to be positive for expansion and negative for compression. From experimental results it follows that the surface dilational viscosity of a surfactant solution depends strongly on the value of $d\ln A/dt$. Higher compression rates result in lower surface viscosities. Surfaces are thus "shear thinning" (Prins (1976)).

The surface dilational viscosity can be determined using a Langmuir trough equipped with barriers which can be moved by means of a caterpillar belt as described by Prins (1986). Results from earlier experiments have shown that for practical systems such as milk and beer a powerlaw can be used to describe the surface rheological behavior in compression (Prins (1988)):

$$\sigma = \sigma_e - 10^n(\,|d\ln A/dt|\,)^{m+1} \qquad [5.10]$$

The absolute value of the surface dilational viscosity depends strongly on the value of n. The shear thinning behavior of the surface is mainly characterized by m. The disproportionation model can now be adjusted for dynamic surface properties with the aid of *Eq.* [5.9] and [5.10].

The ideal-gas equation of state of Boyle and Gay-Lussac is used to describe the total amount of gas in the bubble in relation to the bubble radius:

$$n_{tot} = \frac{(P_{atm}+(2\sigma/r))(\frac{4}{3}\pi r^3)}{RT} \qquad [5.11]$$

During the derivation of the model, the atmospheric pressure and the Laplace pressure of *Eq.* [5.11] go hand in hand. The Laplace pressure is small compared to the atmospheric pressure and can therefore be neglected in *Eq.* [5.11]. The neglect of the expansion effect is also discussed by Yung (1989).

Eq. [5.8], for different gases, combined with *Eq.* [5.9] and [5.10] and the law of Boyle and Gay-Lussac *Eq.* [5.11], can be numerically solved by an appropriate computer technique in order to obtain radius-versus-time curves and the prevailing circumstances for shrinking bubbles under different conditions.

5.4. Experimental

The solution of *Eq.* [5.8], [5.9], [5.10] and [5.11] was carried out on a VAX 8600 computer using Fortran as a programming language and standard IMSL routines to perform numerical integration. The numerical integration gives the radius, gas composition, compression rate, and the surface tension as a function of time for given values of m, n, r_o, σ_e, ϑ, gas composition etc.

A Langmuir trough equipped with a caterpillar belt was used to determine the surface viscosity and the powerlaw parameters m and n of *Eq.* [5.10]. The trough is shown in figure 4.7. Surface tensions are simultaneously measured in the expanded and compressed area with the Wilhelmy plate technique. The relative compression rate (dlnA/dt) was varied over three decades from 5×10^{-1} to 5×10^{-4} s^{-1}.

In addition to surface rheological experiments with the caterpillar belt, single compression measurements were carried out. With a single barrier a surface area of 450 cm^2 was compressed to a surface of 90 cm^2 using different speeds. The experiment was carried out to simulate the

compression of the bubble surface as good as possible and
to examine whether the predicted low surface tensions
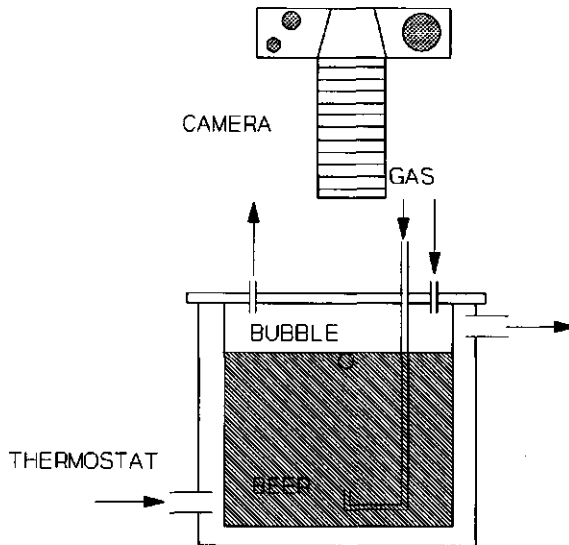could be measured. (figure 4.6).

Figure 5.1: Apparatus to measure the bubble radius as a function of time.

Bubble radius-versus-time curves were determined with
the apparatus shown in figure 5.1. With a syringe needle
bubbles (radius = ±500 μm) were produced in a temperature
controlled vessel. The size of the bubble situated at the
liquid surface is measured as a function of time with a
macroscope unit and a camera. Gas conditions in the
atmosphere above the bubble is controlled using constant
flow of the desired gas, saturated with water vapor. The
temperature was maintained at 20°C.

The surface rheological experiments were carried out
with eight different beers (beer A to H). To measure the
bubble radius with time beer E, G and H were used.

5.5. Results

In order to be able to determine whether the observed
deceleration of the bubble dissolution and the occurrence

of an inflection point in the radius-versus-time curve is caused by changes in gas composition or by surface rheological properties, model calculations were carried out with several different gas compositions and surface dilational viscosities.
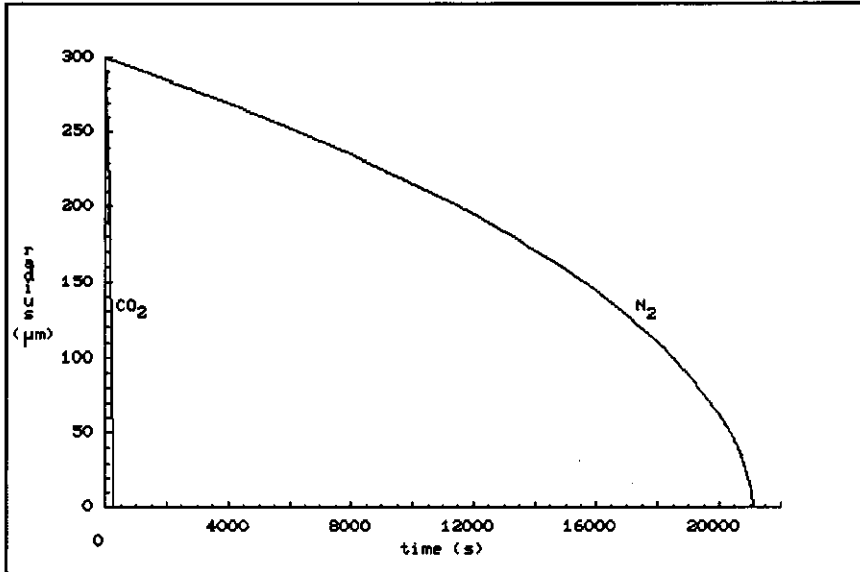

Figure 5.2: The influence of gas solubility on the bubble dissolution rate.

Figure 5.2 shows the large effect of the gas solubility on the bubble dissolution rate of a bubble, situated at a gas-liquid interface. The solubility of carbon dioxide in water is about 50 times higher than the solubility of nitrogen. The initial bubble radius is 300 μm and the topology factor ϑ=10 μm. The equilibrium surface tension is 40 mNm^{-1}. The gas above the liquid surface is identical to the gas in the bubble. Surface viscosity has little effect on both bubbles since the values of m=-0.9 and n=-1.9 express very low surface viscosity. A carbon dioxide bubble, situated at a liquid surface under a carbon dioxide atmosphere, disappears much quicker than a nitrogen bubble under a nitrogen atmosphere. The gas solubility clearly is a very important parameter for gas diffusion processes.
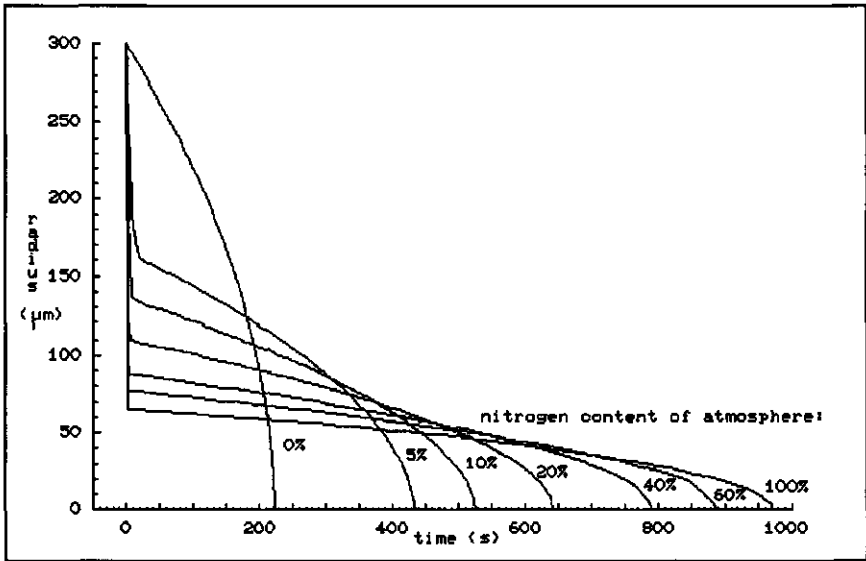
Figure 5.3: The influence of the gas composition in the atmosphere on the radius of a carbon dioxide bubble.

Figure 5.3 illustrates the effect of two gases with different solubility in the surrounding atmosphere on the disproportionation behavior of carbon dioxide bubbles having an initial radius of 300 μm. The viscosity of the bubble surface is very low and does not influence the shrinking rate of the bubble. If nitrogen is introduced into the atmosphere above the carbon dioxide bubble, the shape of the radius-versus-time curve changes dramatically. The driving force in this case is not only the Laplace pressure, but also a difference in partial gas pressure. Carbon dioxide diffuses outward rapidly, because the partial carbon dioxide pressure in the atmosphere is lower than in the bubble. Nitrogen diffuses inward because the partial nitrogen pressure in the atmosphere is higher than in the bubble. The diffusion rate of nitrogen however is much lower than the diffusion rate of carbon dioxide because the solubility of nitrogen is much lower. Therefore, initially the bubble shrinks rapidly until the gas compositions inside and outside the bubble are practically equal. Then, the gas diffusion rate decreases abruptly, and the Laplace pressure becomes the only driving force.
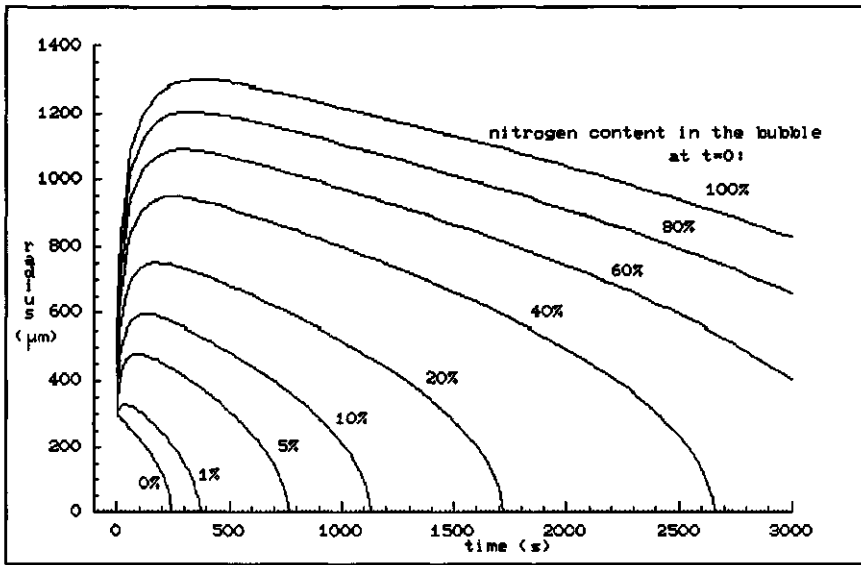
60

Figure 5.4: Behavior of N_2/CO_2 bubbles with low surface viscosity under a CO_2 atmosphere.

To further emphasize that the gas composition inside and outside the bubble is an important parameter for the rate of gas diffusion, figure 5.4 shows a radius-time diagram for a bubble containing varying percentages of carbon dioxide and nitrogen. The atmosphere contains 100% carbon dioxide. The bubble has low surface dilational viscosity.

If a bubble contains nitrogen it starts to grow against the Laplace pressure because diffusion of carbon dioxide inward proceeds much faster than diffusion of nitrogen outward. (The values of m and n of the powerlaw were adjusted for expansion in order to describe the surface rheological behavior of the expanding bubble surface). This process continues until again the gas compositions in- and outside the bubble are equal. Then, the Laplace pressure remains as the driving force of gas diffusion and the bubble starts to shrink.

To illustrate the role of the surface viscosity in gas diffusion, examples are given in figure 5.5 of results of calculations on carbon dioxide bubbles situated at a liquid surface. The gas phase above the liquid surface is also carbon dioxide. The initial bubble radius was 300 µm. The surface dilational viscosity is characterized by

61

m=-0.9 and the value for n varies between -1.9 and -1.15. The equilibrium surface tension was chosen 40 mNm^{-1}.
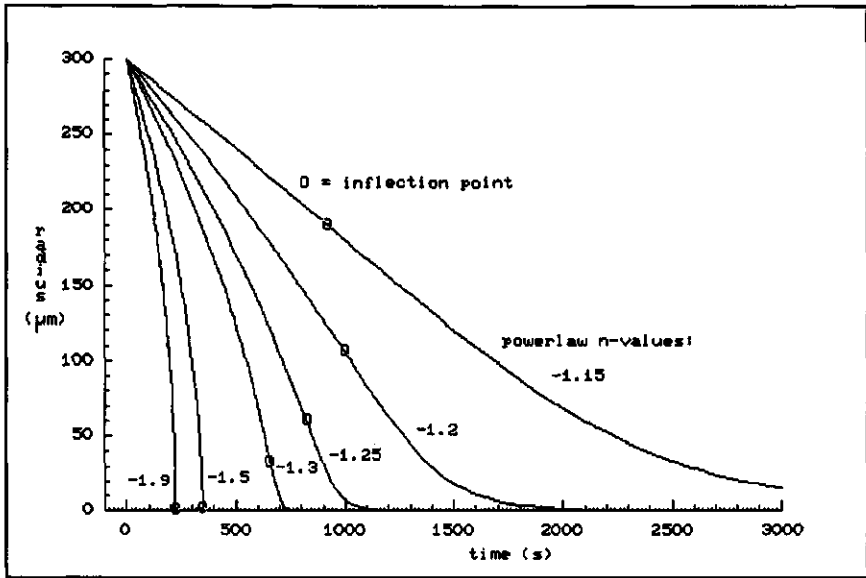
Figure 5.5: Calculated radius versus time curves of carbon dioxide bubbles situated at a liquid–carbon dioxide interface. The bubbles have different surface dilational viscosities.

Table 5.1: Surface dilational viscosities for given values of n. m=-0.9, $dlnA/dt=10^{-3}$ s^{-1}.

n	σ	η_s
	(mNm^{-1})	$(mNsm^{-1})$
-1.9	33.7	$6.3\times10^{+3}$
-1.5	24.2	$1.6\times10^{+4}$
-1.3	14.9	$2.5\times10^{+4}$
-1.25	11.8	$2.8\times10^{+4}$
-1.2	8.4	$3.2\times10^{+4}$
-1.15	4.5	$3.6\times10^{+4}$

In table 5.1 values of the surface tension and surface dilational viscosity at $dlnA/dt=10^{-3}$ s^{-1} are given for different values of n, illustrating that higher values of n represent higher surface dilational viscosities. The value n=-1.9 is quite common for a low concentration protein solution with surfaces of low viscosity. As can be seen in figure 5.5, the shape of the radius-versus-time

curve is about the same as found by De Vries (1958,1972)
for surfaces with low surface dilational viscosity (n=-1.9
and n=-1.5). He assumed that the surface tension remains
constant during the shrinking process of the bubble.
Results given in figure 5.6 show that, for n=-1.9, the
surface tension of the bubble has normal values for
compressed surfaces (25-30 mNm^{-1}) at realistic bubble
sizes.
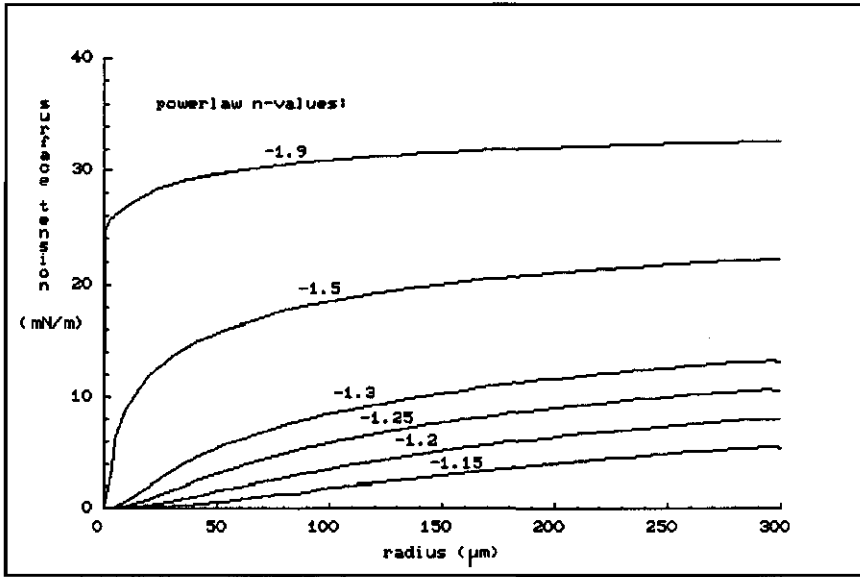
Figure 5.6: Surface tension against radius plot of the bubbles presented in figure 5.5.

However, when the surface dilational viscosity is
increased (by means of increasing the value of n), the
surface tension and the dissolution rate decrease. In
figure 5.5, where the radius is plotted against time, an
inflection point is found for bubbles of considerable
size. The surface conditions at the inflection point are
of great interest because at the inflection point dispro-
portionation starts to slow down as shown in table 5.2.

From these data it appears that for n varying from -1.9
to -1.15 the value for the radius at the inflection point
(r_i) increases by 4 orders of magnitude. For n=-1.9 and
n=-1.5 r_i is so small and the surface deformation rate
(dlnA/dt)$_i$ is so high that there is little effect on the
life-span of the bubble.

Table 5.2: Conditions at the inflection point, $m=-0.9$.

n	r_i	$(d\ln A/dt)_i$	σ_i	$(\eta_s)_i$
	(μm)	(s^{-1})	(mNm^{-1})	(mNsm^{-1})
-1.9	0.03	$4.0\times10^{+4}$	3.6	9.0×10^{-4}
-1.5	3.4	$4.0\times10^{+0}$	3.6	$9.0\times10^{+0}$
-1.3	34.1	4.0×10^{-2}	3.6	$9.0\times10^{+2}$
-1.25	60.6	1.3×10^{-2}	3.6	$2.8\times10^{+3}$
-1.2	107.8	4.0×10^{-3}	3.6	$9.0\times10^{+3}$
-1.15	191.8	1.3×10^{-3}	3.6	$2.8\times10^{+4}$

For higher values of n the bubble dissolution rate clearly starts to slow down: $(d\ln A/dt)_i$ decreases by 8 orders of magnitude. Because the surface tension at the inflection point (σ_i) is constant for all values of n the surface dilational viscosity at the inflection point $(\eta_s)_i$ increases by 8 orders of magnitude. The surface tension at the inflection point only depends on the values of m and σ_e and is independent of the value of n, as can be seen in *Eq.* [5.12]:

$$\sigma_i = \sigma_e \frac{m+1}{m+2} \qquad [5.12]$$

Although the compression rate decelerates for higher surface dilational viscosities, very low surface tensions are found. These low surface tensions have not yet been measured in practical systems. The possible occurrence of very low surface tensions however was described earlier by Van den Tempel et al. (1983) and by Boyle III (1982).

What happens to the shape of the radius-versus-time curve if two gases of different solubility are present and surface viscosity is high, is shown in figure 5.7, where the gas composition in the bubble is chosen 100% carbon dioxide and in the atmosphere 60% carbon dioxide and 40% nitrogen. The viscosity of the bubble surface was altered by varying n between -1.9 and -1.1. If the gas composition of the atmosphere and of the bubble are not equal the bubble very rapidly shrinks. Under these conditions the

64
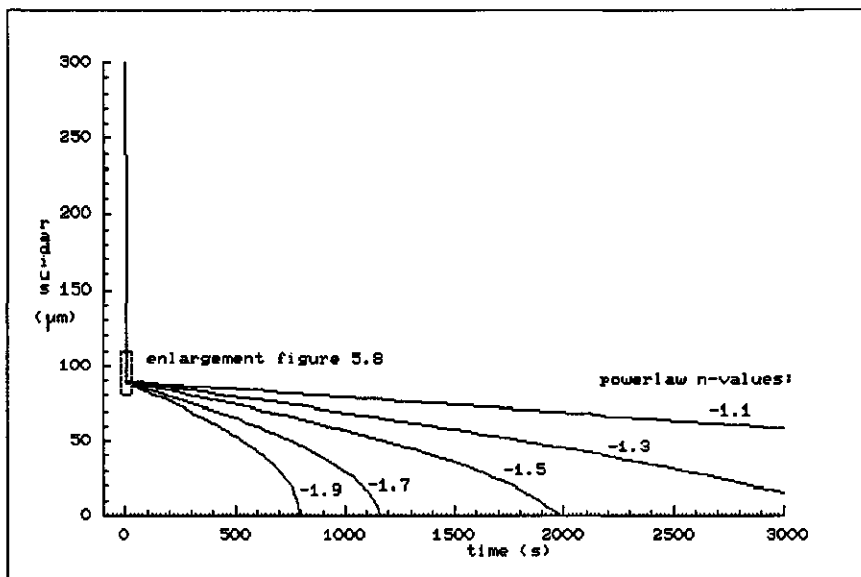
Figure 5.7: Influence of the surface dilational viscosity on gas diffusion of a CO_2-bubble under a 60% CO_2 and 40% N_2 atmosphere.
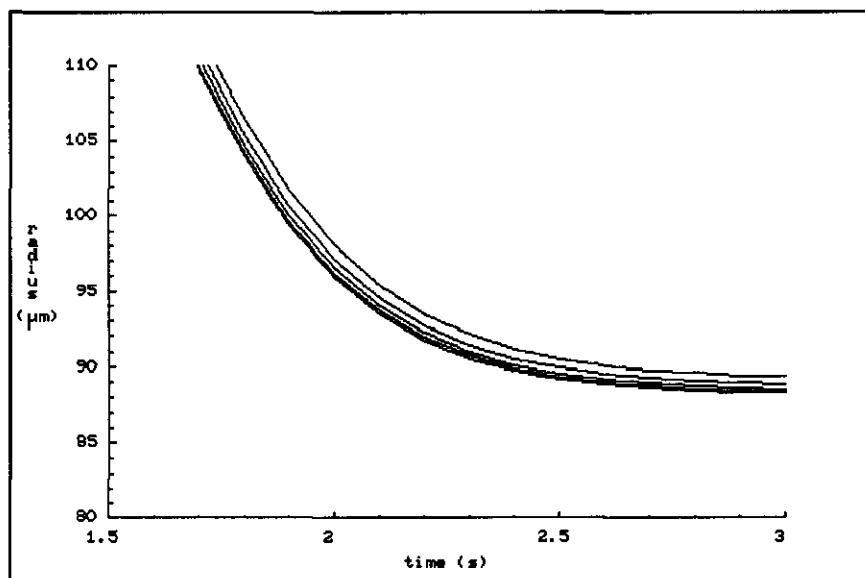
Figure 5.8: Enlargement of the inflection point of figure 5.7, showing that surface viscosity has little effect on gas diffusion when the gas composition in- and outside the bubble is unequal.

surface rheological aspects do not play an important role in gas diffusion as shown in figure 5.8, where an enlargement is displayed of figure 5.7 of the area where the rapid decrease in bubble radius changes abruptly into a

65

much slower decrease. That is roughly speaking when the bubble within a very short period shrinks from about 110 μm to about 90 μm. From figure 5.8 it appears that in this transition zone the behavior of the bubble radius does not very much depend on the surface viscosity. When the gas composition in- and outside the bubble has become equal the Laplace pressure becomes the driving force for gas diffusion and therefore the rheological behavior of the bubble surface determines the bubble shrinking rate. At longer times, the surface viscosity plays a very important role in the decrease of the bubble size as can be seen in figure 5.7.
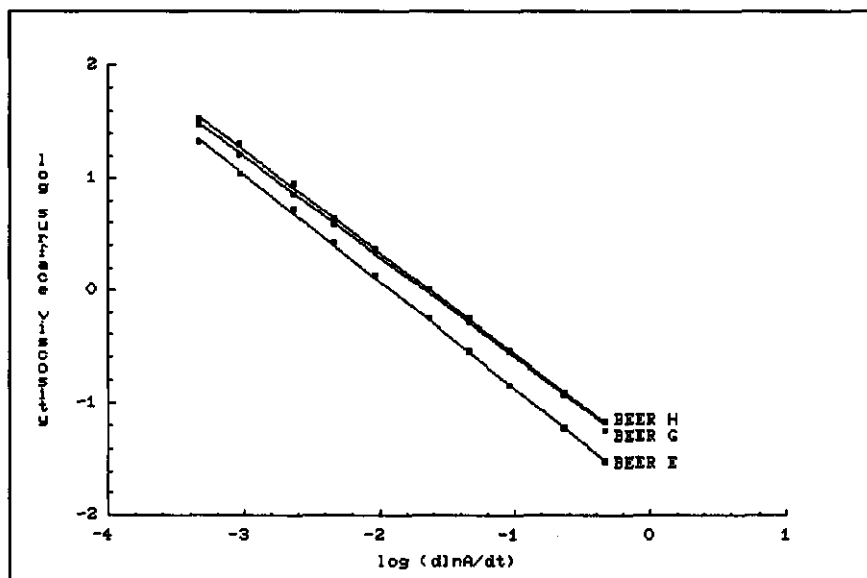

Figure 5.9: Surface rheological behavior in compression of beer E, G, and H, determined with a Langmuir trough equipped with a caterpillar belt, plotted as a powerlaw.

Figure 5.9 shows the results of the caterpillar belt experiments carried out for three different beers. Over the three decades measured, the powerlaw adequately describes the dependency of the surface viscosity on the compression rate. Beer E has a clearly lower viscosity than beer G and H as can also be seen in table 5.3 where the powerlaw values of m and n are given for all beers.

66

Table 5.3: Powerlaw m and n values for the eight different beers as measured with the caterpillar belt method.

Beer	m	n
A	−0.97	−1.74
B	−0.96	−1.80
C	−0.99	−1.81
D	−0.95	−1.74
E	−0.96	−1.78
F	−0.97	−1.73
G	−0.90	−1.50
H	−0.91	−1.48
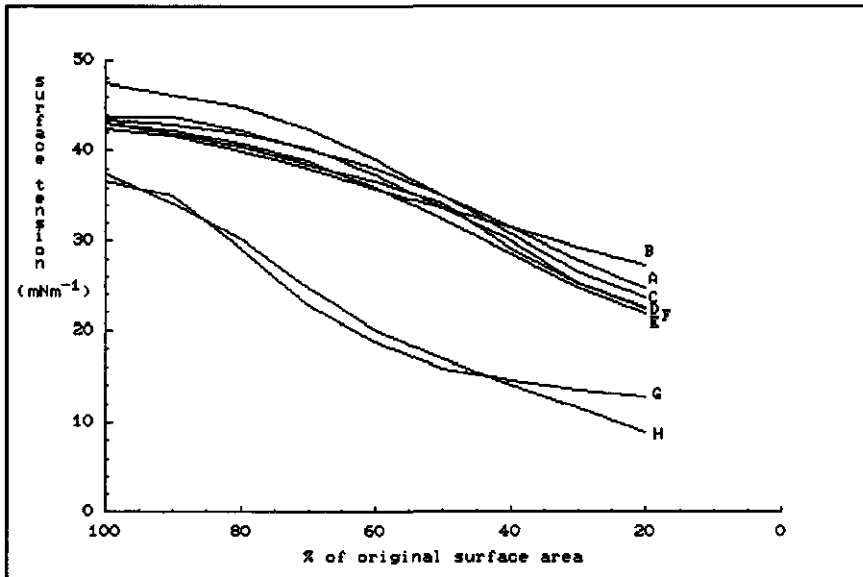
Figure 5.10: The dynamic surface tension of different beers as a function of compression. The original surface area of 450 cm^2 is compressed to 90 cm^2 in 4.5 s.

Differences between the surface rheological behavior of the different beers become even more pronounced with the single compression experiment as shown in figure 5.10. The surface tension of beer G and H becomes very low in compression. The surface tension of beer H, after compression until 20% of the original surface area, is as low as 8.8 mNm^{-1}. This indicates that the surface tension of a

67

shrinking bubble in this beer sample may also become very low in compression.

In figure 5.11 the shrinking rate of a carbon dioxide bubble, situated at a beer surface under a carbon dioxide atmosphere is displayed. The shape of the curve for beer E is similar to the shape of curves found earlier by De Vries. The radius-versus-time curve shows approximately a square root dependency. This observation is in agreement with the expectations, because beer E has a low surface viscosity and only one gas, carbon dioxide, was present. The observed radius-versus-time curve can be well fitted with the model as shown in figure 5.11. The value for ϑ, used to fit the observed radius-versus-time curve was 10 µm, which is of the expected order of magnitude.
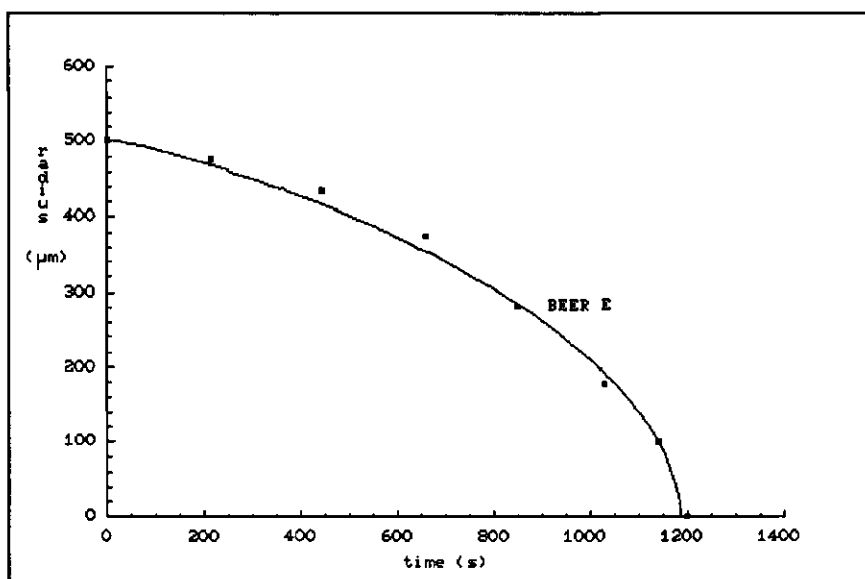
Figure 5.11: Radius versus time curves for a carbon dioxide bubble at a beer–carbon dioxide atmosphere. The beer has low surface viscosity. ▮ measured values, – model calculations.

The disproportionation rate of a carbon dioxide bubble under a nitrogen atmosphere instead of a carbon dioxide atmosphere is shown in figure 5.12. The calculated radius-versus-time curve can be well fitted on the measured values with ϑ=35 µm. As a consequence of a higher carbon

dioxide gradient over the film between the bubble and the surrounding atmosphere the diffusion of carbon dioxide from the bubble outward is accelerated. At the same time nitrogen diffuses into the bubble because there is a nitrogen gradient over the film as well, only inward. The diffusion of nitrogen however goes much slower, because the solubility of nitrogen is much lower than the solubility of carbon dioxide. The result is that the bubble initially shrinks rapidly, until the gas composition in- and outside the bubble has become equal.
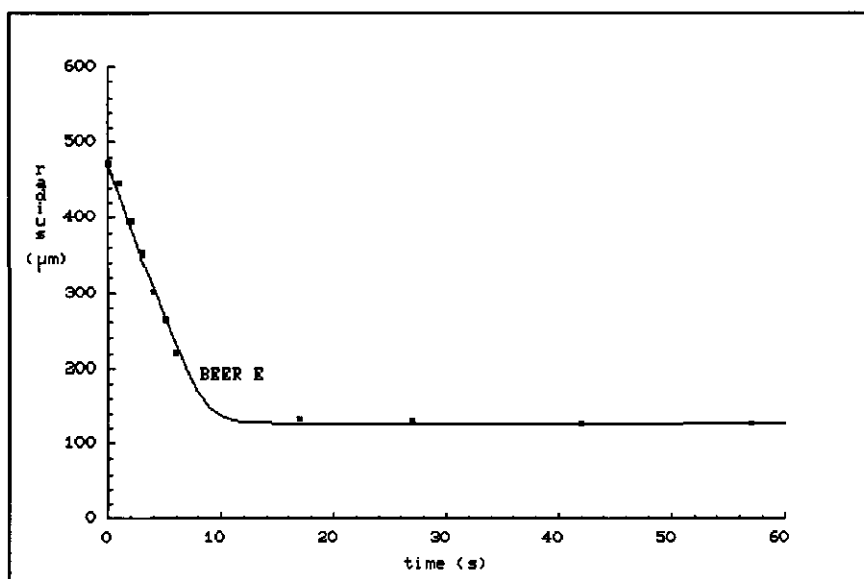
Figure 5.12: Radius versus time curve for a carbon dioxide bubble situated at a beer–nitrogen interface. The beer has low surface viscosity. ∎ measured values, – model calculations.

In the case, given in figure 5.12, the bubble, that initially contained carbon dioxide, within about 10 seconds contains only nitrogen. Thereafter, the bubble will very slowly disappear because the nitrogen gradient over the film depends on the solubility of nitrogen and on the Laplace pressure. After ca. 13×10^3 s, the bubble is completely dissolved according to computer calculations.

The bubble radius belonging to the plateau value in the radius-versus-time curve, that is reached after about 10 seconds, depends mainly on the gas composition of the

bubble and the atmosphere. This is elucidated in figure 5.13, where the initial nitrogen fraction in the bubble is plotted against the quotient of the volume of the bubble when the plateau value is reached (V_e) and the initial bubble volume (V_o). V_e/V_o is proportional to the initial nitrogen fraction in the bubble, giving evidence that, in effect, carbon dioxide diffuses outward and nitrogen diffuses inward and that the diffusion is driven by partial pressure differences.
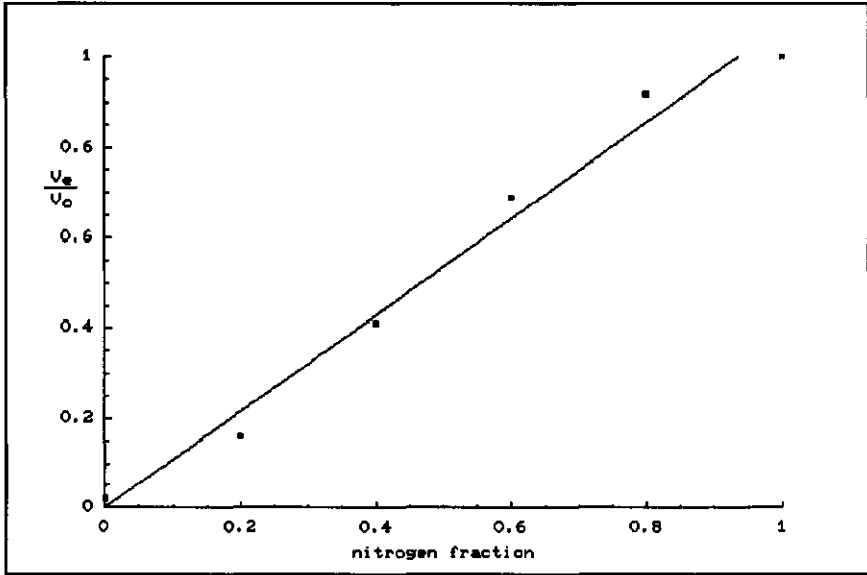
Figure 5.13: A plot of the quotient of the bubble volume at the plateau value and at t=0 plotted against the nitrogen fraction initially present in the bubble.

Table 5.4: Powerlaw n-values determined by model fitting and by the Langmuir trough with caterpillar belt method (m=−0.9).

method	beer E	beer G	beer H
model fitting	−1.95	−1.15	−1.10
caterpillar belt	−1.82	−1.50	−1.48

In figure 5.14 the effect of the surface viscosity on gas diffusion is displayed. A carbon dioxide bubble under a carbon dioxide atmosphere in beer E disappears in about

70

1200 seconds as displayed also in figure 5.11. A similar bubble in beer G however disappears much slower (ϑ=5 µm).
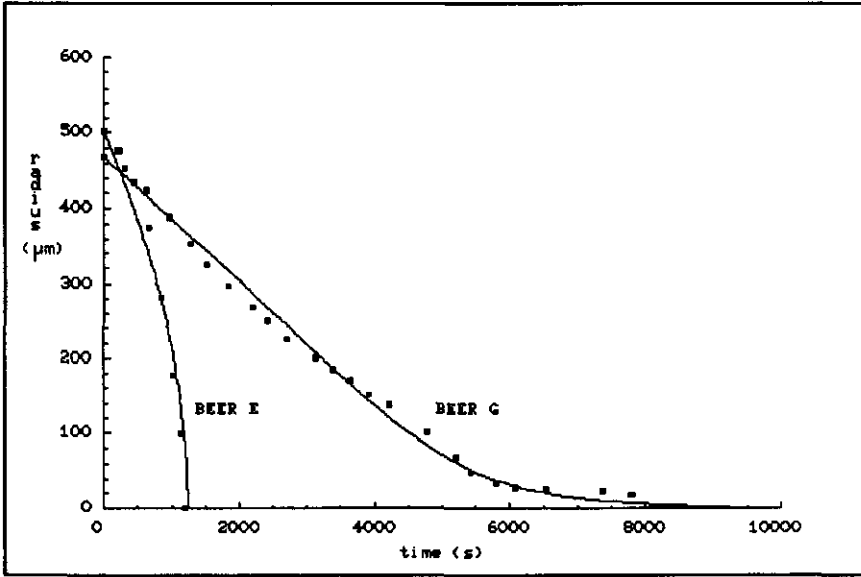
Figure 5.14: Radius versus time curves for carbon dioxide bubbles. Beer E has low surface viscosity and beer G has high surface viscosity. ∎ measured values, – model calculations.
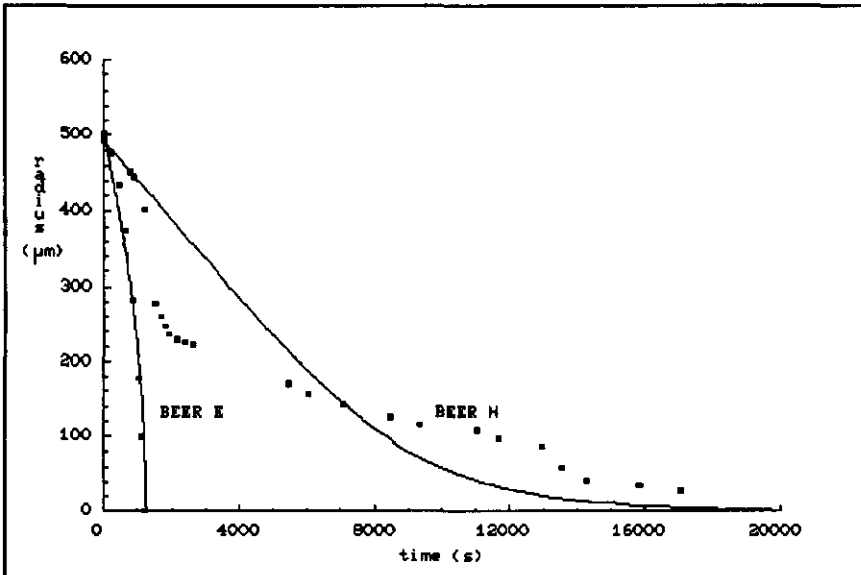
Figure 5.15: Radius versus time curves for carbon dioxide bubbles. Beer E has low surface viscosity and beer H has high surface viscosity. ∎ measured values, – model calculations.

The curve has an inflection point as predicted by the model for high surface viscosity. The shape of the curve changes from convex to concave. Both curves can be fitted with the model calculations, with different values for n as shown in table 5.4. The bubble in beer G shrinks much slower than the bubble in beer E, because the surface viscosity of beer G is higher than the surface viscosity of beer E. A similar plot is made for beer E and beer H as shown in figure 5.15. Here the observed shape of the curve for beer H is different from the shape of beer E and beer G. The observed shrinking rate of the bubble can not be fitted with the model, whatever values for m and n are chosen (ϑ=5 μm).
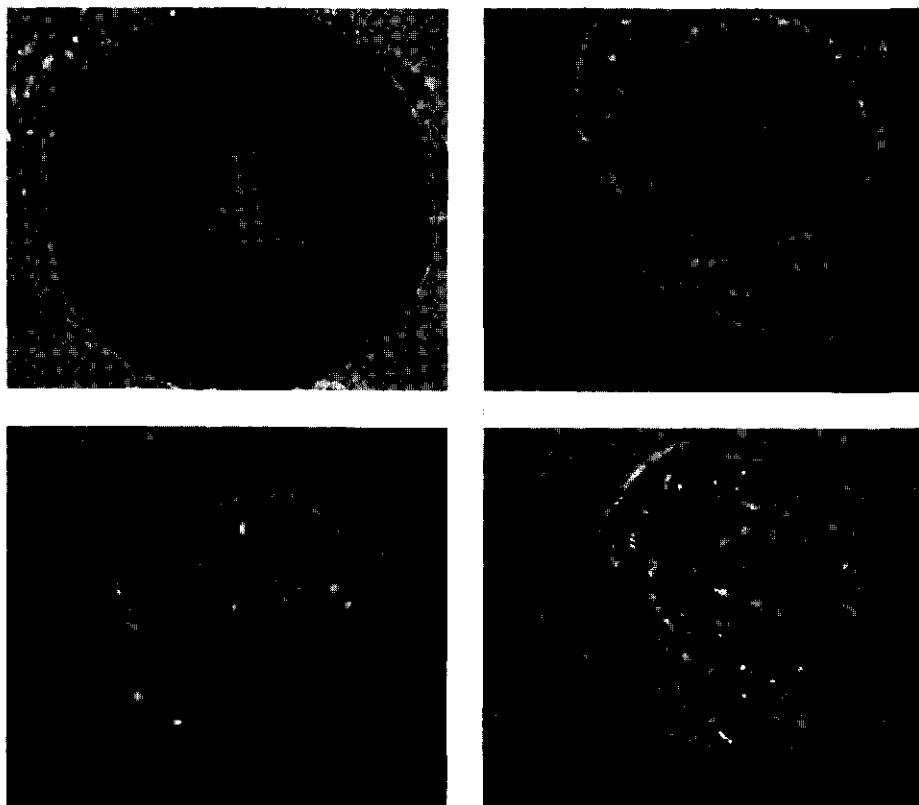
Figure 5.16: A series of photographs, taken at certain time intervals, representing the dissolution of a beer E bubble and the appearance of a bubble ghost. The size of the ghost is ±25 μm.

A possible explanation for this unusual behavior may be that some sort of insoluble skin formation occurs at the bubble surface as a consequence of surface compression. In figure 5.16 a series of photographs displays a shrinking bubble. It can be clearly seen that by compression an insoluble skin is formed at the bubble surface. The skin collapses and a bubble ghost appears. This structured bubble skin may decrease the driving force of gas trans-port. When however the bubble surface separates from the structured skin, gas diffusion may accelerate again and a new skin may be formed. The acceleration of gas diffusion at $t=13 \times 10^3$ s coincides with the first observation of a bubble ghost separated from the bubble surface. This kind of surface rheological behavior appears to be quite common in multicomponent systems (Sebba (1987)). Anderson and Brooker (1988) described the occurrence of bubble ghosts in milk and Johnson and Cooke (1980) have carried out bubble dissolution experiments in seawater and they have shown pictures of bubble ghosts very similar to the bubble ghosts found in beer.

5.6. Discussion

From the results presented in chapter 5.5, it has become evident that the differences in composition of a two phase system are most important for the disproportionation rate in that system. The rate of gas diffusion in foams depends mostly on a difference in partial gas pressures and gas solubilities. Differences in gas composition in- and outside bubbles result in rapid gas diffusion until gas composition in- and outside the bubbles becomes identical.

Under conditions of uniform gas composition the Laplace pressure difference is the only driving force for gas diffusion. This driving force may become very low when the surface tension decreases far enough as a result of the compression of the bubble surface. The surface tension of the bubble surface becomes very low when the surface

dilational viscosity is high. This may cause bubbles to persist much longer than expected from earlier models.

Even the presented model however may overestimate the rate of disproportionation because the powerlaw (*Eq.* 5.10) is not exactly describing the rheological behavior of the bubble surface. The powerlaw describes the surface rheological behavior of a surface under steady-state compression conditions and does neither account for the history of the bubble surface nor for the absolute value of compression. The single compression of a bubble surface is a transient phenomenon, where steady-state is never accomplished. In other words, not only the compression rate of the bubble surface is important, but also the total amount of compression. Generally, total compression of the surface of a shrinking bubble is high because the surface area of a bubble is proportional to the square of the radius. This may result in an even lower surface tension than expected from the caterpillar belt experiments. Thus, a lower Laplace pressure will prevail under practical conditions than was predicted by the powerlaw. These last considerations make it very likely that the disproportionation rate of bubbles depends very much on the rheological behavior of the bubble surface if the gas composition is uniform.

The rate of disproportionation is mainly determined by the geometry of the bubbles, the gas composition in the bubbles and the surface rheological aspects of the liquid.

The geometry parameter ϑ used to fit the measured radius-versus-time curves varies from 5 µm for fits over a longer period of time to 35 µm for fits over a short period of time. Apparently, ϑ is not constant as presumed in the model. During the experiment the film thickness of the bubble cap decreases more than the effective diffusion area. The total effect is that ϑ decreases with time. Nevertheless, it appears to be very well possible to fit observed curves with the model using an average ϑ.

The effect of the gas composition on the rate of dispro-portionation as found with model calculation, is confirmed experimentally. The gas solubility is very important for the rate of gas diffusion. When more than one gas of different solubility is present in a system, rapid gas diffusion will take place until the gas composition is equal throughout all gas compartments. This may have great influence on foam behavior and bubble-size distributions.

The effect, that surface rheological parameters may have on the rate of gas diffusion, is also confirmed experimen-tally. The Laplace pressure is the governing driving force for gas diffusion if the gas composition in- and outside the bubble is equal. Therefore gas diffusion from bubbles depends strongly on the surface tension of the bubble. During gas diffusion, the bubble shrinks and the surface is compressed. Consequently the surface tension decreases. The dynamic surface tension prevailing under compression conditions depends on the surface rheological properties of the bubble. Important parameters determining the dynamic surface tension of the bubble are the surface dilational viscosity, the compression rate of the surface, the history of the bubble surface and the absolute amount of compression. The three experimental methods, described in this chapter, induce different surface compression behavior, because the parameters mentioned above differ for each method.

The surface compression during the actual event of bubble dissolution is a transient phenomenon. The compres-sion rate varies with time while the absolute compression increases in an unpredictable way until the surface is completely compressed. Steady-state compression is not achieved. The history and total compression of the surface is important in addition to the compression rate. The deformation of the bubble surface is determined by the parameters of the system. *E.g.* high surface viscosity slows down the surface deformation rate. Unfortunately it is not possible to describe this transient phenomenon with mathematical formula, and therefore it is not possible to

derive a model that completely satisfactory describes the disproportionation behavior of bubbles in a foam.

The single compression experiment carried out in a Langmuir trough simulates the actual shrinking of the bubble surface. However the absolute compression and the compression rate are not equal in both situations. The absolute compression of a bubble surface, generally, is higher than the maximum absolute compression in the Langmuir trough. Respectively 100% and 80% of the original surface is compressed. Therefore, it may be speculated that the surface tension of the bubble becomes lower than can be measured in the Langmuir trough. In addition, the decrease of the surface tension depends strongly on the compression rate, because visco-elastic surfaces are time dependent as a consequence of relaxation processes. With the single compression experiment the barrier is moved linearly, and therefore dlnA/dt increases during the experiment.

In addition, the compression exerted to the surface in the Langmuir trough is not without shear, whereas the compression of the bubble surface is pure all-sided dilation. The shear forces might influence the results obtained with the Langmuir trough.

From a physical point of view the single compression experiment is a poorly defined experiment. A mathematical expression can not be given that describes the rheological behavior of visco-elastic surfaces on the basis of this experiment.

On the other hand, the caterpillar belt compression experiment is physically rather well defined. Although the dlnA/dt is not entirely constant during the experiment, because the barriers move linearly and because they are a certain distance apart, a stationary-state compression is accomplished. The surface dilational viscosity can be determined at various compression rates, and the powerlaw parameters m and n can be calculated. The experimental results, obtained with the caterpillar belt experiment, can be used to derive a diffusion model that includes

surface rheological aspects as has been proposed in chapter 5.3.

Taking these considerations into' account it is not surprising that the powerlaw parameters m and n found with the caterpillar belt experiment do not coincide with the parameters found with the dissolving bubble method and the model calculations as shown in table 5.4. The simple reason for this deviation may be that the powerlaw, although it rather well describes the rheological behavior of surfaces in the caterpillar belt experiment, does not accurately characterize the rheological behavior of the shrinking bubble surface. However, combining results from the bubble dissolution experiment and model calculations it has been made very clear that the surface tension of the shrinking bubble surface may become very low. In addition the formation of an insoluble skin may occur at the bubble surface caused by the compression of the bubble surface. It can be concluded that gas diffusion from bubbles may be very much inhibited by the surface rheological behavior of the bubble.

References

- Anderson, M., Brooker, B.E., "Dairy Foams." In: Advances in Food Emulsions and Foams. Ed: E. Dickinson, G. Stainsby, Elsevier Applied Science. pp. 221. (1988).
- Boyle III, J., Mautone, A.J., Colloids and Surfaces 4:77 (1982).
- Brown, A.G., Thuman, W.C., McBain, J.W., J. Colloid and Interface Sci. 8:508 (1953).
- Cable, M., Evans, D.J., J. Appl. Phys. 38:2899 (1967).
- Cable, M., Frade, J.R., Glastech. Ber. 60:355 (1987).
- Cable, M., Frade, J.R., Proc. R. Soc. Lond. A. 420:247 (1988).
- Cheng, H.C., Lemlich, R., Ind. Eng. Chem. Fundam. 24:44 (1985).
- Clark, N.O., Blackman, M., Trans. Farad. Soc. 44:1 (1948).
- Cook, R.L., Tock, R.W., Separation Sci. 9(3):185 (1974).

- De Vries, A.J., Receuil des Traveaux Chimiques des Pays-Bas **77**:209 and 283 (1958).
- De Vries, A.J., "Morphology, Coalescence and size distribution of foam bubbles" In: Adsorptive bubble separation techniques. Ed: R. Lemlich, Academic Press. New York, London. pp. 7. (1972).
- Dewar, I., Proc. R. Inst. Cr. Brit. **22**:179 (1917).
- Duda, J.A., Vrentas, J.S., AIChE J. **15**:351 (1969).
- Duda, J.A., Vrentas, J.S., Int. J. Mass Heat Transfer **14**(3):395 (1971).
- Epstein, P.S., Plesset, M.S., J. Chem. Phys. **46**:1505 (1950).
- Gal-or, B., Hoelscher, H.E., AIChE J. **12**(3):499 (1966).
- Haas, F.W., Tock, R.W., Separation Sci. **10**(6):723 (1975).
- Johnson, B.D., Cooke, R.C., Limnol. Oceanogr. **25**(4):653 (1980).
- Lifshitz, I.M., Slyozov, V.V., J.Phys. Chem. Solids **19**:35 (1961).
- Markworth, A.J., J. Colloid and Interface Sci. **107**(2):569 (1985).
- Monsalve, A., Schechter, R.S., J. Colloid and Interface Sci. **97**(2):327 (1984).
- Narsimhan, G., Ruckenstein, E., Langmuir **2**:494 (1986).
- Onorato, P.I.K., Weinberg, M.C., Uhlmann, D.R., J. Am. Ceram. Soc. **64**(11):676 (1981).
- Owen, M.J., Kendrick, T.C., J. Colloid and Interface Sci. **27**(1):46 (1968).
- Princen, H.M., J. Colloid Sci. **18**:178 (1963).
- Princen, H.M., Mason, S.G., J. Colloid and Interface Sci. **20**:353 (1965).
- Princen, H.M., Overbeek J.T.C., Mason, S.G., J. Colloid and Interface Sci. **24**:125 (1967).
- Prins, A., "Dynamic Surface Properties and Foaming Behavior of Aqueous Surfactant Solutions." In: Foams. Ed: R. J. Akers, Academic Press. London, New York. pp. 51. (1976).
- Prins, A., "Theory and Practice of Formation and Stability of Food Foams." In: Food emulsions and foams. Ed: E.

Dickinson, Royal Society of Chemistry. Leeds. pp. 30. (1986).

- Prins, A., "Principles of Foam Stability." In: Advances in Food Emulsions and Foams. Ed: E. Dickinson, G. Stainsby, Elsevier Applied Science. pp. 91. (1988).
- Ramchandran, N., Didwania, A.K., Sirkar, K.K., J. Colloid and Interface Sci. 83(1):94 (1981).
- Ranadive, A.Y., Lemlich, R., J. Colloid and Interface Sci. 70(2):329 (1979).
- Rieser, L.A., Lemlich, R., J. Colloid and Interface Sci. 123(1):299 (1988).
- Ruckenstein, E., Davis E.J., J. Colloid and Interface Sci. 34:142 (1970).
- Scriven, L.E., Chem. Eng. Sci. 28:2127 (1959).
- Sebba, F., In: Foams and biliquid foams - Aphrons. Ed: J. Wiley and sons. pp. 58. (1987).
- Stavans, J., Glazier., J.A., Phys. Rev. Lett. 62:1318 (1989).
- Subramanian, S.R., Weinberg, M.C., J. Chem. Phys. 72(12):6811 (1980).
- Subramanian, S.R., Weinberg, M.C., AIChE J. 27(5):739 (1981).
- Tao, L.N., J. Chem. Phys. 69(9):4189 (1978).
- Tao, L.N., J. Chem. Phys. 71(8):3455 (1979).
- Van den Tempel, M., Lucassen-Reijnders, E.H., Adv. in Colloid and Interface Sci. 18:281 (1983).
- Van 't Riet, K., Prins, A., Nieuwenhuijse, J.A., "Some Effects of Foam Control by Dispersed Natural Oil on Mass Transfer in a Bubble Column." Eur. Congr. Biotechnol. 3rd, Volume 3, Verlag Chemie: Weinheim, West Germany. pp. 521. (1984).
- Vrentas, J.S., Vrentas, C.M., J. Chem. Phys. 77:5256 (1982).
- Wagner, C., Z. Electrochem. 65:581 (1951).
- Ward, C.A., Tucker, A.S., J. Appl. Phys. 46:233 (1975).
- Ward, C.A., Findley, R.D., Rizk, M., J. Chem. Phys. 76(11):5599 (1982[a]).
- Ward, C.A., Rizk, M., Tucker A.S., J. Chem. Phys. 76(11):5606 (1982[b]).

- Ward, C.A., Tikuisis, P., Venter, R.D., J. Appl. Phys. 53(9):6076 (1982[c]).
- Ward, C.A., Tikuisis, P., Tucker, A.S., J. Colloid and Interface Sci. 113(2);388. (1986).
- Weinberg, M.C., Onorato, P.I.K., Uhlmann, D.R., J. Am. Ceram. Soc. 63(7-8):175 (1980[a]).
- Weinberg, M.C., Onorato, P.I.K., Uhlmann, D.R., J. Am. Ceram. Soc. 63(7-8):435 (1980[b]).
- Weinberg, M.C., Chem. Eng. Sci. 36:137 (1981).
- Yung, C., Brockwell, J.L., McQuillen, J.B., Chai, A., J. Colloid and Interface Sci. 127(2):442 (1989).
- Zak, M., Weinberg, M.C., Chem. Eng. Sci. 35:1749 (1980).

6. BEER FOAM PHENOMENA

The four physical processes, bubble formation, drainage, coalescence and disproportionation, influence the behavior of beer foam in a different way. In this chapter several foam phenomena will be discussed and explained in terms of these physical processes.

6.1. The creaminess of the foam

One of the first eye-catching phenomena of beer foam is the creaminess. Creaminess is a foam characteristic that is determined by the appearance, by the rheological properties and by the mouthfeel of the foam. A creamy foam is believed to be preferred by the consumer.

Creaminess is a foam property that is difficult to define. Creaminess is a foam characteristic, that depends mainly on the bubble-size distribution, on the liquid fraction and the whiteness of the foam. A homodisperse size distribution of small bubbles is desired for a suitable creaminess. In addition, the fraction of liquid in the foam must be high, because it facilitates the flow properties of the foam.

The creaminess of the foam does not remain constant with time. The initial creaminess is determined by the way bubble formation takes place. Therefore, creaminess is mainly determined by heterogeneous bubble nucleation and growth and the moment of bubble detachment. As described in chapter 2, the parameters that influence this process are, amongst others, the carbon dioxide content, the dynamic surface tension of the beer under expansion conditions and convection during the dispense of the beer. This explains, amongst others, that beer dispensed from a tap appears to be more creamy than beer poored from a bottle or can. Since there is more convection in the tap, the bubbles produced from the tap are smaller.

The creaminess of the foam after a certain period of time depends on the rate of drainage, coalescence and disproportionation. As a consequence of these processes the fraction of liquid in the foam decreases and larger bubbles will appear. The bubble-size distribution becomes wider and the creaminess of the foam decreases.

A beer foam with small bubbles is favored. The way beer is dispensed influences the size of the bubbles. Beer should therefore be dispensed in such a manner that small bubbles are produced.

6.2. The rise of the foam-liquid interface

The rise of the foam-liquid interface is, primarily, a result of drainage. Coalescence and disproportionation do not directly affect the rise of the foam-liquid interface. However, these processes increase the rate of drainage and therewith indirectly the rate of the rise of the foam-liquid interface.

Simple calculation gives insight in the importance of this phenomenon. The situation is considered that the only process occurring in the foam is drainage. Suppose that a foam initially is 3 cm high, and contains 60% gas and 40% liquid. For fresh beer foam these figures are quite realistic. Also suppose that as a result of drainage the foam contains 90% gas and 10% liquid after a certain period of time. Then, the foam height is 2 cm. The total foam height has decreased by a third. The decrease in foam height may take place in about two minutes, depending on various parameters, like the viscosity. This means that by drainage alone, the foam volume can partly disappear whereas the total bubble volume remains the same.

6.3. The influence of temperature

Beer foam is more stable at low temperatures as measured with a Rudin tube (figure 8.2). This phenomenon can not be

easily explained since the influence of temperature is many fold. The temperature has a dominant effect on various other parameters that influences the rate of the four physical processes. At low temperature the solubility of the gas is higher, the viscosity of the beer is higher, the (dynamic) surface tension is higher and the density of gas is higher.

The nucleation of bubbles is greatly affected. As a result of a higher solubility of the gas the number of bubbles that nucleate becomes less. In addition, the bubbles will become smaller because the bubble growth rate decreases.

Drainage is influenced by the change in viscosity. The drainage rate is believed to be inversely proportional to viscosity (*Eq.* [3.1]) and therefore drainage will proceed slower at lower temperature. As can be seen in figure 8.3 the drainage rate as measured with a Rudin tube is proportional to the viscosity, if viscosity is manipulated by varying temperature.

The direct effect of temperature on coalescence is not well known. When film rupture occurs according to the spreading mechanism, coalescence is increased as a result of the increase of bulk viscosity. In addition, the surface tension of beer is higher at lower temperature and therewith the spreading of surface active material and thus film rupture may be enhanced (see chapter 4).

The effect of temperature on gas diffusion is by its indirect effect on the density of the gas, the solubility of the gas, and the surface tension. The density of the gas is inversely proportional to the absolute temperature and will therefore hardly contribute to differences in the rate of gas diffusion. The variations in surface tension as a result of variations in temperature are rather small compared to the variations in gas solubility. As a result gas diffusion and disproportionation will proceed more rapidly at lower temperatures.

The most important effect of temperature is believed to be the effect on bulk viscosity. At low temperatures the viscosity of the liquid is higher and therefore drainage

proceeds slower. Consequently, the beer-foam interface rises slower if the temperature is lower. In addition, the films between the bubbles remain thicker. This brings about that coalescence becomes less likely and that the rate of disproportionation decreases. Summarizing the above considerations, the conclusion may be drawn that at lower temperature less foam appears, but that it is more stable against breakdown processes.

6.4. The coarsening of the foam

Coarsening of the foam means that the bubbles in the foam become larger. Consequently, the appearance of the foam becomes less attractive. Coarsening of the foam can be caused by either coalescence or by disproportionation within the foam. These processes however have to occur within the foam, because if they occur at the top of the foam coarsening does not take place. Instead the foam will collapse as discussed in chapter 6.5.

The coarsening of the foam by coalescence will proceed somewhat different than the coarsening by disproportiona- tion. As a result of coalescence only larger bubbles appear, while as a result of disproportionation also smaller bubbles appear. The smaller bubbles however can hardly be seen by the naked eye and consequently the general impression of the coarsening phenomenon will be equal for both physical processes.

Drainage only influences the coarsening of the foam indirectly. By drainage the film becomes thinner and therefore the chance that coalescence occurs increases. Disproportionation will proceed more rapidly as a result of drainage, because the diffusion distance decreases.

6.5. The collapse of the foam

Foam collapse is the reduction of foam height. Foam collapse is mainly the result of the escape of gas from

the foam. Gas escapes from the foam either when gas diffuses from the upper bubble layer to the surrounding atmosphere or when the film between a bubble in the upper layer and the surrounding atmosphere ruptures. The final result in both cases is that the foam height reduces.

By simple observation of the upper bubble layer, it appears that, under normal conditions, coalescence does not much contribute to foam collapse. The bubbles in that layer appear to be stable against coalescence. Only when external surface active material is added (chapter 4) or when larger air bubbles rise to the top layer of the foam (chapter 6.7) coalescence may occur. However, in normal situations, this does not happen very often.

In contrast, gas diffusion from the foam to the surrounding atmosphere takes place rapidly. As described in chapter 5 for a single bubble, the driving force for gas diffusion from the upper layer of the foam is high as a consequence of the difference in gas composition between the interior of the foam and the surrounding atmosphere. Partial gas pressure differences as high as 1 Bar dominate the gas diffusion process because initially the bubble contains only carbon dioxide and the atmosphere contains practically only nitrogen and oxygen. Therefore, carbon dioxide will diffuse outward and nitrogen and oxygen inward. However, the solubility of nitrogen and oxygen is much lower than the solubility of carbon dioxide. Since the diffusion rate is also determined by the solubility of the gas, carbon dioxide diffuses outward more rapidly than nitrogen and oxygen inward. The result is that the bubble in the upper layer of the foam shrinks to about 2% of its original volume. This shrinking process does not take more than several seconds (figure 5.12). Thereafter, the gas composition in and outside the bubble is the same. The only driving force for the diffusion of nitrogen and oxygen outward again is the Laplace pressure. The Laplace pressure however is very low because the surface tension of the bubble has become very low as a consequence of the shrinking process. In addition, an insoluble layer of surface active material may be present at the bubble

surface (figure 5.16). For these reasons the gas diffusion outward will proceed very slowly. The small air bubbles in the top layer of the foam will be relatively stable against gas diffusion over a long period of time.

As a consequence of the shrinking of bubbles in the top layer of the foam, bubbles from the next layer can come to the surface of the foam. These bubbles are subjected to exactly the same diffusion process and they shrink to about 2% of their original volume as well. This series of events will repeat itself over and over again, until all bubbles have shrunken, or until the top layer is entirely filled with small air bubbles.

Gas diffusion from the top layer to the surrounding atmosphere is not the only gas diffusion that takes place as a consequence of partial pressure differences. In addition, upward carbon dioxide and downward air diffusion from and to the layers underneath the top layer occurs. The partial pressure differences will penetrate the foam. However, the diffusion of gas through various layers, and thus through various liquid films, will proceed slower than diffusion from the top layer to the surrounding atmosphere.

An order of magnitude calculation can give information about the importance of gas diffusion from the top layer of the foam for the collapse of the foam. Suppose that gas diffusion is the only process that takes place in the foam, and that coalescence does not occur. A foam of 3 cm height, in a glass with a diameter of 6 cm is considered. Suppose the gas fraction is initially 0.6 and all bubbles have an initial radius of 200 μm. In that case the foam contains approximately 1.5 million bubbles distributed over about 100 layers. If the bubbles in the top layer go through the diffusion process until their volume is about 2% of their original volume, then the area they occupy in the surface becomes about $1/14^{th}$ of the original area. This means that, after 14 layers of bubbles have been subjected to the diffusion process, the surface is completely occupied with shrunken air bubbles. The bubbles originally present in 14 layers are, after a certain period of time,

present in the top layer. After that, diffusion of gas has to take place over a longer distance and through more than one liquid film and will therefore proceed slower. The process will repeat itself over and over again for all bubble layers, but the rate of gas diffusion decreases because in the course of the process diffusion has to take place through more and more layers. When all bubbles have gone through the diffusion process the foam will consist of about 7 layers of bubbles with a radius of about 50 μm. The height of the foam will then be 0.4 mm, taking into account that the gas fraction in the foam has become 0.9. The ultimate result of this diffusion process is very much in agreement with the practical observation that after a certain period of time the foam has collapsed, but that a single layer of very small bubbles appears to persist on top of the beer.

From these calculations it can be concluded that a beer foam can almost completely collapse as a consequence of gas diffusion. It is amazing that it happens without the disappearance of a single bubble. The number of bubbles does not change and remains 1.5 million bubbles in the above given example.

If the rapid carbon dioxide and air exchange through a single foam film takes 1 second (chapter 5.5), and if every 14 layers of foam bubbles becomes one layer in the course of the diffusion process in a consecutive way, the 100 layers of bubbles collapse in about 400 seconds. This is a result of the fact that layer after layer goes through the diffusion process. The total collapse time of the foam is the sum of the diffusion times required for all layers. It becomes apparent, that the total collapse time of the foam is very susceptible to the rate of the diffusion process through a single film. An increase of 0.1 second in diffusion time for a single bubble results in an increase of about 40 seconds in foam collapse time in the above given example. It may be concluded that the collapse proceeds within the average consumption time of the consumer.

The observation that smaller bubbles give better beer foam behavior can now easily be explained. After 14 layers of small bubbles shrunken to 2% of their original volume less gas has diffused out of the foam than when the bubbles would have been larger. In other words, a foam that contains smaller bubbles also contains more layers and therefore the same amount of gas must diffuse through more layers if the foam contains smaller bubbles.

The practical observation, that the bubbles in the top layer of the foam are much smaller than the bubbles underneath, can be understood with the knowledge of this gas diffusion process.

Now also the observation, that a nitrogen foam is much more stable against collapse than a carbon dioxide foam, can be explained. Gas diffusion from a nitrogen foam to the surrounding atmosphere proceeds much slower than the diffusion of carbon dioxide, because the partial pressure differences and the solubility of nitrogen are much smaller. In fact, if the foam contains 100% nitrogen and the surrounding atmosphere is air (80% nitrogen, 20% oxygen), the foam expands. In that case, the partial pressure differences for oxygen and nitrogen are equal ($0.2\ P_{atm}$), but the direction of the gradient is opposite. The solubility of oxygen is about twice the solubility of nitrogen. Therefore, two times more oxygen diffuses inward than nitrogen outward. Consequently, the size of the bubbles in the top layer initially increases and the foam level rises. This phenomenon can not be observed by the naked eye, because the increase is very small.

A little amount of nitrogen in a predominantly carbon dioxide foam already greatly improves the stability of the foam against collapse. If nitrogen is present the bubbles shrink more slowly. In addition, the bubbles do not shrink rapidly until 2% of the original volume. Instead, the transition from rapid gas diffusion, driven by partial pressure differences, to slow gas diffusion, driven by the Laplace pressure, will be at a larger volume. This means that less area will become available for the layer underneath the top layer to come to the foam surface and also

88

that it will take longer. Therefore, the overall collapse of the foam will be significantly slowed down. This explains why the addition of nitrogen to beer is such a successful way to improve head retention times, Carroll (1979), Kuzniarski (1983), Butterworth (1983), Hedderick (1984).

A carbon dioxide foam under a carbon dioxide atmosphere is more stable against collapse than a carbon dioxide foam under a nitrogen atmosphere. If a carbon dioxide blanket covers the beer foam, the diffusion of carbon dioxide is driven only by the Laplace pressure and not by large partial pressure differences. Therefore, gas diffusion is comparatively slow, and the foam is more stable against collapse. The bubbles in the top layer of this foam remain larger than when the surrounding atmosphere contains nitrogen (compare figure 5.11 and 5.12). The appearance of the foam therefore is less attractive if carbon dioxide covers the foam.

A last observation gives evidence that foam collapse takes place by the described gas diffusion mechanism. After foam collapse, a monolayer of small bubbles remains on the beer surface for a long period of time. If foam collapse takes place by coalescence, as for example is the case if spreading material is added to the foam, all bubbles disappear. In that case, the monolayer of very small air bubbles will not remain on the surface of the beer. The beer then appears to be completely flat. Thus, a very easy distinction between foam collapse by gas diffusion and by coalescence can be made this way. By gas diffusion bubbles become smaller and remain on the beer surface. By coalescence the bubbles become initially larger and then disappear completely.

Coalescence does apparently not take place in the top layer of the foam. This confirms the hypothesis postulated in chapter 4, that coalescence mainly takes place if films are expanded and the dynamic surface tension is high. The compressed bubble surfaces in the top layer of the foam are not very susceptible to coalescence.

6.6. Cling

Cling is the phenomenon that a part of the foam adheres to the wall when the upper level of the foam decreases. The first observation made is that the gas diffusion process of carbon dioxide outward and air inward is essential for the deposition of cling. The small bubbles at the foam surface adhere more strongly to the wall than larger ones. The ability of bubbles to adhere to the wall and to stick together appears to be dependent on the shrinking of the bubble. This is confirmed by an experiment carried out by Glenister at al (1966). When a glass is covered with a glass plate and the foam is allowed to collapse, no bubbles adhere to the glass wall. In an equal glass that is not covered and contains the same amount of beer foam, cling is formed.

When a sip is taken from the glass, the shrunken bubbles in the upper layer turn to the wall. Apparently, they stick together. Somewhere at some arbitrary place breakage occurs in the top layer. The bond between the bubble and the glass wall seems to be stronger than the bond between bubbles.

As a result of cling the foam collapses in an uneven way. Next to the glass wall a ring-shaped depression in the layer of small air bubbles appears as a result of cling. Therefore gas diffusion of carbon dioxide from the foam is locally accelerated there. As a consequence, foam collapses more rapidly near the glass wall than in the middle of the glass. Consequently, a small heap-shaped buildup of foam may appear in the center of the glass.

6.7. The influence of air entrapment

As discussed in chapter 2.1 foam bubbles can be formed by agitation. While dispensing beer into a glass, a plunging motion can be produced. As a result air bubbles come into the beer foam. In general these air bubbles are larger than the carbon dioxide bubbles. A similar partial

pressure difference between the air bubbles and surrounding carbon dioxide bubbles is present as between the surrounding atmosphere and the carbon dioxide bubbles in the top layer of the foam. Consequently, carbon dioxide diffusion takes place into the air bubble. Very minor amounts of air diffuses to the bubbles in the immediate periphery of the air bubble. The air bubbles suck the carbon dioxide from the surrounding bubbles and become larger. The buoyancy force of these large air containing bubbles increases and consequently they may rise to the surface. As a result the foam becomes less attractive. Also these bubbles may coalesce. In this manner gas escapes from the foam. Entrapped air bubbles can thus contribute to foam collapse by transporting carbon dioxide to the atmosphere above the foam. Therefore, the way that beer is poured out can make a lot of difference for the behavior of the foam. As a rule, air entrapment should be avoided.

6.8. The influence of chemical composition

Foams, with the same chemical composition, may have different foam behavior. The essence of this statement is that in a foam the chemical components may be distributed throughout the foam in a different way. Three examples will be given.

Two foams with exactly the same chemical composition, but with different bubble-size distributions may behave different. The creaminess of the foam and therefore the appreciation of the consumer will be different. In general the foam with the smaller bubbles is favored. In addition, the foam with smaller droplets is more stable against collapse by gas diffusion as explained in chapter 6.5.

Two foams with the same chemical composition, containing the same amount of nitrogen, can have a different collapse behaviour. The only difference between the foams may be that in one foam all nitrogen in enclosed in a single bubble, whereas in the other foam the nitrogen is evenly

91

distributed throughout the bubbles. The collapse of a foam containing a single nitrogen bubble can be enhanced as explained in chapter 6.7. When all bubbles contain the same amount of nitrogen however, the foam is stabilized against collapse.

When two foams have the same chemical composition and contain the same amount of lipid material, the negative effect of this lipid material on the behavior of the foam may be different. This difference can be caused by the fact that the lipid material in one case is present as droplets, and in the other case is molecularly dissolved. Lipid droplets can initiate coalescence and thus enhance foam collapse enormously as explained in chapter 4. When lipid material is dissolved a relatively small negative effect on foam behavior can be observed.

References

- Butterworth, M.J., The Brewer 69:407 (1983).
- Carroll, T.C.N., Tech. Quart. MBAA 16(3):116 (1979).
- Hedderick, J.B., The Brewer 70:116 (1984).
- Kuzniarski, J.N.S., The Brewer 69:362 (1983).
- Glenister, P.R., Segel, E., Koeppl, K.G., ASBC Proc. pp. 150 (1966).

7. BEER FOAM STABILITY

The poor definition of foam stability has often lead to misunderstandings and confusion of tongues. Therefore the need of an appropriate and straightforward definition arose soon after the beginning of this research work on beer foam. However the effort to redefine the concept of foam stability has failed. The main reason for this failure is that the word stability can only be used in relation to a single property, *i.e.* a momentary measurable characteristic, of a system. Therefore, it is possible to define the stability of a single foam property. Foam itself is not a property but a system that has various properties like: (i) total volume (ii) the amount of gas, (iii) the amount of liquid, (iv) bubble-size distribution, (v) distribution of bubbles throughout the foam, (vi) optical properties like colour and shine, (vii) several rheological properties like viscosity and elasticity, (viii) organoleptical properties, and (ix) temperature.

Aqueous foams, once formed, are in thermodynamic terms unstable. Consequently the physical processes, drainage, coalescence and disproportionation take place. This means that the foam properties will vary as a function of time. Every single foam property has its own stability.

The stability of a beer foam property indicates how this property varies as a function of time.

A foam may have very stable and unstable properties. It is impossible to define foam stability. Stability, itself is not a property either, because it can not be measured momentary. Therefore, foam behavior can not be expressed with a single foam number. Unfortunately, different foam numbers must be measured to obtain a complete picture of the behavior of the foam. This will be discussed in chapter 8 in more detail.

It may be difficult to accept for the brewing industry that foam behavior cannot be expressed with a single foam

number. Of course, the desire for simplicity dominates in the day to day practice of brewing.

A way to elucidate the argument, that a single foam number can not express the overall foam behavior, is to compare foam behavior with taste. It is generally accepted that a single taste number can not be given. Always a single taste property, like lightstruck flavour, bitterness, or one of the numerous other tastes, is measured and presented separately. An enormous effort is made by larger breweries to test the taste of beer in all its aspects and detail. The use of taste panels is common practice. Chemical analysis are continuously carried out on many identified taste components with sophisticated equipment, like GLC and HPLC. Even if foam behavior is not as complex as taste the analogy is perfect. The only difference is, that it is not generally accepted that for the proper characterization of foam a similar effort should be made. In addition, the interpretation of taste numbers is more or less common knowledge, while, in contrast, the interpretation of different foam numbers is not. In other words, the available knowledge about foam behavior is very limited compared to the knowledge about taste.

8. MEASUREMENT OF FOAM BEHAVIOR

8.1. Introduction

In chapter 6 and 7 it was concluded that the overall behavior of a foam can not be measured with a single apparatus, nor can it be expressed by one foam number. An argument in favor of this statement is that an enormous amount of methods and procedures have been proposed to determine foam characteristics. In practice, beer foam is measured with several readily available methods. The Blom method, the Rudin tube and the Nibem foam stability tester are among the most well known examples.

The method described by Blom (1934) is based on the measurement of the rate of liquid drainage from the foam. With this method degassed beer is put in a separation funnel and carbon dioxide is diffused into the beer through a porcelain candle in order to produce a certain amount of foam. The separation funnel is then placed on a balance. The liquid that drains from the foam is separated from the foam and directed away from the balance to a separate container. The decrease of the weight of the foam is measured at certain time intervals. Blom (1934) found that the rate of drainage can be described as a first order kinetic. After a short lag period, the logarithm of the weight of the foam is proportional to time, following the next empirical equation:

$$W_t = W_o \, e^{-kt} \qquad [8.1]$$

With the obtained results a half-life time of the foam can be determined:

$$t_{\frac{1}{2}} = \frac{\ln 2}{k} \qquad [8.2]$$

where W_t is the weight of the foam after a certain time t, W_o is the initial weight of the foam, k is a constant and

$t_{\frac{1}{2}}$ is the foam half-life time.

The Blom method is improved upon and automatized in the Carlsberg laboratories as reported by Rasmussen (1981) and Rosendal and Rasmussen (1982). The apparatus can run a measuring and rinsing program for the determination of 50 samples during normal working hours. The initial foam volume and half-life time of the foam are automatically obtained. One of the improvements made is that the foam is no longer produced by diffusing carbon dioxide through a brittle porcelain candle. The candle is difficult to replace by a candle that gives the same reproducible results. Instead the foam is formed by pressing the carbonated beer through a nozzle with well defined dimensions. The foam is thus produced in a similar way as by a tap in a bar, and therefore it may be expected that the initial bubble-size distribution and the gas composition is almost the same as in practical situations. With the automated apparatus, different initial foam volumes are produced and therefore also a "foamability" number is obtained. The "foamability" number depends mainly on the carbon dioxide content of the beer. The initial height of the foam and the rising of the foam-liquid interface is measured with a conductivity probe. However, the probe may interfere with the physical processes occurring in the foam. For example, the probe may induce coalescence. In a second generation apparatus, developed at the Carlsberg research laboratories, the foam measurement with the conductivity probe is replaced by an optical technique. Also the sampler has been improved upon. Nowadays, the samples can be directly drawn from a large variety of bottles and tins.

The Rudin tube, developed and described by Rudin (1957), is based on a method described by Ross and Clark (1939). The similarity between the Rudin tube and the Blom method is that with both measurements the rate of drainage is obtained. The Rudin tube is a long tube of small diameter. At the bottom of the tube there is a sintered glass filter, through which a gas (e.g. nitrogen or carbon dioxide) can be sparged into the primarily degassed beer.

96

The time, that elapses while the foam-liquid interface rises between two marks at the lower end of the tube, can be taken as a characteristic foam number. Also a foam half-life time or Head Retention Value (HRV) can be defined. Instead of the weight of the foam (Eq. [8.1]), the height of the liquid-foam interface can be taken as a measure of the drained liquid. Ross and Clark (1939) defined a Σ-value for the rate of drainage from a foam. The definition of the Σ-value is based on the logarithmic relation between the amount of drained liquid and time:

$$\Sigma = \frac{t}{2.303 \ \log((a+b)/b)} \qquad [8.3]$$

where a is the volume of beer drained from the foam and b is the volume of beer that remained in the foam at time t. The Σ-value is equal to 1/k (Eq. [8.1] and [8.2]).

A Foam Flashing Value (FFV) was defined by Hudson (1960). After the foam was produced by expanding beer with an orifice the drainage of 200 ml of foam was measured.

$$FFV = \frac{200 \ (B_2 - B_1)}{B_2} \qquad [8.4]$$

where B_1 is the amount of beer that drains from the foam in 90 s and B_2 is the total amount of liquid in the foam. The FFV is not often used in the brewing industry as a beer foam characteristic.

Pierce and Pursell (1959) closely investigated the validity of the empirical relation [8.1], [8.2] and [8.3]. They found that these equations can only be used after a certain time-lag, and within certain limits of time, especially if other gasses than carbon dioxide are used.

An explanation for the unusual behavior of different gasses in the Rudin tube was given by Bishop et al (1975). He stated that the half-life time value of the foam is very susceptible to impurities in the carbon dioxide gas. The influence of these impurities can be explained with

differences in gas solubility (see chapter 6.5) and not with the occurrence of oxidation.

Another explanation for deviations of the logarithmic relation between the rate of drainage and the time is suggested by Ross and Cutillas (1955). They state that the decrease of the total interfacial area in a foam as a result of gas diffusion is logarithmically related to time as well. The rate of liquid drainage depends on the progress of the three physical processes involved in the breakdown of the foam, drainage, coalescence and dispro-portionation. It may be argued that initially drainage is the main process, and that at a later stage coalescence and disproportionation become more important. The most dominant process determines whether the empirical relation of *Eq.* [8.1] or *Eq.* [8.3] is valid. Consequently, the validity of these equations may very much depend on the time interval that is used to measure foam drainage. Ross and Cutillas (1955) explained that with a light transmis-sion method a separation can be made between the effects of drainage of liquid in foam from that of gas diffusion, which causes a decrease of interfacial surface area. Similar results were obtained by Segel et al (1967). They stated that, assuming first-order kinetics, two straight lines can be drawn to fit a logarithm-of-drained-beer versus time curve and two reaction constants can be determined. They concluded that the two reaction constants must reflect on separate processes.

A review on the Rudin drainage tube technique is given by Bamforth (1985). He repeated the statement of Klopper (1954), that results of drainage measurements must be used with reservation because the consumer assesses the foam itself and not the drainage rate.

The use of the Rudin tube or other methods based on the rate of drainage have several disadvantages. These disad-vantages are mainly that the foam and the measurement are very different from the practical situation as observed by the consumer.

(i) The beer is degassed previous to measurement. The samples are then sparged with a different gas and foam is

98

produced. The gas composition in the foam may be different from the gas composition in the practical situation. In that case, a meaningful foam number will not be observed, even if the same phenomena could be assessed as the consumer does. For example, the effect of nitrogenation on the rate of beer foam collapse can not be measured with the Rudin tube.

(ii) In the Rudin tube the bubbles are produced through a porous glass filter. Therefore, the initial bubble-size distribution in the foam is, amongst others, determined by the gas flow rate and the size of the pores. This initial bubble-size distribution may be very different from the initial size distribution in practice and therefore the progress of drainage, coalescence and disproportionation, and thus the behavior of the foam may be influenced. The effect of the initial bubble-size distribution on beer phenomena, like creaminess and foam collapse, have been described respectively in chapter 6.1 and 6.5. *E.g.* The effect of the initial bubble-size distribution on the rate of gas diffusion was also discussed by Lemlich (1978) and Ranadive and Lemlich (1979). Bamforth (1985) also stressed that the method is very susceptible to the size of the pores in the filter used to sparge gas bubbles in the beer. Apparently, the initial bubble size in the Rudin tube has a great effect on drainage. The drainage rate of a foam with smaller bubbles appears to be lower than the drainage rate of a foam with larger bubbles.

(iii) Another drawback of the Rudin tube is that the geometry of the tube is very different from the geometry of a normal beer glass. Wall effects may influence the breakdown of the foam. The rate of gas diffusion to the atmosphere above the foam will be lower than in the practical situation because the surface area is very small. That the geometry of the tube is very important for the obtained results is confirmed by Ross and Suzin (1985), who carried out experiments in cylindrical- and conical-shaped vessels.

(iv) The composition of the atmosphere above the foam in the Rudin tube will be different. The rate of carbon

dioxide diffusion from the foam to the surrounding atmosphere as described in chapter 6.5. will be influenced. Therefore, the foam will not collapse as in practice. In fact, the collapse of the foam is not even assessed with this method, since only the rate of drainage is observed.

(v) In the Rudin tube much foam is produced from a small amount of beer in comparison with the practical situation. This may mean that the surface concentration in the foam of adsorpted surface active material is smaller than in a practical system. The depletion of surface active material will influence the reliability of the measurement in a negative way.

The Rudin tube technique is the most widespread method used in the brewing industry nowadays. However, each brewery has made its own modification and defined its own procedures. Therefore, the numbers can not be compared to each other.

Not all beer foam measurement techniques are based on the rate of drainage of liquid from the foam. Three methods have been put forward that are based on the measurement of foam collapse. One of the methods is known as the method of De Clerck and De Dijcker (1957). With this method foam is dispensed into a glass at standard conditions. Afterwards, the collapse of the foam is measured by focussing a microscope onto the foam surface. The second method is based on the measurement of vertical transmission of light through the foam. With this method, amongst others, reviewed by Wilson and Mundy (1984), the total height of the foam is measured, because both the rise of the foam-liquid interface and the collapse of the foam contributes to a gradual increase of light transmission. A similar apparatus was described by Savel and Basaravá (1989) who used an optical glass detector to measure the transmission of light. By moving the detector they could separately measure the level of the foam-liquid interface and the foam height. They claimed that the breakdown of foam can be described by a rather complex empirical relation, that will not be repeated here.

The most well known method to measure foam collapse is

the Nibem foam stability tester. The method was developed by Klopper (1977) and Klopper and Vermeire (1977[a,b]). The foam is produced in a glass with a foam flasher. The flasher works very similar to a tap, and is available for bottles and tins. With the Nibem foam stability tester the collapse of the foam in the glass is measured with a conductivity probe. The probe follows the upper foam level as a function of time. The time elapse from 1 cm to 4 cm below the top of the glass is measured every cm. In general the total time elapse from 1 cm to 4 cm is taken as a measure for foam behavior. The method gives only information about the collapse of the foam. Information about other beer foam phenomena is not obtained. In general, the reproducability of the results of the Nibem foam stability tester is lower than the reproducability of foam numbers obtained with the Rudin tube, although controversial standard deviations are presented in the literature (Piendl and Legat (1980), Wackerbauer and Greif (1980), Ullmann (1982) and Weyh (1988)). From experience, the reproducability of the Nibem foam stability tester depends mostly on the control of the temperature, of the cleanness of the glass and of the gas composition of the atmosphere surrounding the glass. The temperature of the sample is preconditioned at 20°C but the apparatus is not temperature controlled, and therefore the laboratory temperature can influence the outcome of the measurement. Since the collapse of the foam is measured, the gas diffusion from the top layer to the surrounding atmosphere and coalescence in the top layer of the foam are measured. The cleanness of the glass may influence the coalescence rate, and therewith the collapse time as discussed in chapter 4. The gas composition above the glass is very important for the rate of gas diffusion to the atmosphere. During foam collapse a carbon dioxide blanket settles on top of the foam. As a result, the gas diffusion rate from the foam decreases. When the carbon dioxide blanket is disturbed by air turbulence, the collapse rate is altered. This effect on the foam collapse rate is so pronounced that the reproducability of the measurement may depend on

the slamming of a door, the opening of a window or the occasional passing by of a colleague.

The Nibem foam stability tester was compared to the Rudin tube method by Weyh (1987). In the same study, a comparison of both methods with a dispense test, described by Plank (1963), was made. This method is very similar to the method developed by De Clerck and De Dijcker (1957). The dispense test is based on the controlled, motor-driven dispense of beer into a glass, followed by the measurement of foam collapse with a microscope. The Σ-values, obtained with the Ross and Clark method, poorly correlate with the Nibem number. The correlation depends very much on the kind of beers that are examined. This is not surprising since, with the two methods, different foams and different phenomena are measured under different conditions. A somewhat better relation appears to exist between the Nibem numbers and the results of the dispense test. This can be explained because, in principle, the same phenomena are measured. Still the correlation between the methods is not as good as might have been expected. The way the beer is poured into the glass seems to influence the collapse rate of the foam.

Cling can be measured with a photocell that scans the glass wall, where upon cling was previously produced under well defined conditions. A method based on this principle was described by Klopper (1973). A photographic technique was presented by Glenister and Segel (1964) who also came up with the concept of primary and secondary cling. They defined primary cling as the first ring obtained in a glass where beer was previously sucked out at successive, regular intervals. Secondary cling is defined as the consecutive rings. Although the first ring is always larger than the others, as can be understood from chapter 6.6, there is no fundamental basis for the distinction between two kinds of cling. Yet another method to measure cling was presented by Jackson and Bamforth (1982). The cling can be produced in a similar way as described by Glenister and Segel (1964). The cling is then rinsed from the glass with water and the absorbance at 230 nm of the

102

resulting solution is then taken as a measure for the total amount of cling.

Although the above mentioned methods and techniques give ample information on foam characteristics, even more beer foam properties were studied by Glenister et al (1966) and Segel et al (1967). They discussed methods to asses the whiteness of a foam, the density of a foam, the foam strength and the foam viscosity. The whiteness can simply be measured with a reflectometer. The density of the foam is defined as the ratio of the liquid in the foam and the foam volume. The density of the foam is therefore equal to the liquid fraction of the foam and can be measured in various obvious ways. Foam strength (or robustness) is a measure for resistance of a foam against externally added surface active material. Under standard conditions, cetyl trimethyl ammonium bromide was added to the beer and foam characteristics were determined as normal. Glenister et al (1966) measured the viscosity of the foam by dropping glass beads through a foam column and applying Stokes law as also described by Waniska and Kinsella (1979). For all sorts of reasons, not discussed here, the proper viscosity of a foam is not measured with this technique (see *e.g.* Princen (1983)). However, the result of this measurement may very well be a good characteristic for the creaminess of a foam.

Other method to establish foam characteristics are described. However, they are not commonly used for the characterization of beer foam. With these methods other foam properties than drainage rate or collapse rate can be measured.

One of these methods was described by Nishioka and Ross (1981,1983), Nishioka (1986). The method is based on the measurement of the pressure build-up in a confined volume, that is a result of the coarsening of the foam. The loss of total surface area with time can be related to the pressure increase as described by the authors. Therefore, with these results quantitative information is obtained about the combined progress of disproportionation and coalescence.

Other methods are based on the measurement of the conductivity of a foam. Chang and Lemlich (1980) stated that the ratio of foam conductivity to liquid conductivity is proportional to the liquid hold-up in a foam. Agnihotri and Lemlich (1981) and Datye and Lemlich (1983) later added that this relation is mostly independent of the surfactant used and the inhomogeneity in bubble size. The size of the bubbles somewhat influences the conductivity of the foam. The conductivity of a foam with smaller bubbles is lower than the conductivity of a foam with larger bubbles.

Substantial research work has been done on the determination of bubble-size distributions in aqueous foams. The bubble-size distribution in foams can be determined in various ways. For beer foam, Glenister et al (1966) and Segel et al (1967) described a method to measure the bubble-size distribution. The bubble-size distribution was measured from photographs taken of the top of the foam. This method may adequately give the size distribution of the bubbles in the top layer of the foam, but, as was discussed in chapter 6.5, under practical conditions the bubbles in the top layer of the foam are much smaller than the bubbles inside the foam. Therefore, the bubble-size distribution of bubbles in the top layer by no means represent the size distribution of bubbles inside the foam.

Other methods to measure the bubble-size distribution in a foam are based on the measurement of observed bubble diameters in a cross section of the foam. This cross section can either be obtained by photographing the foam through a glass wall or by freezing and cutting the foam (De Vries (1972)). Seleki and Wasiak (1984) described a different method. With this experiment the foam is led through a capillary, and the distance between the foam films in that capillary is taken as a measure for the bubble size. The method was used by Rieser and Lemlich (1988) to determine the gas diffusion rate in a foam from the evolution of an initially bimodal bubble-size distribution. The determination of the bubble-size distribution

of a foam by measuring the chord length distribution obtained running a conductivity probe through a gas-liquid dispersion was described by Lewis at al (1984). They calculated the bubble-size distributions from the chord length distribution, using a statistical method of Thang and Davies (1979).

8.2. Aim and Approach

With the methods, described above, foam numbers can be obtained. Here a modified Rudin tube, a modified Nibem meter and the original Nibem meter were used. These foam numbers give information about the progress of one or more foam phenomena as a function of time. In some cases, total drainage is measured, in other cases foam height. However, these foam numbers are a reflection of the occurrence of one or more physical processes. Since the progress of the physical processes depends on the apparatus used, and since different properties are measured with different methods, the foam numbers, that are obtained with diffe-rent methods, do not necessarily have to correlate with each other, nor with the consumers assessment of the beer foam behavior. With the methods for measuring beer foam characteristics a foam number is obtained that is a result of some total effect of bubble formation, drainage, coalescence and disproportionation. If it were possible to measure the progress of the four physical processes in a foam separately, a better insight in the characteristics of a foam could be obtained.

Strictly, there is only one objective method to measure foam behavior and that is to measure the bubble-size distribution as a function of time and place. The measure-ment of the evolution of the bubble-size distributions has not yet been used to make a distinction between bubble formation, drainage, coalescence and disproportionation, although theoretically it must be possible. The initial bubble-size distribution gives information about the bubble formation process. The measurement of the volume

fraction of liquid in the foam as a function of time is a measure for the rate of drainage. A distinction between coalescence and disproportionation can be made because there is a fundamental difference between the effect of coalescence and disproportionation on the evolution of the bubble-size distribution. Only larger bubbles appear as a result of coalescence, whereas disproportionation results in both larger and smaller bubbles. Hence, a bimodal distribution is obtained in the latter case. A distinction can be made between coalescence and disproportionation using gases of different solubility. The rate of disproportionation depends very much on the gas solubility. By using gases of different solubility like nitrous oxide or carbon dioxide on the one hand and nitrogen or oxygen on the other the disproportionation rate can be influenced. Coalescence will mostly be independent of the used gas. Therefore, using gases with very different solubilities, an estimate can be made of the contribution of disproportionation and coalescence to the evolution of the size distribution in a foam.

In this chapter a new method to assess a number of foam phenomena will be introduced. The method is based on the simultaneous measurement of the bubble-size distribution, the level of the foam-liquid interface and the level of the foam height as a function of time. The drainage rate, the changes in the gas fraction, the foam collapse rate, and the changes in foam volume are thus obtained. In order to measure all these features an optical glass-fibre probe was pierced through the foam at consecutive intervals. The results obtained with the new method were compared with the bubble-size distributions measured with a photographic method.

8.3. Experimental

The characteristics of beer foam were assessed in three different ways. A Rudin tube, a Nibem foam stability tester and a new method to measure amongst others the

bubble-size distribution in a foam were used.

The Rudin tube was made of a temperature controlled Pharmacia Chromatography column (600x25 mm). At the bottom of the inner tube a G_2-glass filter was melted. With this filter bubbles of approximately the same size are produced as when a beer is dispensed from a bottle. The beer was degassed by shaking regularly in air. Prior to measurement the column was filled with the same gas as the gas that was used during the actual measurement. Then, 50 ml of beer sample was put into the column and foam was produced by sparging gas (CO_2 or N_2) into the column until the total system had reached a height of 33 cm above the filter. The gas flow rate was maintained at $2.1x10^{-6}$ m^3s^{-1}. The time, that elapses when the foam-liquid interface rises between two marks on the column (at 3 and 8 cm above the glass filter), was measured. Measurements were carried out at 25°C, unless indicated otherwise. The Σ-value, HRV, or half-life time were not calculated.

The Nibem foam stability tester was used in two ways. The first way is exactly as described by Klopper (1977) and Klopper and Vermeire (1977[a,b]). The modification, that was also used, was made to enable the measurement of previously degassed beer samples. In a glass, of the same dimensions as used for the standard measurement, 100 ml of degassed beer was added. The foam could be produced by diffusing gas through a porous G_2-glass filter. Only CO_2 was used, because the nitrogen foam is too stable against collapse to allow reproducible measurement. The collapse rate of the foam was measured with a conductivity probe as usual, with the exception that during the measurement the glass was covered with a small container to avoid air turbulence and therewith to improve the reproducability of the measurement.

The bubble-size distribution, the foam height and the level of the foam-liquid interface were measured with a newly developed technique. The apparatus is based on the use of an optical glass-fibre technique developed at the Technical University of Delft, The Netherlands (Frijlink et al (1986) and Frijlink (1987)). The apparatus consists

of three major parts, as shown in figure 8.1: firstly a mechanism for moving the fibre up and down the foam at known speed, secondly the fibre itself combined with the opto-electronic unit, and thirdly equipment for data acquisition and for the calculation of the bubble-size distributions and other foam properties.
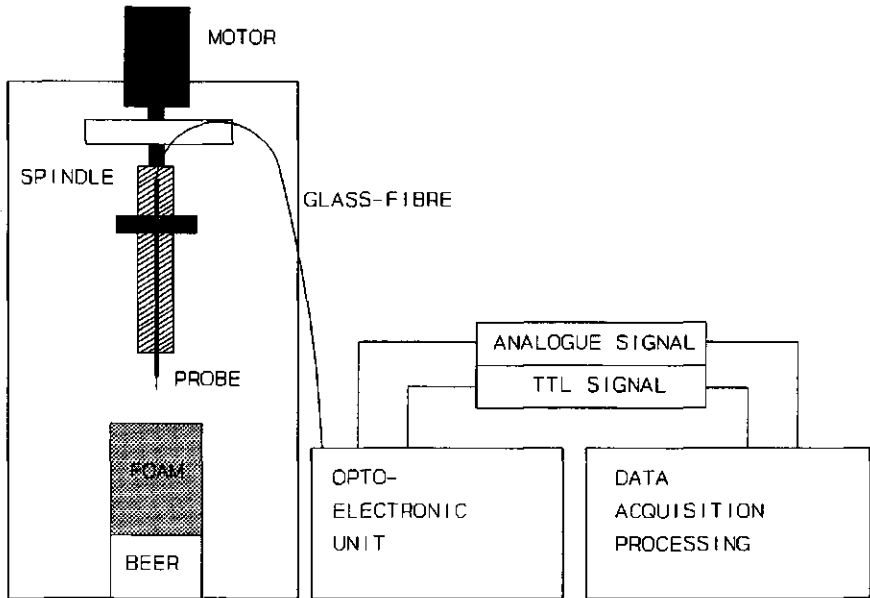

Figure 8.1: The optical probe method to determine bubble size distributions.

From the opto-electronic unit light is emitted into the fibre. The end of the fibre consists of a very small rounded tip of diameter ca. 20 μm, the diameter of the fibre itself being 200 μm. The essence of the method is that the amount of light reflected at the tip of the fibre depends on the refractive index of the medium surrounding the tip. If the refractive index of the medium is approximately the same as the refractive index of the glass almost no light is reflected. However, if the refractive index of the medium is much lower than the refractive index of the glass, part of the light is reflected. Therefore, when the tip is surrounded with gas, more light is reflected than when the tip is in liquid. A beam splitter separates the returning beam; half is returned to

108

the source and lost and the other half is received by a light-sensitive cell and converted into an electronic signal. The opto-electronic unit also contains a analogue-digital converter to make data acquisition easier.

On moving the fibre through a foam, that was produced in an identical way as for the modified Nibem method, an alternating signal corresponding to gas and liquid is obtained. If the speed of the probe is known (ca. 10 cms^{-1}), the time intervals of gas and liquid are a measure for the bubble-size distribution in the foam. Either the analogue or the digital signal can be used to calculate the bubble-size distribution.

With the calculation of the bubble-size distribution a problem similar to the 'tomato salad' problem is to be solved. The observed one-dimensional gas lengths are not equal to the actual three-dimensional bubble radii because a cross section of a bubble is hardly ever made through two polar ends. Furthermore, bubbles of large diameter have a greater chance of being pierced by the optical probe than bubbles of smaller diameter. A statistical method can be used to calculate the three-dimensional bubble-size distribution from the one-dimensional chord length distribution. Several methods are available for this purpose (Thang and Davies (1979), Kawakami et al (1988), Clark and Turton (1988), Ruan et al (1988)). A method described by Weibel (1980) was used here. The method makes use of the gas fraction of the foam, which follows from the measurement of the upper level of the foam and the level of the foam-liquid interface. If the experiment is carried out at consecutive time intervals the rate of drainage, the collapse of the foam and the changes in foam volume are detected in addition to the evolution of the bubble-size distribution.

The results of the optical glass-fibre method were compared with a photographic method. In that case, the bubble-size distributions were obtained by measuring and counting bubbles on a photograph taken through a glass wall. The photographic method has several disadvantages e.g. (i) the glass wall might distort the bubbles, (ii)

the glass wall might enhance coalescence, (iii) the
bubbles at the glass wall are not representative of the
foam bubbles, and (iv) the method is very time consuming.
Although the photographic method has these disadvantages
an order of magnitude comparison of both methods can be
made.

8.4. Results

In figure 8.2 the dependence of the Rudin foam number on
temperature is displayed for beer E. It can be clearly
seen that the foam number, as measured with this method,
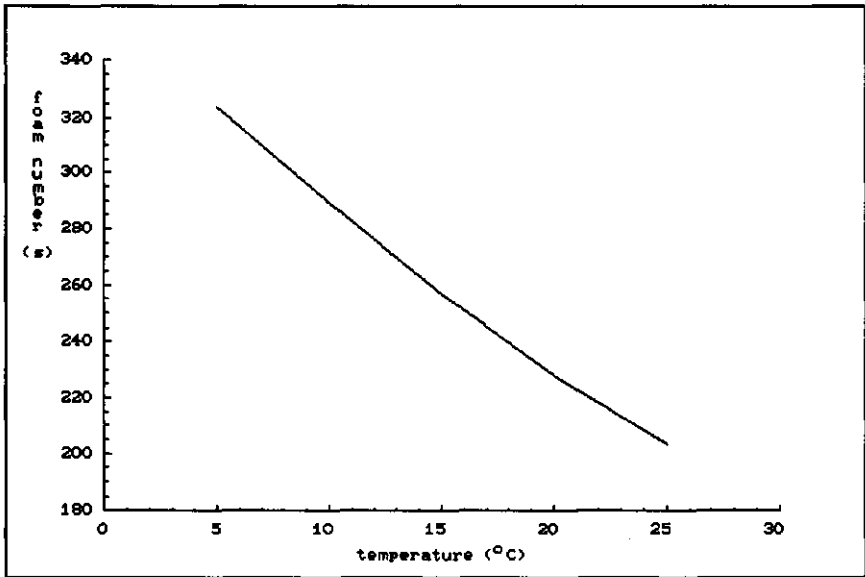increases with lower temperatures.

Figure 8.2: The foam number as a function of the temperature measured with the Rudin
tube.

This is in correspondence with expectations. With the
Rudin tube drainage is measured. Because the rate of
drainage is proportional to bulk viscosity (Eq. [3.1]) and
because bulk viscosity increases with lower temperatures,
an almost linear relationship between the temperature and
the Rudin foam number can be expected. From this result
the conclusion can be made that the foam number obtained

with a Rudin tube very much depends on the bulk viscosity of the beer under investigation and on the temperature of the measurement.
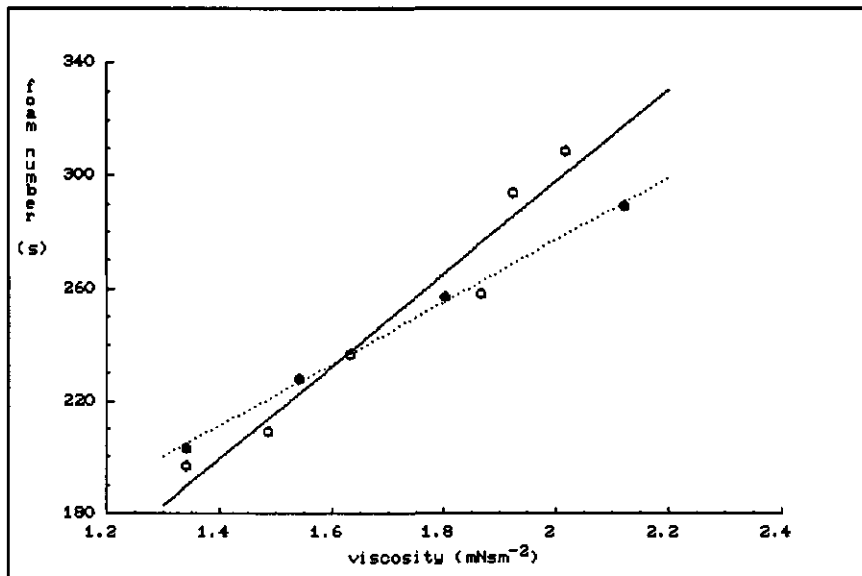

Figure 8.3: The foam number as a function of the viscosity, measured with the Rudin tube. The viscosity was adjusted with temperature (···) and with dextran (—).

In order to establish whether temperature is related to the Rudin foam number by its effect on bulk viscosity only or by its effect on other parameters as well, the bulk viscosity was also increased with dextran. The foam number of the samples was again measured with the Rudin tube. In figure 8.3 the results are given. As can be seen the relation between the foam number and the bulk viscosity shows a linear correlation when the bulk viscosity is varied by means of the temperature. The linear relationship becomes less pronounced when the bulk viscosity is increased by adding dextran. In addition the slope of both lines is different, giving evidence that more parameters than only the bulk viscosity influences the rate of drainage. In addition, there is not a good correlation between the bulk viscosity and the Rudin foam number when measured with different beers as can be seen in table 8.1.

However, the lines in figure 8.3 show more than enough similarity to conclude that the bulk viscosity of the beer

is a very important parameter for the foam number determined with the Rudin tube. The observation that beer foam is more stable at lower temperatures can thus be explained (see also chapter 6.3).

In table 8.1 the foam numbers obtained with 7 beers are displayed as measured with the Nibem meter and with the Rudin tube, using carbon dioxide and nitrogen. In addition the bulk viscosity of the beers is given.

Table 8.1: Foam numbers for various beers as determined with the Rudin tube with CO_2 and N_2 and with the standard and modified Nibem foam stability tester.

beer	Rudin CO_2 (s)	Rudin N_2 (s)	η (mNsm^{-2})	Nibem (s)	modified Nibem (s)
A	142	643	1.21	175	137
B	235	757	1.34	215	92
C	206	633	1.34	224	108
D	250	715	1.29	254	165
E	241	727	1.34	278	163
F	293	654	1.34	–	176
G	273	722	1.32	422	285

There appears to be a very large difference between foam numbers determined with carbon dioxide and nitrogen. With nitrogen much higher foam numbers are obtained. Mostly, drainage and coalescence appear to occur in a nitrogen foam. Disproportionation will proceed very slow, because the solubility of nitrogen is low. In a carbon dioxide foam disproportionation will contribute significantly to the amount of liquid drainage, because gas diffusion proceeds rapidly as a result of the high solubility of carbon dioxide. Consequently, much lower foam numbers are found for carbon dioxide foams. Apparently, disproportionation contributes indirectly to drainage and is therefore an important process for the foam number as measured with the Rudin tube. The upper level of the foam in the Rudin tube remains the same for most beers. Therefore, coalescence does not seem to be an important process in beer foam.

The foam numbers, determined with the modified Nibem

foam stability tester, are lower than the numbers with the standard Nibem meter. This must be a consequence of the difference in bubble formation. The bubbles produced by the foam flasher are smaller than the bubbles produced with the porous glass filter. The difference may also be explained by a difference in gas composition. With the standard Nibem method the foam contains the original gas of the beer, whereas with the modified Nibem method purified carbon dioxide is used.

The beers all have approximately the same bulk viscosity except beer A and to a lesser extent beer D. This must be one of the main reasons that the foam numbers for beer A are low compared to the foam numbers of the other beers. From the obtained foam numbers, in particular from the numbers obtained with the Rudin tube using carbon dioxide and the standard Nibem method, it may be concluded that the overall behavior of the foam of beer A is very poor.

Beer B very rapidly collapses as can be concluded from the results obtained with both the standard and the modified Nibem foam stability tester. Even in the Rudin tube foam collapse can be observed for beer B. In the Rudin tube the upper level of the foam of the other beers remains almost at the initial height. The Rudin number of beer B, measured with nitrogen, is extremely high, meaning that coalescence does not contribute to the collapse of the foam to a large extent. Therefore, the rapid collapse measured, when carbon dioxide was used, must be a result of gas diffusion. The foam number of beer B, obtained with the standard Nibem foam stability tester is high compared to the number, obtained with the modified Nibem foam stability tester. This can only be explained if the original gas of beer B contains less soluble gas, that stabilizes the foam against collapse.

The foam behavior of beer C is comparatively poor. In particular, the foam number, obtained with the Rudin tube using nitrogen, is lower than the foam numbers of the other beers. This must be a result of coalescence and not of drainage, because the bulk viscosity of beer C is not lower than the bulk viscosity of the other beers. It

appears that in the foam of beer C more coalescence occurs than in the foam of the other beers.

The foam numbers of **Beer D** and E are rather normal, although the standard Nibem foam number for beer D is somewhat low. This may be a result of the composition of the original gas. The bulk viscosity of beer D is somewhat lower than the bulk viscosity of beer E.

The numbers of beer F are also rather normal although it appears that more coalescence and less gas diffusion occurs in this foam than in the foams of beer D and E.

Beer G has unusual high foam numbers as measured with both Nibem methods. This can be explained by the extreme high surface dilational viscosity in compression and the ability to form bubble ghosts as explained in chapter 5.5. After beer G was degassed, the beer was somewhat turbid. This phenomenon was not observed by using the other beers. The liquid of beer G can completely drain from the foam if the foam is protected against collapse by a carbon dioxide blanket on top of the foam. In that case, a dry, aerated structure remains after drainage. The creaminess of the foam becomes very low and the color of the foam becomes grey-brown within a short period of time. The collapse of the foam is uneven and the appearance of the foam is not very attractive. In the case of beer G, the high foam numbers certainly do not represent good foam behavior from a consumer point of view.

Figure 8.4 shows the bubble-size distribution of a fresh beer E foam generated by sparging nitrogen through a G_2-glass filter with well defined pores. The foam is almost homodisperse directly after generation and the bubbles have a mean radius of about 100 μm (note that the number of bubbles is plotted on a logarithmic scale).

Figure 8.5 shows the same foam, but three minutes later. The bubble-size distribution has widened and the mean bubble radius has increased. Most important is the observation that no bubbles have become smaller, meaning that disproportionation did not occur.

Using carbon dioxide instead of nitrogen practically the same bubble-size distribution is obtained directly after

generation of the foam (figure 8.6). After three minutes
however a completely different picture is obtained. A very
large number of smaller bubbles than initially present was
measured. From figure 8.7 it is clear that bubbles have
shrunken as a consequence of gas diffusion and the bubble-
size distribution has widened much more than when the foam
contained nitrogen. It is evident that disproportionation
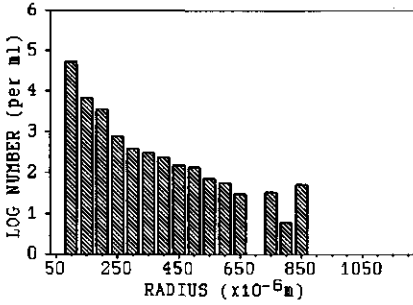has taken place.

Figure 8.4: Bubble size distribution of a
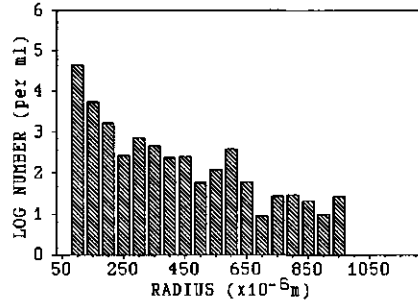nitrogen beer foam at t=0 min.

Figure 8.5: Bubble size distribution of a
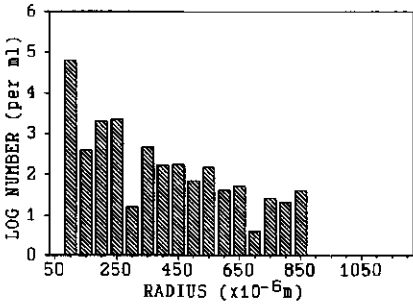nitrogen beer foam at t=3 min.

Figure 8.6: Bubble size distribution of a
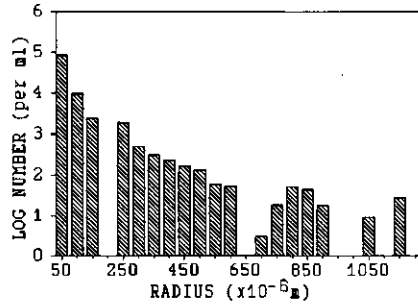carbon dioxide beer foam at t=0 min.

Figure 8.7: Bubble size distribution of a
carbon dioxide beer foam at t=3 min.

The distributions determined with the photographic
method on the same foams are presented in figures
8.8-8.11. The discrepancy between the two methods is
smaller than appears from the distributions, because the
number of bubbles is on a logarithmic scale. In general,
somewhat larger bubbles are observed with the optical
probe method than with the photographic method. This may
be a result of the fact that larger bubbles are not seen
at the glass wall with the photographic method, or because
the optical probe method induces some coalescence. In

115

addition, the initial bubble-size distribution is wider
when measured with the optical glass-fibre probe method.
The explanation for this observation is most likely that
the bubble-size distribution as measured with the optical
glass-fibre probe method is a representation of the entire
foam, whereas the bubble-size distribution, measured
photographically, gives the bubble-size distribution at a
specific foam height. All in all, the conclusion may be
drawn that the distributions determined with the optical
glass-fibre probe method and the photographic method,
correspond qualitatively and quantitatively very well.
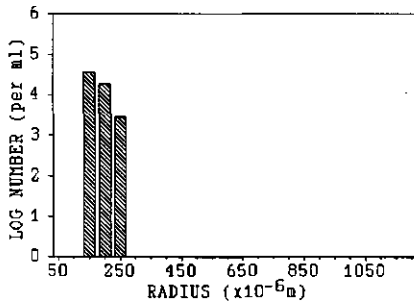
Figure 8.8: Bubble size distribution of a nitrogen beer foam at t=0 min.

Figure 8.9: Bubble size distribution of a nitrogen beer foam at t=3 min.
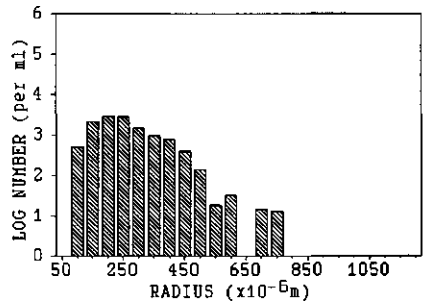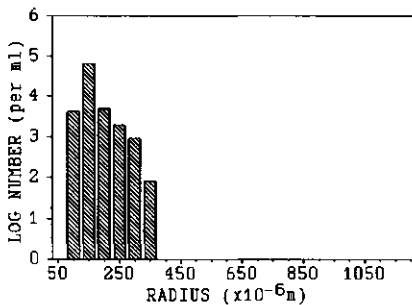

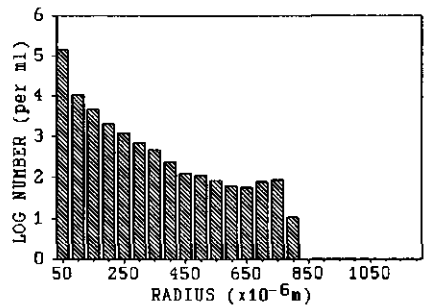**Figure 8.10:** Bubble size distribution of a carbon dioxide beer foam at t=0 min.

Figure 8.11: Bubble size distribution of a carbon dioxide beer foam at t=3 min.

8.5. Discussion

   The measurement of foam behavior is not a simple task.
Although it is not difficult to measure some kind of beer
foam characteristic with one of the described, readily

available, methods that have been developed within the last decades, the obtained results may be very misleading.

These beer foam numbers, in general, do not give a good impression of the foam behavior as it is assessed by the consumer. The methods do not correlate with each other either. Apparently, only part of the total information is obtained. A good example of the latter is given in table 8.1, where several methods, to characterize beer foam, are compared. At the most, a tendency can be found that the behavior of the foam increases from beer A to beer G. Although these beers are very extreme in their foaming behavior, the ranking for the beers is different for different methods. The main reasons are that; (i) with most methods the foam is not produced in the same way as in practice, and therefore the initial bubble-size distribution is different. (ii) in some methods beers are degassed prior to measurement and foamed with a gas of a different composition. In that case, effects of gas composition and concentration in the original beers can not be measured. (iii) the geometry of the measuring cylinder does not correspond with the practical situation. (iv) for some methods, the composition of the surrounding gas atmosphere is not identical with the normal drinking conditions. In that case, the collapse by gas diffusion is not measured correctly, although this is the main process for the breakdown of the foam in practice. (v) the ratio beer to foam is often different, resulting in a different depletion of surface active material. (vi) mostly, the temperature during the measurement is not the drinking temperature. (vii) last but not least, different phenomena are observed, *e.g.* drainage instead of collapse.

A better impression of the foam behavior is obtained when more sophisticated experiments are carried out. In addition, to the rise of the foam-liquid interface and collapse the foam, the bubble-size distribution can be measured as a function of time to obtain more information about the foaming behavior. Gasses with a different solubility, preferentially nitrogen and carbon dioxide, can be used to discriminate between different processes as

described. Additionally, the viscosity of the beer can be measured to find out whether a distinctive behavior of a foam can be explained by a difference in drainage rate or by the progress of other processes. If atypical behavior is found, that can not be readily explained, the composition of the dissolved gas in the beer may be responsible. Therefore, foam characteristics with the "natural" gas and the gas composition can be measured. If all the relevant experiments are carried out a complete impression of foam characteristics can be obtained.

Nevertheless, it remains difficult to make a quantitative distinction between the different physical processes occurring in the foam. The quantitative distinction can not be given because the four physical processes, bubble formation, drainage, coalescence and disproportionation are interrelated. The interrelations are complicated.

The initial bubble-size distribution influences the rate of drainage, coalescence and disproportionation. Drainage will proceed slower if smaller bubbles are present because there are more motionless surfaces to slow down drainage. When smaller bubbles are present coalescence will not be as destructive as when larger bubbles are present, because there are much more films to rupture. The effect of the initial bubble-size distribution on gas diffusion from the top layer of the foam to the surrounding atmosphere has been discussed before in chapter 6.5; a foam with smaller bubbles is more stable against outward gas diffusion. A wide bubble-size distribution will enhance disproportionation inside the foam, because the Laplace pressure differences in that case are larger. As a result of drainage the film thickness between the bubbles decreases with time, and this in general results in faster disproportionation and more coalescence. If coalescence or disproportionation occur more drainage will be observed. In addition, coalescence will accelerate disproportionation because, owing to coalescence, the bubble-size distribution becomes wider and the Laplace pressure differences increase. Furthermore, disproportionation may enhance coalescence. As a consequence of disproportiona-

118

tion film rearrangements in the foam may lead to an increase in coalescence.

These are only a few of the possible interrelations between bubble formation, drainage, coalescence and disproportionation. Because of these interrelations it is impossible to distinguish between these processes in a quantitative way. However, a good qualitative or even a semi-quantitative distinction can be made.

The measurement of the evolution of bubble-size distributions in foams with gasses of different solubility can make a contribution to a specified determination of foam characteristics. Therefore, the optical glass-fibre probe technique may contribute to the assessment of foam characteristics. For beer foam it is a good working method that gives rapid and conclusive information about the progress of the four physical processes. In addition, the method is comparatively easy to operate.

References

- Agnihotri, A.K., Lemlich, R., J. Colloid and Interface Sci. 84(1):42 (1981).
- Bamforth, C.W., J. Inst. Brew. 91:370 (1985).
- Bishop, L.R., Whitear, A.L., Inman, W.R., J. Inst. Brew. 81:131 (1975).
- Blom, J., Petit J. Brass. 42:388 (1934).
- Chang, K.S., Lemlich, R., J. Colloid and Interface Sci. 73(1):224 (1980).
- Clark, N.N., Turton, R., Int. J. Multiphase Flow 14(3):413 (1988).
- Datye, A.K., Lemlich, R., Int. J. Multiphase Flow 9(6):627 (1983).
- De Clerk, J., De Dijker, G., EBC Proc. Copenhagen pp. 43 (1957).
- De Vries, A.J., "Morphology, Coalescence and Size Distribution of Foam Bubbles." In: Adsorptive Bubble Separation Techniques. Ed: R. Lemlich, Ac. Press, N.Y. London. pp. 7.

(1972).

- Frijlink, J.J., van Halderen, P.A., Hofmeester J., War-moeskerken, M.M.C.G., I^2-procestechnologie 3:19 (1986).

- Frijlink, J.J., Physical Aspects Of Gassed Suspension Reactors, PhD. Thesis, Technical University Delft, Netherlands (1987) pp. 119.

- Glenister, P.R., Segel, E., ASBC Proc. pp. 55. (1964).

- Glenister, P.R., Segel, E,. Koeppl, K.G., ASBC Proc. pp. 150. (1966).

- Hudson, J.R., Development of Brewing Analysis 1st ed. London (1960).

- Jackson, G., Bamforth, C.W., J. Inst. Brew. 88:34 (1980).

- Kawakami, M., Tomimoto, N., Kotazawa, Y., Ito, K., Trans. Iron. Steel. Inst. Jpn. 28(4):271 (1988).

- Klopper, W.J., J. Inst. Brew. 60:217 (1954).

- Klopper, W.J., EBC Proc. Salzburg pp. 363 (1973).

- Klopper, W.J., The Brewers Digest 52(1):51 (1977).

- Klopper, W.J., Vermeire, H.A., Brauwissenschaft 30(9):276 (1977[a]).

- Klopper, W.J., Vermeire, H.A., Voedingsmiddelentechnologie 10(3):7 (1977[b]).

- Lemlich, R., Ind. Eng. Chem. Fundam. 17(2):89 (1978).

- Lewis, D.A., Nicol, R.S., Thompson, J.W., Chem. Eng. Res. Des. 62:334 (1984).

- Nishioka, G., Ross, S., J. Colloid and Interface Sci. 81(1):1 (1981).

- Nishioka, G., Ross, S., Whitworth, M., J. Colloid and Interface Sci. 95(2):435 (1983).

- Nishioka, G.M., Langmuir 2:649 (1986).

- Piendl, A, Legat, H, Brauwissenschaft 33(2):32 (1980).

- Pierce J.S., Pursell, J.R., EBC Congr. proc. 7th. Rome pp. 246. (1959).

- Plank, H., PhD Thesis, TH München-Weihenstephan. (1963).

- Princen, H.M., J. Colloid and Interface Sci. 91(1):160 (1983).

- Ranadive, A.Y., Lemlich, R, J. Colloid and Interface Sci. 70(2):392 (1979).

- Rasmussen, N.J., Carlsberg Res. Commun. 46:25 (1981).

- Rieser, L.A., Lemlich, R., J. Colloid and Interface Sci.

123(1):299 (1988).

- Rosendal, I., Rasmussen, N.J., MBAA Tech. Quart. 19(4):153 (1982).
- Ross, S., Clark, G.L., Wallerstein Lab. Commun. 6:46 (1939).
- Ross, S., Cutillas, M.J., J. Phys. Chem. 59:863 (1955).
- Ross, S., Suzin, Y, Langmuir 1(1):145 (1985).
- Ruan, J.Z., Litt, M.H., Krieger, I.M., J. Colloid Interface Sci. 126(1):93 (1988).
- Rudin, A.D., J. Inst. Brew. 63:506 (1957).
- Savel, J., Basarová, G., Monatschrift für Brauwissenschaft 6:249 (1989).
- Segel, E, Glenister, P.R., Koeppl, K.G., Tech. Quart. MBAA 4:104 (1967).
- Selecki, A., Wasiak, R., J. Colloid Interface Sci. 102(2):557 (1984).
- Thang, N.T., Davis, M.R., Int. J. Multiphase Flow 5:17 (1979).
- Ullmann, F., Brauerei Rundschau 93(12):249 (1982).
- Wackerbauer, K., Greif, H., Brauwissenschaft 33(4):123 (1980).
- Waniska, R.D., Kinsella, J.E., J. Food. Sci. 44:1398 (1979).
- Weibel, E.R., Estimation of Particle Size Distribution from Measurements of Intercept Lenght on a Random Line. In: Stereological Methods, Vol. 2. Ed: Academic. Press N.Y. London. pp. 215. (1980).
- Weyh, H., Monatschrift für Brauwissenschaft, 3:108 (1987).
- Weyh, H., Monatschrift für Brauwissenschaft, 11:441 (1988).
- Wilson, P.J., Mundy, A.F., J. Inst. Brew. 90:385 (1984).

9. CONCLUSIONS

The appearance of the foam is one of the important aspects of beer quality. The appearance of the foam is foremost determined by the progress of four physical processes, *i.e.* bubble formation, drainage, coalescence and disproportionation.

Bubble formation is an important process because it initially determines creaminess, the amount of foam, the bubble-size distribution in the foam, the bubble wall composition and the gas composition throughout the foam. Bubble formation depends on beer properties, like the dynamic surface tension under expansion conditions, the wetting properties, the gas content and the gas composition. This process also depends on the conditions during the dispense of the beer. A very effective way to improve beer foam behavior is by dispensing the beer in such a way that small carbon dioxide bubbles are formed. In addition, a proper control of the gas composition and the temperature is essential. Large hydrodynamic shear forces and small nucleation sites with good wetting properties may contribute to the formation of small bubbles. The entrapment of air during the dispense of the beer should be avoided. The bubble formation process is very important for foam behavior because the initial foam properties very much influence the progress of the three other physical processes.

Drainage and disproportionation appear to be the most important processes for the disappearance of the foam. The drainage rate is mainly determined by bulk viscosity and therefore the temperature of the beer is one of the main parameters, that influences the behavior of the foam. For disproportionation two different situations can be distinguished. If gas diffusion occurs inside the foam, large bubbles grow at the expense of smaller bubbles. This coarsening process proceeds rapidly as shown in chapter 8.4. If gas diffuses from the top layer of the foam to the surrounding atmosphere, the foam collapses. This is the

most important process for the breakdown of the foam. If this diffusion process can be slowed down for just a small period of time for each bubble layer, the foam will last much longer. This is a result of the fact that the whole diffusion process elapses in a time that is equal to the sum of the time required for each bubble layer in the foam. Improvement of the stability of the foam against collapse can be made effectively by nitrogenation as explained in chapter 6.5. Gas diffusion can also significantly be slowed down by surface viscosity. The surface tension in compression must be low in order to decelerate gas diffusion, because the Laplace pressure is the driving force for gas diffusion if the gas composition throughout the foam is uniform. The formation of insoluble surface layers in compression appears to go hand in hand with the decrease of the surface tension. However, for the deceleration of gas diffusion, a low surface viscosity is less effective than nitrogenation. In addition, the initial bubble-size distribution is important. A narrow initial size distribution of small bubbles is in favor of good foam behavior.

Coalescence does not contribute to the collapse of beer foam to a large extent under normal conditions. However, coalescence becomes a very dominating process if external spreading material is added to beer foam. Dirty beer glasses or consumer lips may be a source of spreading material, that can initiate coalescence. The effect on beer foam behavior can be disastrous for the appreciation of the consumer. Normally, a collapsed foam may still be appealing because a monolayer of small bubbles remains on top of the beer. If coalescence takes place the beer looks completely flat. The only way to avoid coalescence by the spreading mechanism appears to be to avoid spreading. Therefore, the beer must have a low surface tension in expansion. However, beers have very similar surface rheological behavior in expansion, especially at higher expansion rates. Therefore, beer foam will remain very susceptible for spreading material.

LIST OF SYMBOLS

Roman symbols

a	= drained beer volume	[m^3]
A	= area	[m^2]
b	= beer volume in a foam	[m^3]
B_1	= drained beer volume in 90 s	[ml]
B_2	= total drained beer volume	[ml]
c	= activity	[mole m^{-3}]
c_i	= activity of component i	[mole m^{-3}]
d	= thickness of the spread layer	[m]
d_{vs}	= volume/surface mean diameter	[m]
dlnA/dt	= relative deformation rate	[s^{-1}]
$(dlnA/dt)_i$	= dlnA/dt at inflection point	[s^{-1}]
$\mathbb{D}$	= diffusion coefficient	[$m^2 s^{-1}$]
$\mathbb{D}_i$	= $\mathbb{D}$ of component i	[$m^2 s^{-1}$]
F	= force	[N]
FFV	= Foam Flashing Value	[-]
g	= gravity	[ms^{-2}]
HRV	= head retention value	[s]
k	= constant	[s^{-1}]
k_i	= fraction of gas i in the atmosphere	[-]
l	= slit length	[m]
m	= powerlaw parameter	[-]
n	= powerlaw parameter	[-]
n_i	= amount of gas i	[mole]
n_{tot}	= total amount of gas	[mole]
O	= perimeter of bubble attachment	[m]
p	= penetration depth	[m]
P_{atm}	= atmospheric pressure	[Nm^{-2}]
P_c	= capillary pressure	[Nm^{-2}]
P_i	= partial pressure of gas i	[Nm^{-2}]
P_{tot}	= total pressure	[Nm^{-2}]
P_1	= pressure in bubble 1	[Nm^{-2}]
P_2	= pressure in bubble 2	[Nm^{-2}]
Q	= flow rate	[$m^3 s^{-1}$]
r	= radius	[m]
r_o	= bubble radius at t = 0	[m]
r_t	= bubble radius at t = t	[m]

124

r_1	= radius of bubble 1	[m]
r_2	= radius of bubble 2	[m]
R	= initial radius of a droplet	[m]
R	= gas constant	[Jmole^{-1}K^{-1}]
S	= gas solubility	[mole m^{-3}]
S_i	= gas solubility of component i	[mole m^{-3}]
t	= time	[s]
$t_{\frac{1}{2}}$	= half-life time	[s]
t_c	= critical drainage time	[s]
T	= temperature	[K]
u	= bursting velocity	[ms^{-1}]
v	= velocity	[ms^{-1}]
v_o	= initial velocity	[ms^{-1}]
V	= bubble volume	[m^3]
V_e	= bubble volume at plateau value	[m^3]
V_o	= bubble volume at t = 0	[m^3]
W_o	= weight of beer foam at t = 0	[m]
W_t	= weight of beer foam at t = t	[m]
z	= diffusion distance	[m]

Greek symbols

α	= Mach angle	[-]
η	= bulk viscosity	[Nsm^{-2}]
η_s	= surface dilational viscosity	[Nsm^{-1}]
π	= disjoining pressure	[Nm^{-2}]
ρ	= density	[kgm^{-3}]
σ	= surface tension	[Nm^{-1}]
σ_{dyn}	= dynamic surface tension	[Nm^{-1}]
σ_e	= equilibrium surface tension	[Nm^{-1}]
σ_i	= σ at inflection point	[Nm^{-1}]
σ_o	= σ in the oil phase	[Nm^{-1}]
σ_{ow}	= interfacial tension oil-water	[Nm^{-1}]
σ_s	= spreading tension	[Nm^{-1}]
σ_w	= σ in the water phase	[Nm^{-1}]
Σ	= foam characteristic (*Eq.* [8.3])	[s]
θ	= film thickness	[m]
θ_o	= initial film thickness	[m]
θ_c	= critical film thickness	[m]
ϑ	= topology factor	[m]

SUMMARY

The foaming behavior is one of the main quality charac-
teristics of beer. The appearance and behavior of the foam
has to be in accordance with the expectations of the
consumer. The foam characteristics of beer foam are
determined by the progress of four physical processes,
viz. bubble formation, drainage, coalescence and dispro-
portionation.

In beer foam two kinds of bubbles are initially present.
The first kind of bubbles is formed by heterogeneous
nucleation from the supersaturated beer solution. These
beer bubbles are comparatively small and contain carbon
dioxide. Homogeneous nucleation does not take place in
beer, because an enormous supersaturation would be neces-
sary for the spontaneous formation of bubbles. The second
kind of bubbles is formed in beer by air entrapment during
the dispense of the beer. These bubbles are in general
larger than the carbon dioxide bubbles and contain air.

Drainage occurs in beer foam. The rate of drainage is a
result of a complex interplay of gravity, Plateau border
suction, geometry aspects and balancing parameters. The
parameters that slow down drainage are bulk and surface
viscosity.

Coalescence in beer foam can be caused by externally
added lipid components. The two mechanisms that may be
responsible for this phenomena are the hydrophobic par-
ticle mechanism and the spreading mechanism. A number of
parameters can be used to distinguish between these
mechanisms. In the case of the hydrophobic particle
mechanism the size of a lipid droplet that initiates film
rupture must be at least equal to the film thickness,
whereas the droplets may be smaller in the case of the
spreading mechanism. In addition, the spreading particle
mechanism can only work when the spreading condition is
met. Therefore, the composition of the lipid droplet and
the prevailing, dynamic surface tension of the film must
allow spreading. The viscosity of the film liquid is an
important parameter to distinguish between the two film

rupture mechanisms, because at a higher bulk viscosity coalescence is more easily initiated by the spreading mechanism and more difficult by the hydrophobic particle mechanism. A falling film apparatus was used to examine the stability of a free falling beer film under various conditions. Emulsions of different composition and droplet-size distribution were added to stable free falling beer films. Some emulsions caused hole formation in the falling film. The number of holes formed in the film depended on droplet size and droplet composition. Droplets of approximately the same size as the film thickness had to be put in the beer and a certain minimum amount of emulsifier had to be added to the emulsion in order to cause hole formation. A number of spreading experiments and various surface rheological experiments were carried out in order to study the relation between the spreading of surface active material and the (dynamic) surface tension. A good correlation between the spreading of surface active material and hole formation in the free falling film was found. After some time of operation the droplet-size distribution of the added emulsion appeared to shift to smaller droplets when holes were formed in the falling film. An increase of the bulk viscosity of the beer resulted in an enormous increase of the number of holes that were formed in the film per unit of time. Thus, from these results arguments in favor of the spreading mechanism were obtained.

The radius-versus-time curves of bubbles, that shrink as a result of gas diffusion, often showed an inflection point. Therefore, the effect of the gas composition in- and outside the bubbles and the rheological aspect of the bubble surface on the rate of disproportionation was examined. A gas diffusion model was developed, including the possible presence of gases with different solubilities and including a powerlaw that describes the dependence of the surface viscosity on the surface deformation rate in compression and expansion. Experiments were carried out to measure a number of surface rheological aspects in compression. The dissolution rate of bubbles was measured.

127

Large partial pressure differences appear to dictate the rate of disproportionation. Additionally, the solubility of the present gases determines the gas diffusion rate to a large extent. When the gas composition throughout the foam is uniform the rate of disproportionation is determined by the surface dilational viscosity of the bubble. Experimental results are very much in agreement with model calculations, unless an insoluble skin formation takes place at the bubble surface as a consequence of surface compression. As a result of insoluble skin formation, bubble ghosts may be present in beer after foaming.

Several beer foam phenomena can, at least qualitatively, be explained with the knowledge of the four physical processes. The creaminess of the foam, the rise of the foam-liquid interface, the influence of temperature, the coarsening of the foam, foam collapse, cling, the influence of air entrapment and the influence of the composition of beer are described. The disappearance of the foam is mainly caused by liquid drainage and gas diffusion from the top layer of the foam to the surrounding atmosphere. Only when externally added spreading material initiates film rupture, coalescence contributes to foam collapse.

Because there are so many beer foam phenomena and properties, an overall foam stability number can not be given. Consequently, different methods must be used to measure different foam phenomena in order to fully characterize beer foam behavior. A newly developed optical glass-fibre probe technique was used to measure the bubble size distribution, the height of the foam and the level of the foam-liquid interface as a function of time. With this technique and the use of gases of different solubility a qualitative distinction can be made between the four physical processes.

SAMENVATTING

Het gedrag van het schuim is één van de belangrijkste kwaliteitskenmerken van bier. Het uiterlijk en het gedrag van het schuim moeten zijn zoals dat door de klant wordt verwacht. Het schuimgedrag wordt bepaald door het verlopen van vier fysische processen. Deze processen zijn bellenvorming, drainage, coalescentie en disproportionering.

In pas gevormd bierschuim komen twee soorten bellen voor. De eerste soort bellen ontstaat door heterogene kiemvorming in een oververzadigd bier. Deze bellen zijn betrekkelijk klein en bevatten koolzuur. Homogene kiemvorming van bellen komt in bier niet voor omdat een enorme oververzadiging nodig is voor spontane bellenvorming. De tweede soort bellen in bier ontstaat door de inslag van lucht tijdens het inschenken van bier. Deze bellen zijn in het algemeen groter dan de koolzuurbellen en bevatten lucht.

De snelheid, waarmee drainage plaatsvindt in bierschuim, is het resultaat van een ingewikkelde wisselwerking tussen de zwaartekracht, de zuiging van de Plateauzomen, compenserende parameters en geometrische aspecten. De parameters die drainage tegenwerken zijn o.a. de oppervlakte- en bulkviskositeit.

Coalescentie in bierschuim kan worden veroorzaakt door van buiten toegevoegde, vetachtige deeltjes. De twee mechanismen, die verantwoordelijk kunnen zijn voor dit verschijnsel, zijn het hydrofobe deeltjes mechanisme en het spreidingsmechanisme. Een aantal parameters kan worden onderzocht om onderscheid te kunnen maken tussen deze mechanismen. In het geval van het hydrofobe deeltjes mechanisme moet de diameter van het deeltje minstens gelijk zijn aan de filmdikte, terwijl het deeltje kleiner mag zijn in het geval van het spreidingsmechanisme. Daar komt nog bij dat aan de spreidingsconditie moet worden voldaan om het spreidingsmechanisme te laten werken. Daarom moet de deeltjessamenstelling en de heersende, dynamische oppervlaktespanning dusdanig zijn dat het spreiden van oppervlakte-aktief materiaal kan optreden.

Ook de viskositeit van de filmvloeistof is een belangrijke parameter waarmee onderscheid kan worden gemaakt tussen beide mechanismen, omdat bij een hogere viskositeit filmbreuk makkelijker kan worden veroorzaakt in het geval van het spreidingsmechanisme en moeilijker in het geval van het hydrofobe deeltjes mechanisme. Een vallende film apparaat werd gebruikt om de stabiliteit van een vrij vallende bierfilm te onderzoeken onder verschillende condities. Emulsies van verschillende samenstelling en met een verschillende deeltjesgrootteverdeling werden aan de stabiele vallende bierfilm toegevoegd. Sommige van die emulsies veroorzaakten gatvorming in de vallende film. Het aantal gaten dat wordt gevormd in de film is afhankelijk van de grootte en de samenstelling van de deeltjes. Druppels van ongeveer dezelfde grootte als de filmdikte moesten aan het bier worden toegevoegd om gatvorming te veroorzaken. Bovendien moest aan de druppels een zekere hoeveelheid emulgator worden toegevoegd. Een aantal spreidingsproeven en oppervlaktereologische experimenten werd uitgevoerd om het verband tussen het spreiden van oppervlakte-aktief materiaal en de dynamische oppervlakte-spanning te bestuderen. Een goede correlatie tussen het spreiden van oppervlakte aktief materiaal en het optreden van gatvorming in de vrij vallende film werd gevonden. De deeltjesgrootteverdeling van de toegevoegde emulsies bleken te verschuiven in de richting van kleinere deeltjes wanneer gaten werden gevormd in de vallende film. Een verhoging van de bulkviskositeit van het bier resulteerde in een sterke toename van het aantal gaten in de vallende film per tijdseenheid. Het coalescentiemechanisme in bierschuim, dat optreedt wanneer vetachtige componenten van buitenaf worden toegevoegd, blijkt dus het spreidings-mechanisme te zijn.

De straal-tegen-tijdcurves van bellen die krimpen als gevolg van disproportionering vertonen vaak een buigpunt. Daarom is de invloed van de gassamenstelling in en buiten de bellen en de invloed van de reologische eigenschappen van het beloppervlak op de disproportioneringssnelheid onderzocht. Een gasdiffusiemodel werd ontwikkeld, waarbij

rekening is gehouden met de mogelijke aanwezigheid van twee gassen met een verschillende oplosbaarheid en waarbij een machtwet is gebruikt om de afhankelijkheid van de oppervlaktedilatatieviskositeit van de vervormingssnelheid in zowel compressie als expansie te beschrijven. Enkele experimenten zijn uitgevoerd om een aantal oppervlakte-reologische aspecten in compressie te bepalen. De snelheid waarmee bellen oplossen werd gemeten. Partiële gasdrukver-schillen blijken de disproportioneringssnelheid in belang-rijke mate te bepalen. Bovendien is de oplosbaarheid van de aanwezige gassen bepalend voor de gasdiffusiesnelheid. Wanneer de gassamenstelling in het gehele schuim gelijk is wordt de disproportioneringssnelheid bepaald door de oppervlaktedilatatieviskositeit van de bel. De verkregen experimentele resultaten kunnen goed worden beschreven met modelberekeningen tenzij in het beloppervlak een onoplos-bare laag wordt gevormd door de oppervlaktecompressie. Wanneer onoplosbare lagen worden gevormd tijdens de compressie van het bieroppervlak kunnen "bubble ghosts" in bier voorkomen nadat het bier heeft geschuimd.

Verschillende verschijnselen die voorkomen in bierschuim kunnen worden verklaard met behulp van de kennis van de vier verschillende fysische processen. De romigheid van het schuim, het optrekken van het vloeistof-schuimgrens-vlak, de invloed van de temperatuur, het vergroven van het schuim, het inzakken, cling, de invloed van de inslag van lucht en de invloed van de samenstelling van het bier is beschreven. Het verdwijnen van het schuim blijkt vooral te komen door drainage en gasdiffusie vanuit de bovenste bellenlaag van het schuim naar de atmosfeer boven het schuim. Alleen wanneer vetachtige componenten, die van buitenaf worden toegevoegd, het breken van films veroor-zaken, draagt coalescentie wezenlijk bij tot het inzakken van het schuim.

Omdat er zoveel verschillende verschijnselen en eigen-schappen van bierschuim zijn, is het niet goed mogelijk om de stabiliteit van schuim in één getal uit te drukken. Dit heeft tot gevolg dat verschillende methodes moeten worden gebruikt en verschillende verschijnselen moeten worden

gemeten om het schuimgedrag volledig te karakteriseren. Een optische glasvezelkabeltechniek is gebruikt om bellen- grootteverdelingen in schuim, de dikte van de schuimkraag en de hoogte van het vloeistof-schuimgrensvlak te bepalen als functie van de tijd. Met gassen, die een verschillende oplosbaarheid hebben, is een kwalitatief onderscheid gemaakt tussen de vier verschillende fysische processen.

CURRICULUM VITAE

A.D. Ronteltap was born on the 12th of November 1957 in Pladju, Indonesia. He was raised in Holland where he graduated from high school in 1976. After spending one year at the "Vrije Hogeschool" in Driebergen, he started to study Food Technology at the Agricultural University in Wageningen in 1977. In the final years of his study he specialized in Food chemistry, Biochemistry and Proces Technology. After graduating in 1985, he started the research work on beer foam of which this thesis is the final result.